NPS62-78-008 PR

NAVAL POSTGRADUATE SCHOOL

Monterey, California

SENSITIVITY ANALYSIS OF THE XR-3 HEAVE EQUATIONS TO CHANGES IN PLENUM AIR LEAKAGE AND INFLUX RATES

Alex Gerba, Jr. and George J. Thaler

September 1978

Progress Report for Period Ending

June 1978

Prepared for:
Naval Sea Systems Command (PMS-304)
Surface Effect Ship Project Office
P. O. Box 34401
Bethesda, Maryland 20034

NAVAL POSTGRADUATE SCHOOL
Monterey, California

Rear Admiral Tyler F. Dedman
Superintendent

Jack R. Borsting
Provost

The work reported herein was supported by funds provided by the Naval Sea Systems Command, Surface Effects Project Office. Reproduction of all or part of this report is authorized.

This report was prepared by:

Alex Gerba Jr

ALEX GERBA, JR.
Associate Professor of
Electrical Engineering

GEORGE J. THALER
Professor of
Electrical Engineering

Reviewed by:

D. E. KIRK, Chairman
Department of Electrical
Engineering

Released by:

William M. Tolles

W. M. TOLLES
Dean of Research and Dean of
Science and Engineering

UNCLASSIFIED

SECURITY CLASSIFICATION OF THIS PAGE (When Data Entered)

REPORT DOCUMENTATION PAGE		READ INSTRUCTIONS BEFORE COMPLETING FORM
1. REPORT NUMBER NPS62-78-008	2. GOVT ACCESSION NO.	3. RECIPIENT'S CATALOG NUMBER
4. TITLE (and Subtitle) Sensitivity Analysis of the XR-3 Heave Equations to Changes in Plenum Air Leakage and Influx Rates		5. TYPE OF REPORT & PERIOD COVERED Project Report for Period Ending June 1978 6. PERFORMING ORG. REPORT NUMBER
7. AUTHOR(s) Alex Gerba, Jr. and George J. Thaler		8. CONTRACT OR GRANT NUMBER(s)
9. PERFORMING ORGANIZATION NAME AND ADDRESS Naval Postgraduate School Code 62 Monterey, CA 93940		10. PROGRAM ELEMENT, PROJECT, TASK AREA & WORK UNIT NUMBERS 63534N, Task 19824 N0002478WR8G039
11. CONTROLLING OFFICE NAME AND ADDRESS Naval Sea Systems Command (PMS-304) Surface Effect Ship Project Office P.O. Box 34401, Bethesda, MD 20034		12. REPORT DATE September 1978 13. NUMBER OF PAGES 89
14. MONITORING AGENCY NAME & ADDRESS(if different from Controlling Office)		15. SECURITY CLASS. (of this report) Unclassified 15a. DECLASSIFICATION/DOWNGRADING SCHEDULE

16. DISTRIBUTION STATEMENT (of this Report)

Approved for public release: distribution unlimited

17. DISTRIBUTION STATEMENT (of the abstract entered in Block 20, if different from Report)

18. SUPPLEMENTARY NOTES

19. KEY WORDS (Continue on reverse side if necessary and identify by block number)

XR-3 Heave Equation Analysis
Effect of Varying Plenum Air Rate
Linear and 6 DOF Equations of Motion
CAB Surface Effect Ship

20. ABSTRACT (Continue on reverse side if necessary and identify by block number)

A study of the CABSES vertical plane motions using the 6-DOF Program for the XR-3 craft was performed with various values of air flow rates in order to observe the sensitivity of the craft heave, c.g. acceleration and plenum pressure to variations in air flow rate. The frequency response due to regular and complex seas as well as the transient response due to a weight removal were used to observe the effect of changes in air flow rate. A linear heave-only model is shown to provide useful

DD FORM 1 JAN 73 1473 EDITION OF 1 NOV 65 IS OBSOLETE
S/N 0102-014-6601

UNCLASSIFIED
SECURITY CLASSIFICATION OF THIS PAGE (When Data Entered)

information concerning the effect of air flow rate on the high frequency characteristics of the XR-3 craft.

ABSTRACT

A study of the CABSES vertical plane motions using the 6-D.O.F. Program for the XR-3 craft was performed with various values of air flow rates in order to observe the sensitivity of the craft heave, c. g. acceleration and plenum pressure to variations in air flow rate. The frequency response due to regular and complex seas as well as the transient response due to a weight removal were used to observe the effect of changes in air flow rate. A linear heave-only model is shown to provide useful information concerning the effect of air flow rate on the high frequency characteristics of the XR-3 craft.

TABLE OF CONTENTS

I. INTRODUCTION

One important design consideration of any naval vessel is the habitability of the craft for all possible environmental conditions encountered in its operation. For the CAB type surface effect ship, it is important that the vibrations induced by the high speed operations over the full spectrum of the sea surface wave profile do not produce a great discomfort factor for the crew. In particular, the possibility of large vertical accelerations for prolonged periods of operation should be avoided.

The primary purpose of this study is to obtain data relating the effects of plenum air flow leakage, and air influx rates on the vertical motions of The Captured Air Bubble craft. To do this several models and several kinds of simulation tests are used. The models used are a Six Degree of Freedom computer model (originally written by Oceanics, Inc., and modified for the XR-3 craft at USNPGS), and the simplified linear model for heave motions only (written at USNPGS, see Report NPS62-77-002, Ref. 2).

The simulation tests included sinusoidal sea frequency response tests, complex sea frequency response tests, and step weight removal transient tests.

II. SIMPLIFIED XR-3 MODEL

In order to investigate the characteristics of the vertical motion of the CAB craft, it is necessary to obtain a mathematical model that can readily be used for analytical purposes. This was the principal objective in Reference 1 in which a simplified heave-only model of the XR-3 was developed. For the convenience of ready reference, the development of this model has been repeated in Appendix A.

This simplified XR-3 model has proven to be quite useful in developing a scaling method for the heave motion equations as reported in Reference 2. The linear model used was described by the state variable vector

$$\underline{x} = (\delta z, \dot{\delta z}, \delta V_m)^T$$

and the output variable,

$$y = \delta P_b$$

as given in Appendix A where

$x_1 = \delta z$, incremental heave (draft)

$x_2 = \dot{\delta z}$, incremental heave rate

$x_3 = \delta V_m$, incremental air mass volume with $\delta V_m = m_b/\rho_a$

$y = \delta P_b$, incremental plenum pressure

The step weight transient used both in Reference 1 and Reference 2 had the state equation

$$\dot{\underline{x}} = \underset{\sim}{A}\,\underline{x}$$

with initial conditions

$$x(0) = [\delta z(0) \quad 0 \quad \delta V_m(0)]^T$$

which was brought about by the sudden removal of 10% of the craft weight. The characteristic equation for the system

$$\det(sI - A) = 0$$

is shown in Appendix A to be of third order. In this report, the sinusoidal sea input transfer function for this model is developed in the following section. The step weight transient is investigated in Section IV to correlate the results of the sinusoidal sea input investigation.

III. SINUSOIDAL SEA INPUT

The characteristics of the fully developed sea surface can be approximated by a long crested wave obtained by the addition of a finite number of sinusoidal waves of various amplitudes as described in References 3 and 4 and summarized below.

For the CAB-SES frequency response analysis, it is necessary to develop a transfer function for the sinusoidal sea input. What follows is a development of the transfer function for the heave motion equation of the simplified XR-3 craft.

A Development of the Simplified XR-3 Transfer Functions

1. Surface Wave Profile

The surface wave profile for both deep and shallow waves can be represented by a regular swell or wave:

$$WAV(x,t) = A \sin[k_n(x + V_w t)]$$

where: A = surface wave amplitude (half-height from crest to trough) (ft)

k_n = the "wave number", $2\pi/L_w$ (ft^{-1})

L_w = wave length (ft)

V_w = wave velocity or "celerity" (ft/sec)

$$\left(\text{for deep water, } V_w = \sqrt{\frac{gL_w}{2\pi}}\right)$$

A more convenient form can be obtained by using circular (incident) frequency, $\omega_i = 2\pi/T_w$ where T_w is the period, that is, the

time required for the wave to travel one wave length. From the equation for V_w , $T_w = \frac{L_w}{V_w} = \left(\frac{2\pi L_w}{g}\right)^{\frac{1}{2}}$

then $\omega_i = \frac{2\pi}{T_w} = \left(\frac{2\pi g}{L_w}\right)^{\frac{1}{2}} = (k_n g)^{\frac{1}{2}} = k_n V_w$

thus,

$$WAV(x,t) = A \sin(k_n x + \omega_i t)$$

When observed at a fixed point in space with x = 0

$$WAV(0,t) = A \sin(w_i t)$$

Alternately, if the wave profile is observed at t = 0,

$$WAV(x,0) = A \sin(k_n x)$$

The slope of the wave surface is obtained by differentiation,

$$\frac{d}{dx}\left[WAV(x,0)\right] = k_n A \cos(k_n x)$$

and the maximum slope occurs when $k_n x = 0, \pi$, etc., thus

$$\text{max slope} = k_n A = \frac{2\pi A}{L_w} = \frac{\pi h_w}{L_w}$$

where L_w = length of the wave

$h_w = 2A$ = wave height from hollow to crest.

2. Wave Input for the Heave Equation

In the case of the CAB-SES, the wave introduces (1) a change in the plenum volume and thus a change of plenum pressure and (2) a change in sidewall immersed volume and thus a change in the forces

of buoyancy. The additional forces due to the seals will be neglected in this study since they largely affect pitch motion which is not considered in this model. Since the objective is to obtain transfer function of the system to be analyzed for the condition of a forcing function that is sinusoidal in time, it is necessary to recast the wave profile equation from a function of displacement and time to a function of time only. This is readily possible for the heave-only model since all the forces along the hull that result due to the waves can be lumped together into a single force acting at the center of gravity (CG) which is the same point as the center of pressure (C.P.) for this simplified XR-3 model.

Given the wave profile

$$WAV(x,t) = A \sin(k_n x + \omega_i t)$$

and the assumption that the craft is heading into the wave, the wave height, WAV(x,t), as seen by the ship hull is at the apparent or encounter frequency, $\omega_e = \omega_i(1 + \frac{V}{V_w})$ where V is the ship velocity and V_w is the velocity of the wave, thus

$$WAV(x,t) = A \sin(k_n x + \omega_e t)$$

$$= A \sin\left(\frac{\omega_i x}{V_w} + \omega_e t\right)$$

Use of the identity for the sine of the-sum-of-two-angles yields

$$WAV(x,t) = A\left[\sin(\omega_e t)\cos\frac{\omega_i x}{V_w} + \cos(\omega_e t)\sin\frac{\omega_i x}{V_w}\right]$$

The differential volume of the plenum due to the wave input is

$$d[\delta V_p(x,t)] = (W_p)[WAV(x,t)]dx$$

where

δV_p is the incremental plenum volume due to wave.

W_p is the width of the plenum chamber.

dx is the differential length of the plenum.

The total incremental volume of the plenum due to the wave can be established at any time t by integration over the plenum length, L_p. Thus,

$$\delta V_p(t) = W_p A \int_{-\frac{L_p}{2}}^{\frac{L_p}{2}} \left[\sin(\omega_e t) \cos \frac{\omega_i x}{V_w} + \cos(\omega_e t) \sin \frac{\omega_i x}{V_w} \right] dx$$

$$\delta V_p(t) = W_p A \left\{ \left[\sin(\omega_e t) \left(\frac{V_w}{\omega_i} \right) \sin\left(\frac{\omega_i x}{V_w} \right) \right]_{-\frac{L_p}{2}}^{\frac{L_p}{2}} \right.$$

$$\left. - \left[\cos(\omega_e t) \left(\frac{V_w}{\omega_i} \right) \cos\left(\frac{\omega_i x}{V_w} \right) \right]_{-\frac{L_p}{2}}^{\frac{L_p}{2}} \right\}$$

It can be observed that the first term on the right hand side of the equation when the limits are applied will yield a double-amplitude sinusoid (since it is an odd function) and the second term will yield zero (since it is an even function). Thus,

$$\delta V_p(t) = \left[\left(\frac{2 W_p V_w}{\omega_i} \right) \sin\left(\frac{\omega_i L_p}{2 V_w} \right) \right] A \sin(\omega_e t)$$

Now, for each regular wave input with a wave length of L_w and an incident (circular) frequency of $\omega_i = \frac{2\pi V_w}{L_w}$ where $V_w = \sqrt{\frac{gL_w}{2\pi}}$ the coefficient in the brackets above is constant and thus the incremental variation of plenum volume is the result of the sinusoidal input, $\delta W = A \sin(\omega_e t)$.

The transfer function of the incremental plenum volume, δV_p to wave height, δW becomes,

$$\frac{\delta V_p}{\delta W} = k_1(\omega_i) = \left[\left(\frac{2W_p V_w}{\omega_i}\right) \sin\left(\frac{\omega_i L_p}{2V_w}\right)\right]$$

where the coefficient $k_1(\omega_i)$ is a function of the incident frequency.

Following the same path of development, the transfer function of each sidewall volume, δV_s , to wave height, δW is,

$$\frac{\delta V_s}{\delta W} = k_0(\omega_i) = \left[\left(\frac{2W_s V_w}{\omega_i}\right) \sin\left(\frac{\omega_i L_p}{2V_w}\right)\right]$$

where W_s = width of each sidewall.

The transfer function of the total incremental sidewall buoyancy force, δF_s to wave height, δW is

$$\frac{\delta F_s}{\delta W} = k_0(\omega_i)(2\rho_w g)$$

Then

$$\frac{\delta F_{sm}}{\delta W} = k_0(\omega_i) \frac{2\rho_w g}{M}$$

where $\delta F_{sm} = \delta F_s / M$

3. System Block Diagram and Transfer Function

The linear heave motion equations were developed in Ref. 1 and are repeated here for convenience in Appendix A. The block diagram for this linear system is shown in Figure 1 where the output is the incremental variation in heave (or draft) δz, and the input is the sinusoidal variation in wave height about the calm water level of draft. Note that a positive value of wave height reduces the effective plenum volume, δV_b , and therefore requires a negative sign in the signal transmission as shown in Figure 1.

Also it should be noted that a positive value of wave height increases the wetted sidewall volume, δV_s , which cause a larger upward force and therefore requires a negative sign in the signal transmission. The effect of added mass, δF_{am} , was also included in this model. However, in the development of the transfer function of C.G. acceleration to wave height as well as plenum pressure to wave height, it was shown that the effect of added mass can be neglected, as a reasonable first approximation and therefore added mass effects were not included in the analysis that follows.

The algebraic computation of the wave input transfer functions can be performed either by block diagram manipulation or by application of the signal flow graph method. The latter approach was used with the details contained in Appendix B. The resulting transfer functions are of the following forms

$$\frac{\delta z}{\delta W} = \frac{-(a\,s + b)}{s^3 + cs^2 + ds + e} \qquad \text{(Draft/Wave height)} \quad (1)$$

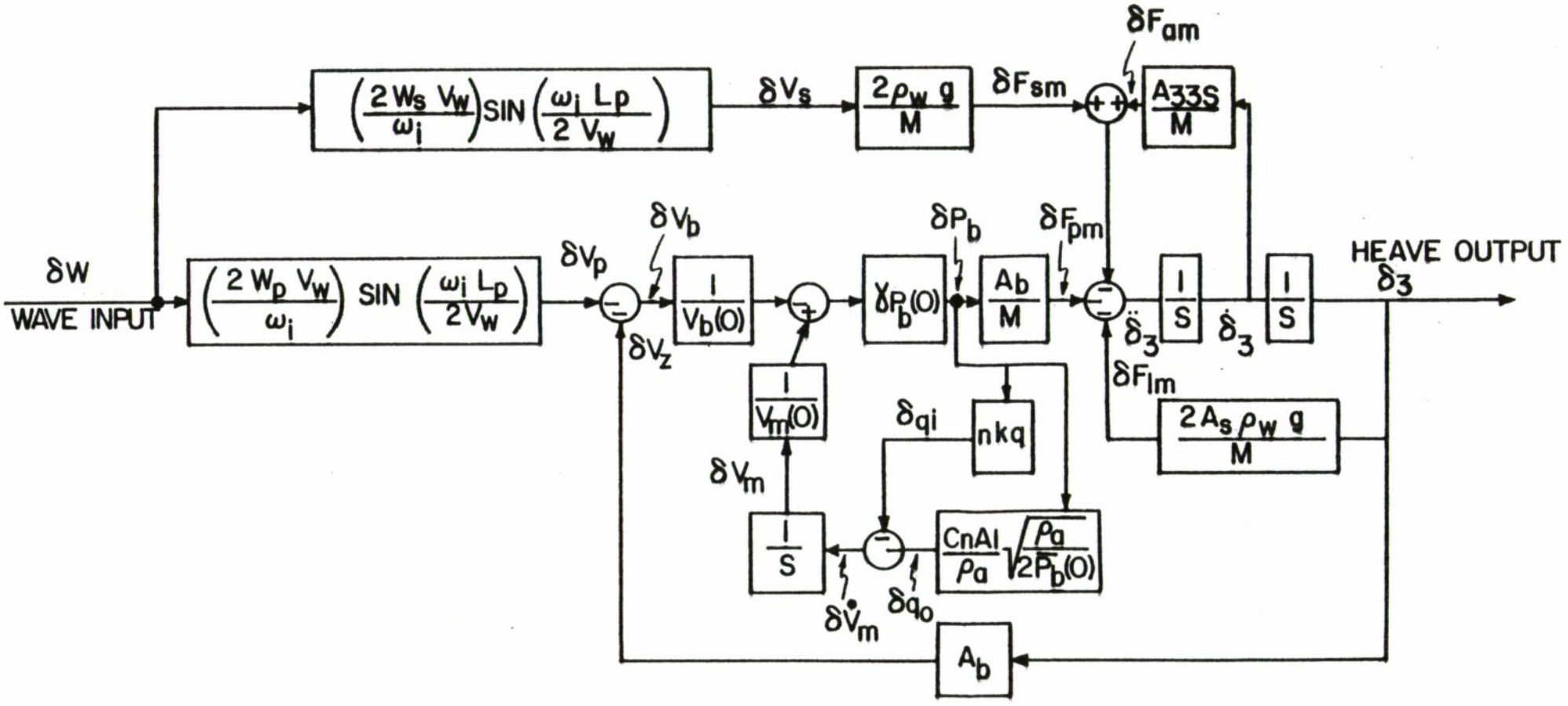

FIGURE 1. BLOCK DIAGRAM OF THE LINEAR HEAVE EQUATION FOR SINUSOIDAL WAVE INPUT.

$$\frac{\ddot{\delta z}}{\delta W} = \frac{-s^2(a\,s + b)}{s^3 + cs^2 + ds + e} \qquad \left(\frac{\text{C.G. acceleration}}{\text{Wave Height}}\right) \quad (2)$$

$$\frac{\delta P_b}{\delta W} = \frac{s^2(a's + b')}{s^3 + cs^2 + ds + e} \qquad \left(\frac{\text{Plenum Pressure}}{\text{Wave Height}}\right) \quad (3)$$

The coefficients a,b,a' and b' are functions of the incident wave frequency since they contain the k_0 and k_1 terms of the plenum volume-wave height transfer function and sidewall volume-wave height transfer function developed in secion III-A-2. It is possible to simplify this functional relationship in k_0 and k_1 by a convenient approximation which is carried out below.

From Appendix B,

$$a = k_0 + k_1k_2k_3k_4$$

where $$k_0 = \left[\left(\frac{2W_sV_w}{\omega_i}\right)\sin\left(\frac{\omega_i L_p}{2V_w}\right)\right]\frac{2\rho_\omega g}{M}$$

$$k_1 = \left(\frac{2W_pV_w}{\omega_i}\right)\sin\left(\frac{\omega_i L_p}{2V_w}\right)$$

$$k_2 = 1/V_b(0)$$

$$k_3 = \gamma P_b(0)$$

$$k_4 = A_b/M$$

For the XR-3 craft operating at 30 knots, the encounter frequency, ω_e , can be approximated, as shown in Appendix C, over the frequency range of interest as, $\omega_e = 2\omega_i^2$. Recognizing that $V_w = g/\omega_i$, it is possible to apply these substitutions into k_0 and k_1 to yield

$$k_0 = \left(\frac{2A_s\rho_w g}{M}\right)\frac{\sin\ \alpha\omega}{\alpha\omega}$$

and

$$k_1 = (A_b)\frac{\sin\ \alpha\omega}{\alpha\omega}$$

where

$$A_b = W_p L_p \qquad \alpha = L_p/4g$$

$$A_p = W_s L_p \qquad \omega = \omega_e$$

Observe now that k_0 and k_1 are now composed of constant terms multiplied by the sine function $\frac{\sin\ \alpha\omega}{\alpha\omega}$. A plot of this function over the encounter frequency range of interest is given in Figure 2. It should be noted that the magnitude of this function is very nearly unity up to 2 rps then attenuates in a manner that approximates a single pole at 8.4 radians/sec up to 15 rps after which it drops at a faster rate and then a lobe of increased magnitude occurs with a peak at approximately 30 rps and repeated attenuated lobes at multiples of the plenum length as reported in reference 7.

The coefficient

$$a = \left[\frac{2A_s\rho_w g}{M} + \frac{\gamma P_b(0)A_b}{V_b(0)M}\right]\frac{\sin\ \alpha\omega}{\alpha\omega}$$

and in like manner

$$b = \left[\frac{2A_s\rho_w g}{M} \cdot \frac{\gamma P_b(0)k_6}{V_m(0)}\right]\frac{\sin\ \alpha\omega}{\alpha\omega}$$

$$a' = b' = \left[\frac{A_b\gamma P_b(0)}{V_b(0)}\right]\frac{\sin\ \alpha\omega}{\alpha\omega}$$

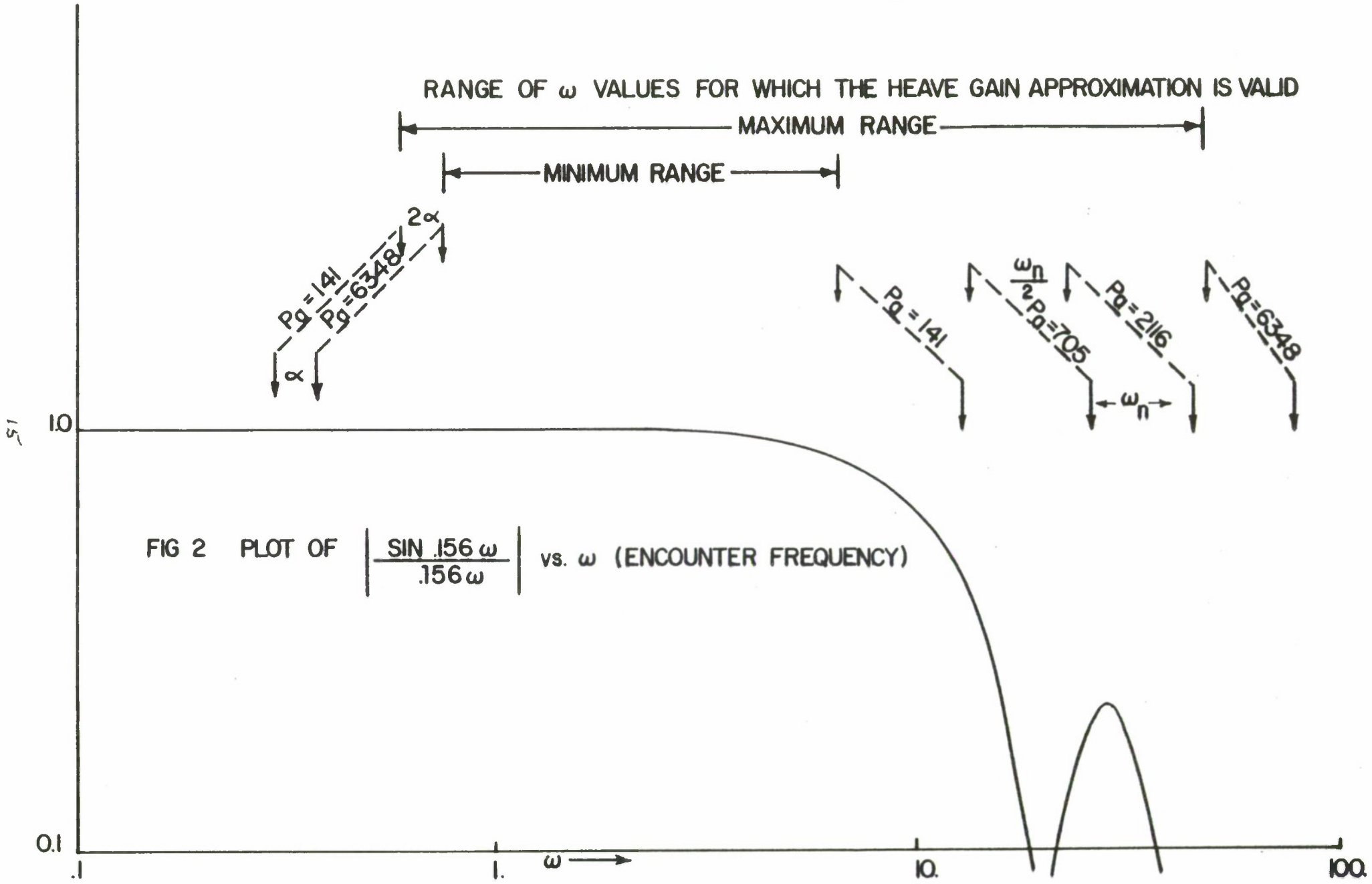

FIG 2 PLOT OF $\left|\frac{\text{SIN } .156\,\omega}{.156\,\omega}\right|$ vs. ω (ENCOUNTER FREQUENCY)

where the added mass coefficient, k_9 , that originally appeared in coefficient b has been set equal to zero.

The transfer functions now become

$$\frac{\delta z}{\delta W} = \frac{-a(s + b/a)}{s^3 + cs^2 + ds + e} \tag{1b}$$

$$\frac{\ddot{\delta z}}{\delta W} = \frac{-a\ s\ (s + b/a)}{s^3 + cs^2 + ds + e} \tag{2b}$$

$$\frac{\delta P_b}{\delta W} = \frac{a'\ s\ (s + l)}{s^3 + cs^2 + ds + e} \tag{3b}$$

where

$$a = \left[\frac{2A_s\rho_w g + \gamma P_b(0) A_b}{M}\right] \frac{\sin \alpha\omega}{\alpha\omega}$$

$$a \doteq \left(\frac{\gamma P_b(0) A_b}{M}\right) \frac{\sin \alpha\omega}{\alpha\omega} \quad (\text{since } \gamma P_b(0) A_b >> 2A_s\rho_w g)$$

$$b = \left[\frac{2A_s\rho_w g\ P_b(0) k_6}{M\ V_m(0)}\right] \frac{\sin \alpha\omega}{\alpha\omega}$$

$$a' = \left[\frac{A_b \gamma P_b(0)}{V_b(0)}\right] \frac{\sin \alpha\omega}{\alpha\omega}$$

and

$$k_6 = \left(n\ k_q + \frac{C_n A_\ell}{\rho_a} \sqrt{\frac{\rho_a}{2\bar{P}_b(0)}}\right)$$

$$c = \frac{\gamma P_b(0)}{V_m(0)} k_6$$

$$d = \frac{2A_s\rho_w g}{M} + \frac{\gamma P_b(0) A_b^2}{V_b(0) M}$$

with added-mass coefficient k_9 = zero

$$d \doteq \frac{\gamma P_b(0) A_b^2}{V_b(0) M} \quad \left(\text{since } \frac{\gamma P_b(0) A_b^2}{V_b(0)} >> 2A_p\rho_w g\right)$$

$$e = \frac{\gamma P_b(0) k_6}{V_m(0)} \left(\frac{2A_s\rho_w g}{M}\right)$$

The value of b/a is dependent upon the magnitude of the air flow rate term, k_6 , thus

$$\frac{b}{a} = \frac{2A_s\rho_w g\gamma P_b(0) k_6}{MV_m(0)} \cdot \frac{M}{(2A_s\rho_w g + \gamma P_b(0) A_b)}$$

which will reduce by the above approximation to yield,

$$\frac{b}{a} = \left[\frac{2A_s\rho_w g}{A_b V_m(0)}\right] k_6$$

Using the parameter values given in Section IV, the transfer functions are

$$\frac{\delta z}{\delta W} = \left[\frac{-3200.\ (s + .045\ k_6)}{s^3 + 11.3\ k_6 s^2 + 2441.8s + 145.3}\right] \frac{\sin(.155\omega)}{(.155\omega)}$$

$$\frac{\ddot{\delta z}}{\delta W} = s^2 \frac{\delta z}{\delta W}$$

$$\frac{\delta P_b}{\delta W} = \left[\frac{2284\ s^2(s + 1)}{s^3 + 11.3\ k_6\ s^2 + 2441.8s + 145.3}\right] \frac{\sin(.155\omega)}{(1.55\omega)}$$

where

$$a = \left[\frac{2\ (\frac{75}{4})\ 2\ (32.17) + 1.4\ (2140.8)\ 200}{188.06}\right] \frac{\sin\ (\frac{20}{4 \cdot 32.17})\ \omega}{(5/32.17)\ \omega}$$

$$b = \left[\frac{2(\frac{75}{4})\ 2(32.17)\ 1.4(2140.8)\ k_6}{188.06(264.63)}\right] \frac{\sin \alpha\omega}{\alpha\omega}$$

$$a' = \left[\frac{200(1.4)(2140.8)}{262.44}\right] \frac{\sin \alpha\omega}{\alpha\omega}$$

$$c = \left[\frac{1.4(2140.8)}{264.63}\right] k_6$$

$$d = \frac{2(\frac{75}{4})\ 2(32.17)}{188.06} + \frac{11.420\ (200)^2}{188.06}$$

$$e = (11.326)(12.83)\ k_6$$

Using the value of $k_6 = 6.28$, the transfer functions become

$$\frac{\delta z}{\delta W} = \frac{-3200(s + .28)\ \frac{\sin(.155\omega)}{(.155\omega)}}{(s + .38)(s + 35.1 + j\ 34.4)(s + 35.1 - j\ 34.4)}$$

$$\frac{\delta z}{\delta W} = s^2\ \frac{\delta z}{\delta W}$$

$$\frac{\delta P_b}{\delta W} = \frac{2284\ s^2\ (s + 1)\ \frac{\sin(.155\ )}{(.155\ )}}{(s + .38)(s + 35.1 + j\ 34.4)(s + 35.1 - j\ 34.4)}$$

where the factored form of the denominator was obtained from Section IV A.

Figure 3 shows the magnitude spectrum for the three transfer functions of the simplified XR-3 model for the value of $k_6 = 6.28$. The curve for acceleration was plotted in g units and the pressure curve in incremental (gage) pressure values.

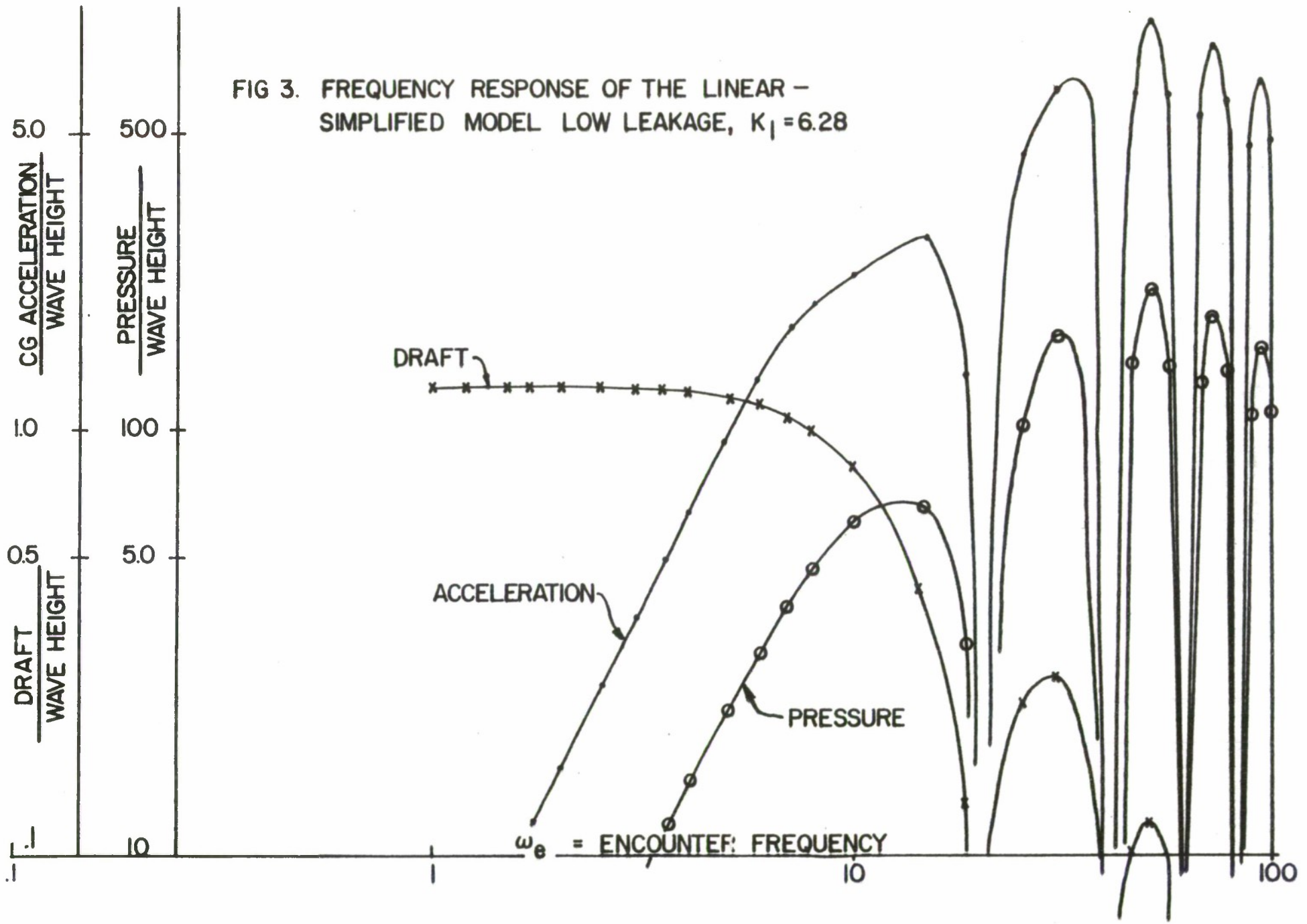
FIG 3. FREQUENCY RESPONSE OF THE LINEAR – SIMPLIFIED MODEL LOW LEAKAGE, $K_1 = 6.28$
CG ACCELERATION / WAVE HEIGHT
PRESSURE / WAVE HEIGHT
DRAFT / WAVE HEIGHT
5.0
1.0
0.5
500
100
5.0
10
.1
1
10
100
DRAFT
ACCELERATION
PRESSURE
ω_e = ENCOUNTEF: FREQUENCY

B. Calculation of the 6 DOF Model Frequency Response.

Using the 6 DOF equations for the XR-3 as given in Ref. 5, the output response to a small amplitude (10% of the average draft) sinusoidal head-on sea was obtained on the IBM 360/67 computer. Two types of wave inputs were used; a single frequency input (regular sea) and a complex frequency input (complex sea). The band of encounter frequencies was extended beyond that used in Ref. 6 to include the range

$$1 < \omega < 100 \text{ rps}$$

1. Regular Sea

The procedure used in the computation of output response to a regular sea input was to compute 35 seconds with the adjustable thrust option to arrive at a steady state sinusoidal response. The average value of thrust, draft, pitch and pressure were then used as input for the operating condition of the final run. The steady-state final run was obtained with constant thrust at a steady-state speed of 30 knots. Data was taken only after at least 30 seconds of compute time to insure true steady-state conditions. The integration method used was a fixed-stepsize Runge Kutta which yielded about 50% saving in compute time over the adjustable R-K method with no observable loss in accuracy.

The ratio of draft to wave height amplitude as well as C.G. acceleration and plenum pressure to wave height were computed for the 6 DOF equations with the results plotted in Figure 4. All 3 frequency response curves clearly show the $\frac{\sin \alpha\omega}{\alpha\omega}$ function

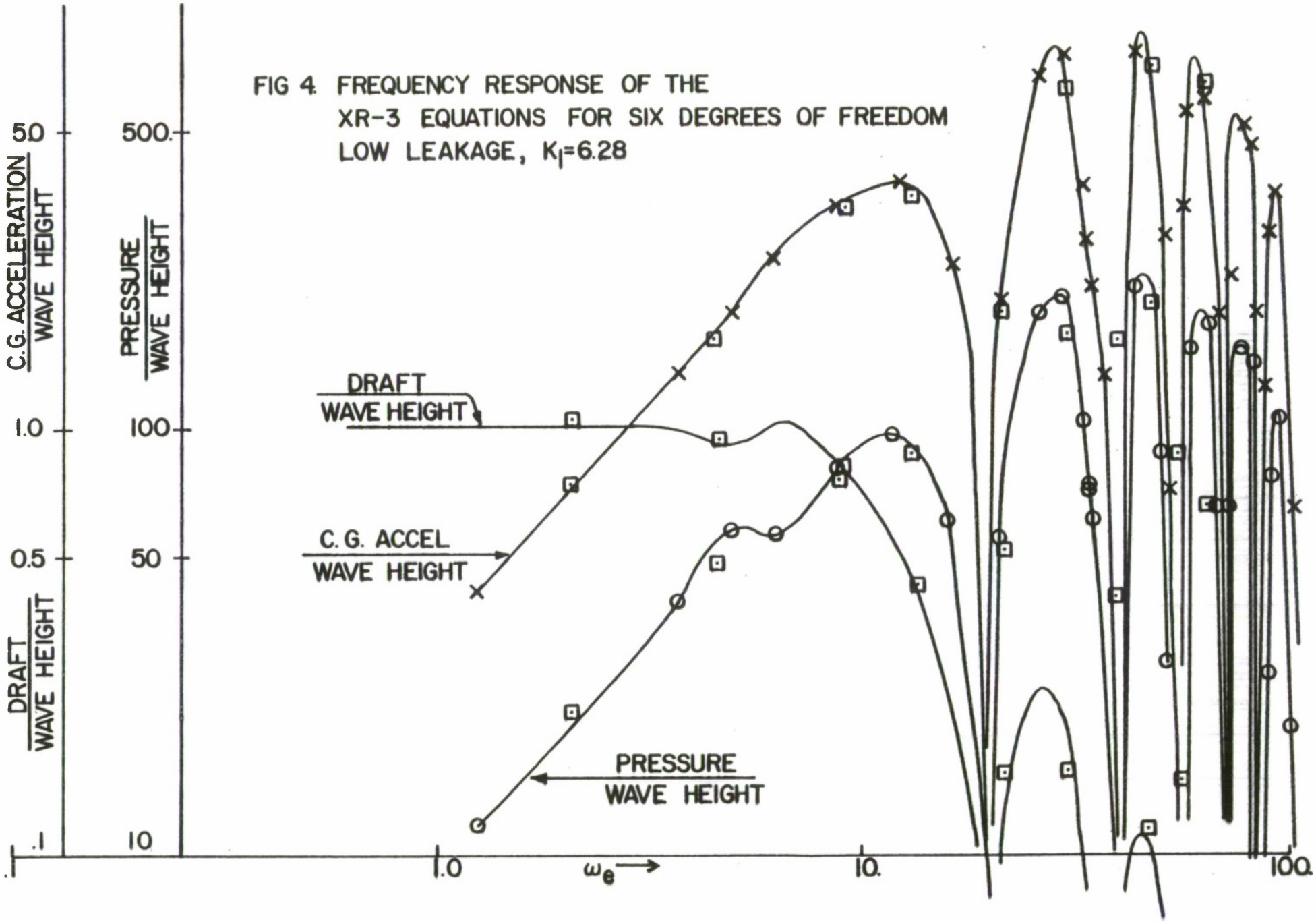
FIG 4. FREQUENCY RESPONSE OF THE
XR-3 EQUATIONS FOR SIX DEGREES OF FREEDOM
LOW LEAKAGE, K_I=6.28
C.G. ACCELERATION / WAVE HEIGHT
PRESSURE / WAVE HEIGHT
DRAFT / WAVE HEIGHT
50
1.0
0.5
.1
500.
100
50
10
DRAFT
WAVE HEIGHT
C. G. ACCEL
WAVE HEIGHT
PRESSURE
WAVE HEIGHT
1.0
ω_e
10.
100.

lobes occuring at approximately 28 rps and above. A comparison of Figure 4 and Figure 3 clearly shows that the simplified XR-3 is in good agreement with the 6 DOF results. For frequencies below 28 rps, the transfer functions can be approximated from the data of Figure 4 using the straight line approximation methods of Bode as follows:

For draft, the frequency response follows very closely the curve of Figure 2 for the sinc function thus

$$\frac{\delta z}{\delta W} \doteq \frac{\sin \alpha\omega}{\alpha\omega} \text{ where } \begin{matrix} \alpha = Lp/4g \\ \omega = \omega e \end{matrix}$$

For pressure, the response is approximated by the transfer function

$$\frac{\delta P_b}{\delta W} \doteq \left(10\frac{\sin \alpha\omega}{\alpha\omega}\right)s$$

For C.G. acceleration, the response is approximated by the transfer function (in g units) as,

$$\frac{\delta \ddot{z}}{\delta W} = \left(0.35\ \frac{\sin \alpha\omega}{\alpha\omega}\right)s$$

These above approximations neglected the small amplitude variations that occur between 3 and 6 radians per second that are most likely introduced by the pitch mode coupling which is not accounted for in the simplified heave-only model of this study.

2. Complex Sea

The complex or irregular sea conditions were approximated by the summation of 10 regular sea components as provided for in the

6 DOF wave subroutine but with sufficient amplitude in each component to introduce an output response without exceeding the total height limitations for maintaining somewhat linear operation. The transfer functions amplitude ratios were computed at these discrete frequencies using the Fast Fourier Transform of Reference 4 and the values plotted in Figure 4 as square points. It can be seen that each of the discrete frequencies produces values that are in reasonable agreement with the regular sea input results. This also has been confirmed by Booth in Reference 4. It should be noted that the complex sea input frequency response computation is a single run technique but limited by the following

1) Discrete frequencies must by necessity be limited in number and so chosen that they are harmonics of the fundamental frequency.
2) Each frequency must introduce a reasonable amplitude to produce a response which in total must be limited to maximum composite wave height.
3) Steady-state speed must exist since encounter frequency must be a multiple of the fundamental frequency to reduce the effect of leakage (a problem with the Discrete Fourier Transform method).

IV. PLENUM AIR FLOW RATE PARAMETER STUDY

During the study conducted on scaling the heave motion equation as reported in Reference 2, it was observed that the air flow influx as well as the leakage rate determined the characteristic response of heave motion for a step weight disturbance. It is of interest, therefore, to study the sensitivity of the craft dynamics to these parameters (air flow influx and leakage rate). The characteristic equation of our simplified linear model is a function of the parameters, so a root locus study permits analysis of their effect on root locations. Alternately the transfer functions may be recomputed and the frequency responses plotted and analyzed. Finally the six degree of freedom simulation program may be exercised to provide both frequency response data and step weight removal transients.

A. Characteristic Equation Root Locus

The linearized equations (see Appendix A) yield the following characteristic equation

$$s^3 + cs^2 + ds + e = 0$$

which in terms of the system parameters becomes,

$$s^3+\gamma\left[nkq+\frac{C_nA_\ell}{\rho_a}\sqrt{\frac{\rho_a}{2P_b(0)}}\right]\left(\frac{P_b(0)}{V_m(0)}\right)s^2+\frac{1}{M}\left(2A_s\rho_\omega g+\gamma A_b^2\,\frac{P_b(0)}{V_b(0)}\right)s$$

$$+2\gamma\rho_\omega g\left(\frac{A_s}{M}\right)\left(nk_q+\frac{C_nA_\ell}{\rho_a}\sqrt{\frac{\rho_a}{2P_b(0)}}\right)\frac{P_b(0)}{V_m(0)} = 0$$

Now let $K_\ell = \left(nk_q + \frac{C_n A_\ell}{\rho_a}\sqrt{\frac{\rho_a}{2P_b(0)}}\right)$ represent the adjustable parameter for the characteristic equation which can be re-organized into the root locus form for a π-type locus,

$$\frac{\left(\frac{\gamma P_b(0)}{V_m(0)}\right)K_\ell\left(s^2 + 2\rho_\omega g A_s/M\right)}{s\left[s^2 + \frac{1}{M}\left(2A_s\rho_\omega g + \gamma A_b^2\frac{P_b(0)}{V_b(0)}\right)\right]} = -1$$

$$-1 = \frac{K_\ell\frac{(1.4)(2140.8)}{264.63}\left[s^2 + \frac{2(1.99)(32.17)(75)(32.17)}{(4)(6050)}\right]}{s\left\{s^2 + \left[\frac{2(75)(32.17)(1.99)(32.17)}{4(6050)} + \frac{(1.4)(200)^2(2140.8)(32.17)}{(262.44)6050}\right]\right\}}$$

Then the equation for the root locus becomes

$$\frac{K_\ell(11.33)(s^2 + 12.83)}{s(s^2 + 2441.8)} = -1$$

To carry out the root locus study numerical values are required for the parameter. We obtained the values used in the following study from the six degree-of-freedom program. These values were also used in the simulation studies for the 10% weight removed transient; thus the root locations can be correlated with the transient response.

An IBM 360/67 subroutine called ROOTLO was used to compute and plot the locus of roots with the results shown in Fig. 5 and in Table I. The values of K_ℓ used in this study covered the range

$$6 < K_\ell < 22$$

with the root locus of Fig. 5 covering the range

$$5 < K_\ell < 50$$

From Fig. 5, and Table I, it can be seen that the roots of the characteristic equation for small values of K_ℓ are one real pole near the origin and a complex pair far removed from the origin. For larger values of K_ℓ, the complex pair become real roots with one root approaching the root near the origin and the other moving towards negative infinity. Note in particular that the real root near the origin moves a relatively short distance during the one decade change of the parameter K_ℓ.

In summary, it is noted that the real root near the origin is not very sensitive to K_ℓ changes in this range of values, whereas the two other roots are quite sensitive to changes in K_ℓ. Since K_ℓ is a function of air flow rate influx (nk_q) and air flow rate leakage $\frac{C_n A_\ell}{\rho_a}\sqrt{\frac{\rho_a}{2\rho_b(0)}}$, it is clear that the oscillatory modes in the ship dynamics depend on these flow rates.

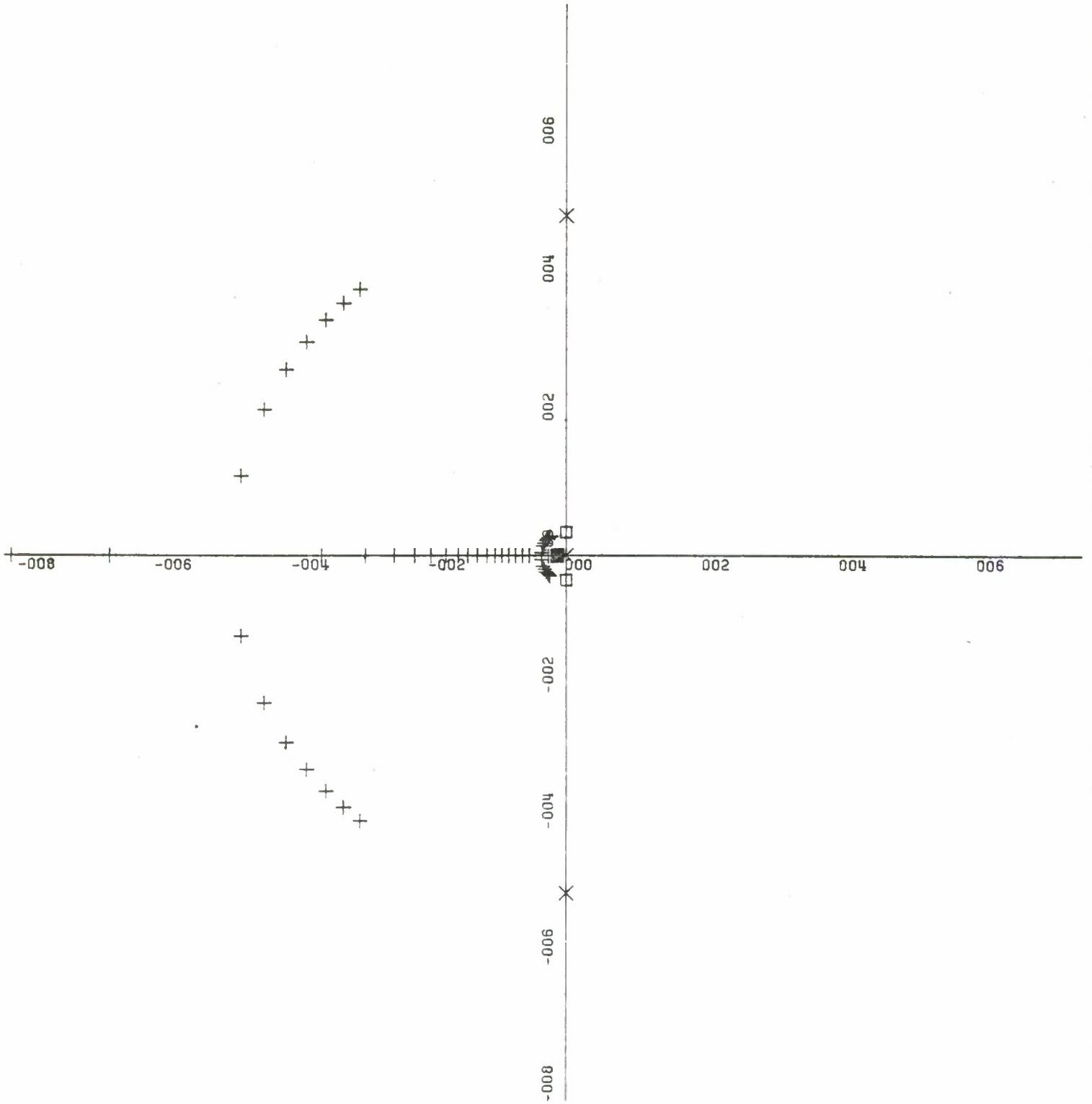

X-SCALE=2.00E+01 UNITS INCH.
Y-SCALE=2.00E+01 UNITS INCH.

BØX 70 GERBA PARAMETER STURY

FIG.5 RØØT LØCUS FØR KL ADJUSTABLE

Table I - Root Location for Various K_ℓ Values for the Characteristic Equation, $(s + \alpha)(s + \beta)(s + \gamma) = 0$

K_ℓ	α	β	γ
5.00	0 + j 49.4	0 - j 49.4	0.0
6.28	-35.1 + j 34.4	-35.1 - j 34.4	-0.38
7.88	-44.0 + j 21.5	-44.0 - j 21.5	-0.47
9.88	-81.3 + j 0.0	-29.2 - j 0.0	-0.60
12.4	-119. + j 0.0	-19.6 - j 0.0	-0.77
15.6	-160. + j 0.0	-14.2 - j 0.0	-0.99
19.5	-208. + j 0.0	-10.4 - j 0.0	-1.31
24.5	-267 + j 0.0	-7.3 - j 0.0	-1.82
28.5	-313 + j 0.0	-5.3 - j 0.0	-2.50
33.2	-366 + j 0.0	-3.31 + j 1.44	-3.31 - j 1.44
38.6	-428 + j 0.0	-2.84 + j 2.23	-2.84 - j 2.23
44.9	-500 + j 0.0	-2.43 + j 2.66	-2.43 - j 2.66

B. Sinusoidal Sea Input Frequency Response

Both the simplified linear model and the six degree of freedom program were used in this part of the study. Figure 6 shows the frequency response of the linear model for high leakage conditions. Comparison of Figure 6 with Figure 3 shows one effect of the leakage conditions: with high leakage the higher frequency motions are substantially attenuated. Note that for encounter frequencies less than 8 rad/sec ($w_e < 8$) the craft's vertical motion is not at all sensitive to air flow and leakage rates, but for $w_e > 10$ the CG acceleration, pressure and heave displacement are all substantially reduced for the case of increased leakage.

Figure 7 shows the frequency response of the six degree of freedom model for high leakage. Comparison of Figure 7 with Figure 4 shows the same general characteristics observed with the linear model: the response to frequencies above 10 radians per second are significantly attenuated when the air flow is increased. Frequencies below 10 radians per second produce somewhat larger responses when the airflow is increased. We believe this is a result of pitch motions, as discussed in the following paragraphs.

C. Comparison of the Linear Model with the 6DOF Model Using the Frequency Response Plots

One purpose of this study is to assess the value of the linear model as a tool for studying the CAB and predicting the salient features in its behavior. Alternately, comparison of results

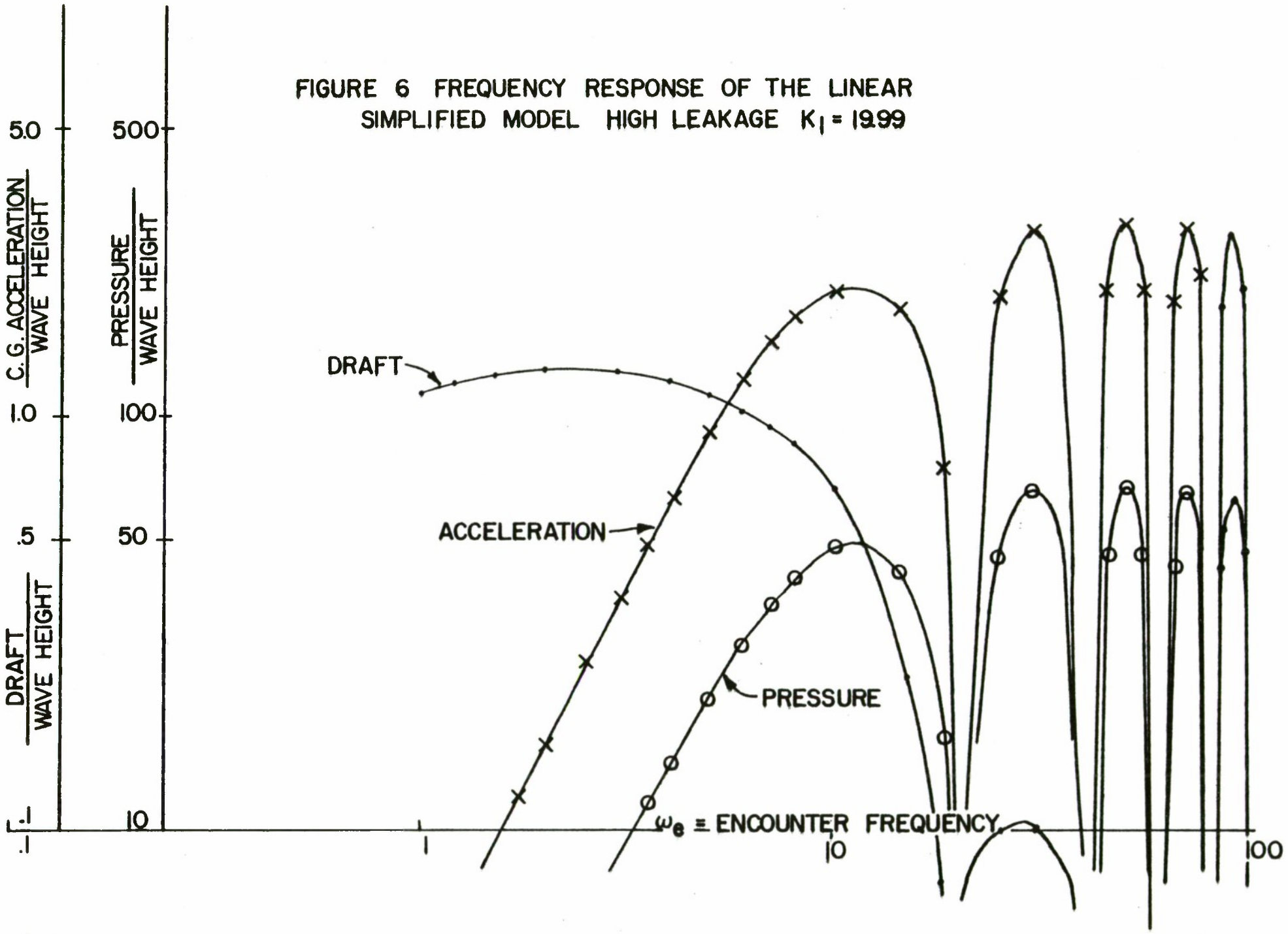
FIGURE 6 FREQUENCY RESPONSE OF THE LINEAR SIMPLIFIED MODEL HIGH LEAKAGE $K_1 = 19.99$
C.G. ACCELERATION / WAVE HEIGHT
PRESSURE / WAVE HEIGHT
DRAFT / WAVE HEIGHT
5.0
1.0
.5
.1
500
100
50
10
DRAFT
ACCELERATION
PRESSURE
$\omega_e \equiv$ ENCOUNTER FREQUENCY
1
10
100

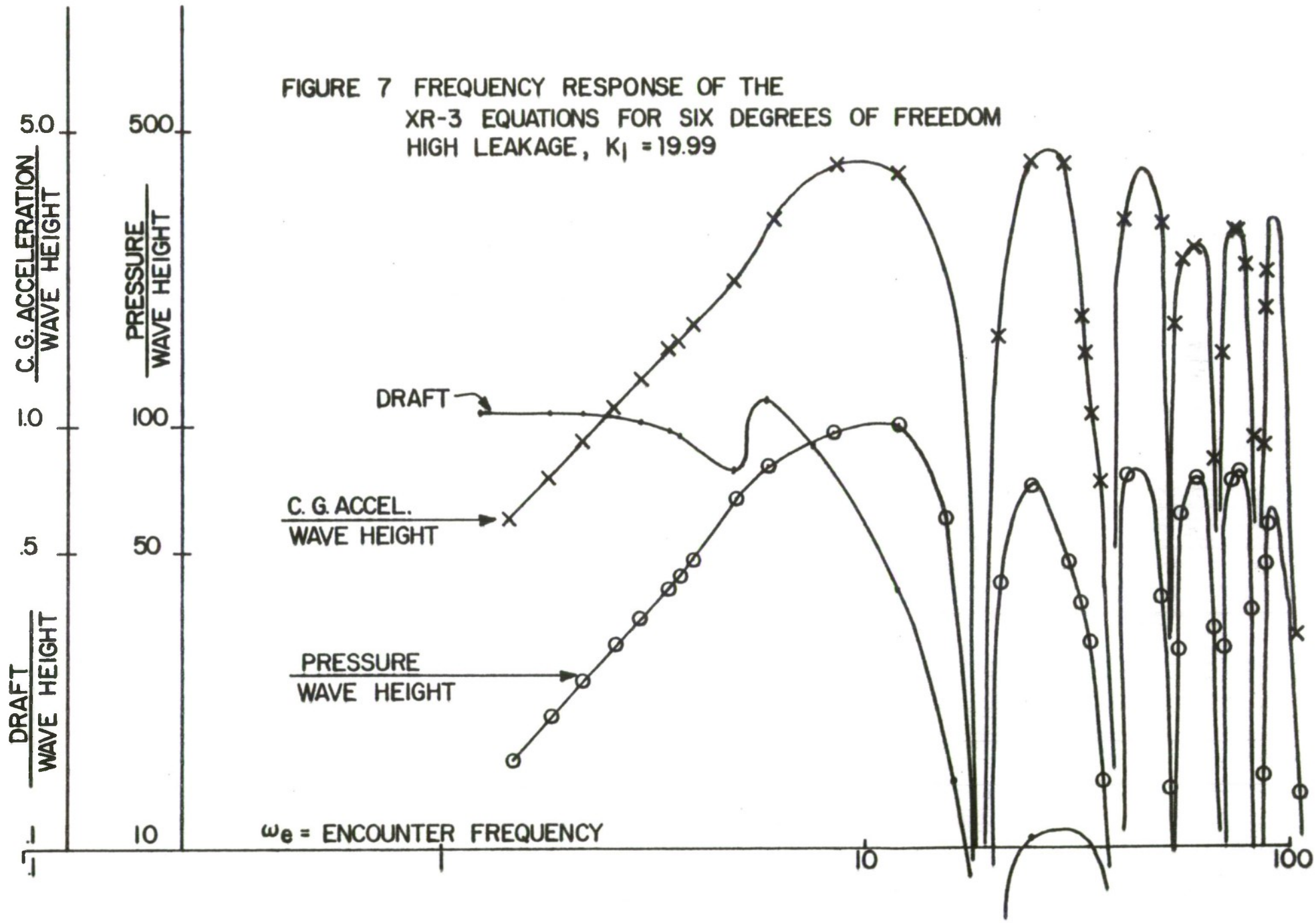
FIGURE 7 FREQUENCY RESPONSE OF THE
XR-3 EQUATIONS FOR SIX DEGREES OF FREEDOM
HIGH LEAKAGE, K_1 = 19.99
C.G. ACCELERATION / WAVE HEIGHT
PRESSURE / WAVE HEIGHT
DRAFT / WAVE HEIGHT
5.0
1.0
.5
.1
500
100
50
10
DRAFT
C. G. ACCEL. / WAVE HEIGHT
PRESSURE / WAVE HEIGHT
ω_e = ENCOUNTER FREQUENCY
1
10
100

between the linear model and the 6 DOF model (or experimental data when available) should lead to an understanding of phenomena which are peculiar to the CAB. On Figure 8 the c.g. acceleration curve of the simplified model and that of the six degree of freedom model are plotted, using the data for $K_{\ell} = 19.99$.

At low frequencies the six degree of freedom curve indicates much larger accelerations than the linear model. At high frequencies both models are in good agreement (the null frequencies are not exactly the same, indicating that the effective plenum length is not precisely the geometric length). In the low frequency range we note that the six degree of freedom frequency response has a slight "dip" or anti-resonance for $4 < w < 6$, while the linear model does not. This frequency range includes the natural frequency of the pitch mode, which is included in the six degree of freedom model, but not in the linear model. We know that the sinusoidal sea will excite the pitch mode, so we are led to a plausible explanation for the discrepancy between the results at low frequencies. It is simply this - with sinusoidal excitation in the range of frequencies about pitch resonance, the pitching motion will have large enough amplitude to increase the air leakage. With the bubble volume thus reduced the incompressible wave will cause higher air pressures and higher heave acceleration. At high frequencies, above the natural frequency in pitch, leakage is not increased and the linear model is a reasonably good one.

FIGURE 8 COMPARISON OF FREQUENCY RESPONSES IN ACCELERATION
K_1 = 19.99

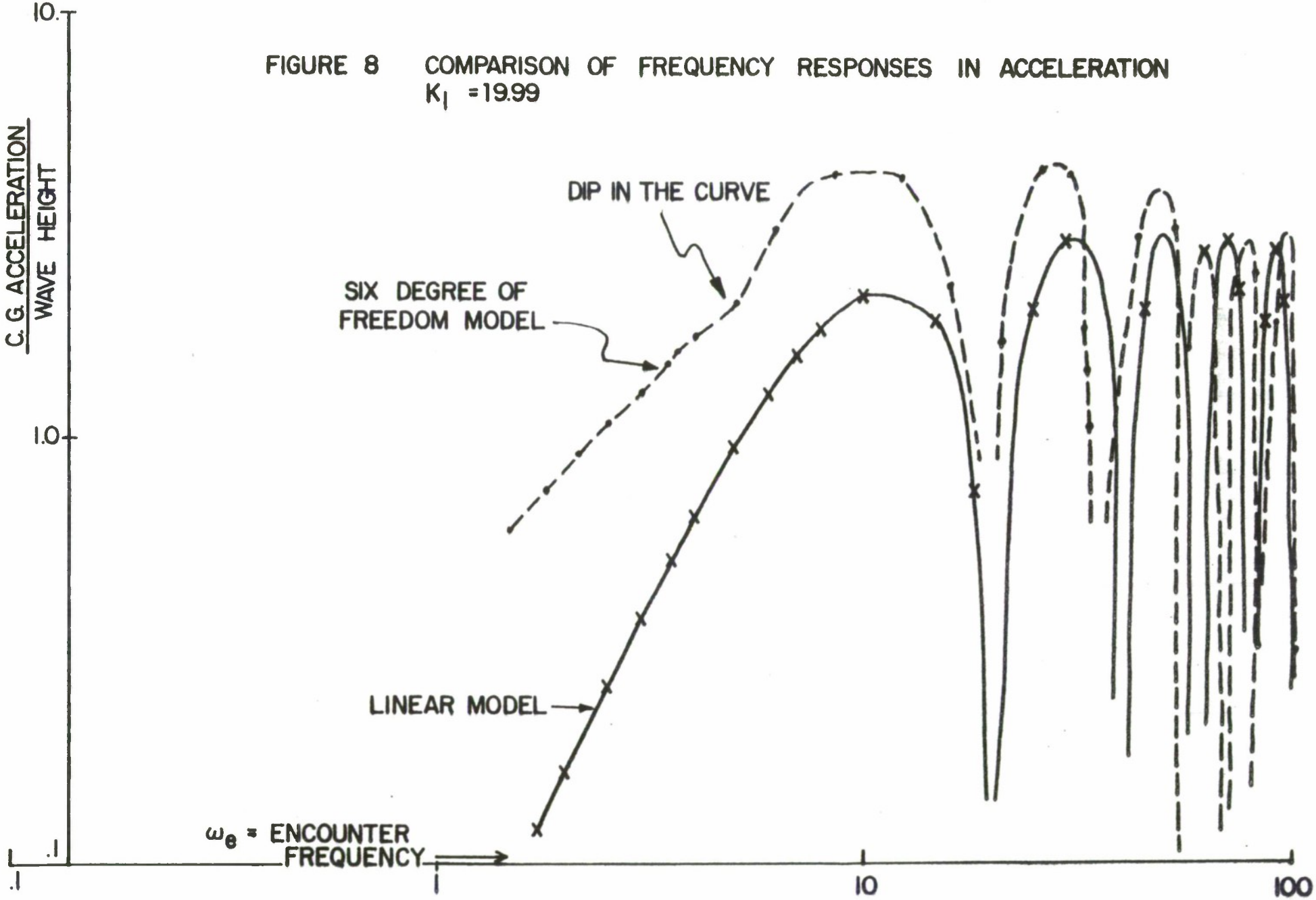

We also note that at low frequencies the slopes of the curves on Figure 8 are not the same. This can be attributed to variation in the leakage as a function of frequency.

D. Simulation of Transient Response due to Step Removal of Weight

The removal of weight by a step change is equivalent to a negative step change in acceleration. The transfer function for draft pressure and C.G. acceleration for the step weight removal can readily be found by Mason's Gain Rule using the signal flow graph given in Figure B-1 of Appendix B. The transfer function for draft becomes

$$\frac{\delta z}{\delta a} = \frac{s + \left(\frac{\gamma P_b(0)}{V_m(0)}\right) K_\ell}{D(s)}$$

where δz = incremental draft

δa = incremental weight (acceleration)

$$D(s) = s^3 + \left(\frac{\delta P_b(0)}{V_m(0)}\right) K_\ell \; s + \left(\frac{2A_s \rho_\omega g}{M} + \frac{\gamma P_b(0) A_b^2}{M V_b(0)}\right) s + \left(\frac{\gamma P_b(0)}{V_m(0)}\right)\left(\frac{2A_s \rho_\omega g}{M}\right) K_\ell$$

For pressure,

$$\frac{\delta P_b}{\delta a} = \frac{\left(\frac{\delta P_b(0) A_b}{V_b(0)}\right) s}{D(s)}$$

And for C.G. acceleration where $\ddot{\delta z}$ = incremental acceleration:

$$\frac{\ddot{\delta z}}{\delta a} = \frac{s^2 \left(s + \frac{\gamma P_b(0)}{V_m(0)} k_\ell\right)}{D(s)}$$

These transfer functions are for the linear simplified model, for which we have the root locations (factors of D(s)) in Table I with corresponding root locus on Figure 5. The transfer functions also indicate the presence of zeros, some of which are functions of the leakage, K_ℓ.

In studying the weight removal behavior, simulation was done with the six degree of freedom model, and the results are conveniently analyzed if we consider Table I and Figure 5, remembering also that the simulation model contains additional pitch mode effects. Figure 9 is a set of 16 curves covering the range of air flow conditions from $6.1 < K_\ell < 21.99$, but recorded for less than a 1.0 second duration after removal of the weight. This expands the scale of the initial transient, and permits correlation with Table I and Figure 5. Figure 10 is a set of 12 curves covering the same air flow conditions, but recorded for a 5.0 second duration, which permits us to recognize the effect of pitch coupling.

Consider first the c.g. acceleration curves of Figure 9 (A1, A2, A3, A4), noting from Table I that for each of these figures the K_ℓ value results in a small negative real root, but gives complex roots only for Figure 9-A1, where $\zeta \approx 0.7$ and $w_n > 50$. Each of these figures shows a very fast initial transient, there is no apparent contribution from the small real root (Table I, column γ), which may have been cancelled by the zero of the

transfer function. Comparison of these four initial transients shows very good agreement with the root values of Table I for low leakage (Figure 9-A1). The initial transient shows a small overshoot, about as expected for roots with $\zeta \approx 0.7$. As K_ℓ increases (Figures 9-A2, A3, A4) the transient does not overshoot (roots are all real) and the settling time increases which agrees with the change in root values in column β of Table I.

Continuing the analysis of Figure 9, the z-displacement and plenum pressure curves show an approximately exponential variation which is very slow but speeds up with increased leakage. This agrees qualitatively with the increase in value of the smallest real root (column γ, Table I). The pitch angle variation of Figure 9 shows a substantial variation, but the short duration does not supply enough information for further analysis. We therefore proceed to Figure 10.

Let us start the discussion of Figure 10 with the pitch angle response curves, 10-D1, D2, D3. On all of these curves it is clear that the pitch transient is an exponentially damped sinusoid plus another exponential response. The frequency of this pitch mode is approximately 5 rad/sec, and increases slightly with increased K_ℓ. We cannot correlate this with the linear model, for it does not include the pitch mode. The second exponential component, however, appears to be due to the small real root of the heave mode (Table I, column γ) and its time constant seems to decrease with increasing K_ℓ, which agrees with the root variation in Table I.

From Figure 10 it is also clear that the pitch mode couples into c.g. acceleration, z-displacement, and plenum pressure. This coupling increases with K_ℓ. The small real root is also seen to contribute -- it is obviously dominant in the z-displacement and pressure curves, and can be recognized in the c.g. acceleration curve of Figure 10-A3.

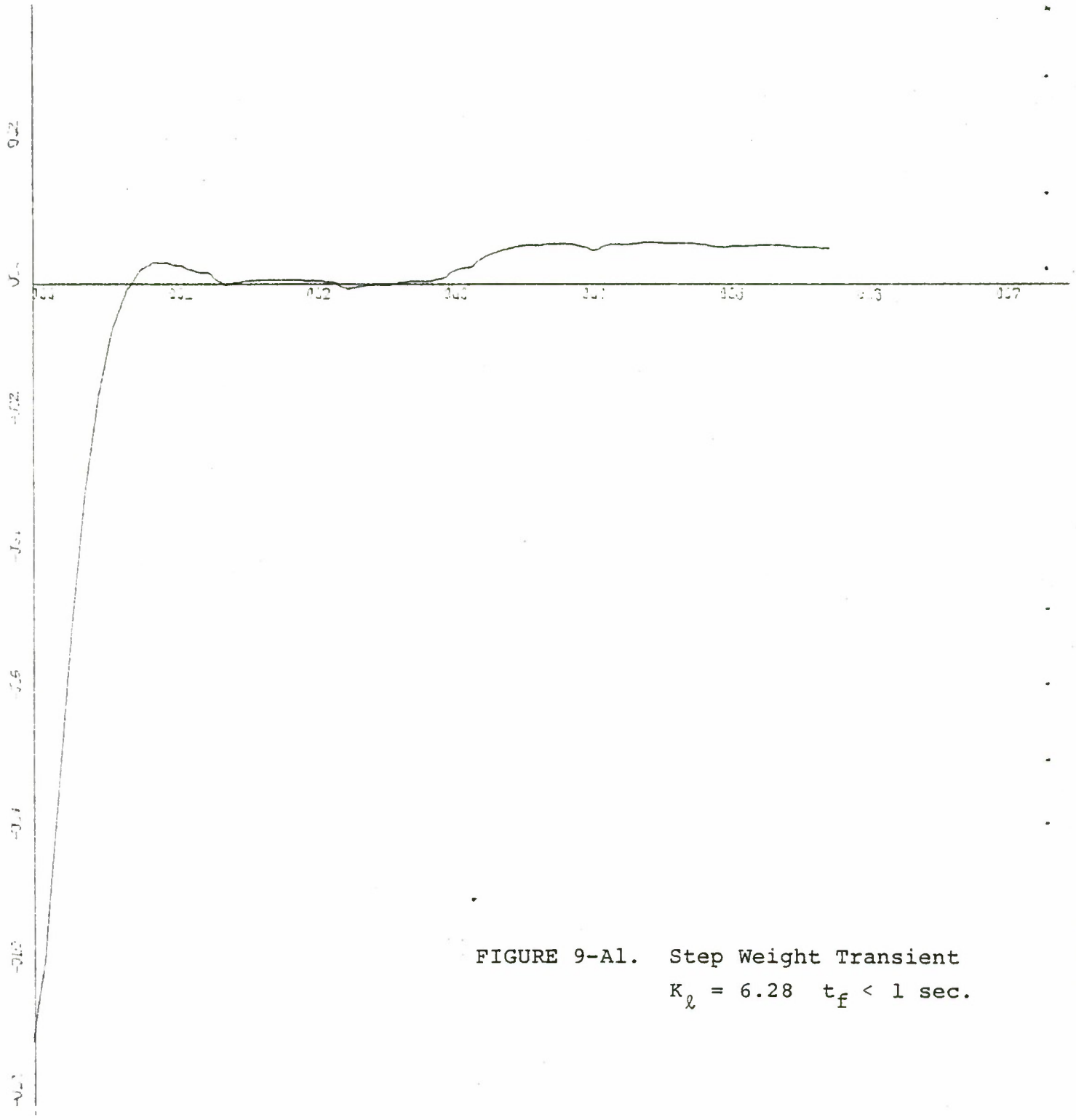

FIGURE 9-A1. Step Weight Transient
$K_\ell = 6.28$ $t_f < 1$ sec.

X-SCALE=1.00E-01 UNITS INCH.
Y-SCALE=2.00E-02 UNITS INCH.
BOX 70 30 KNOT RUN WRT
PLOT IS C.G. ACCELERATION VERSUS TIME

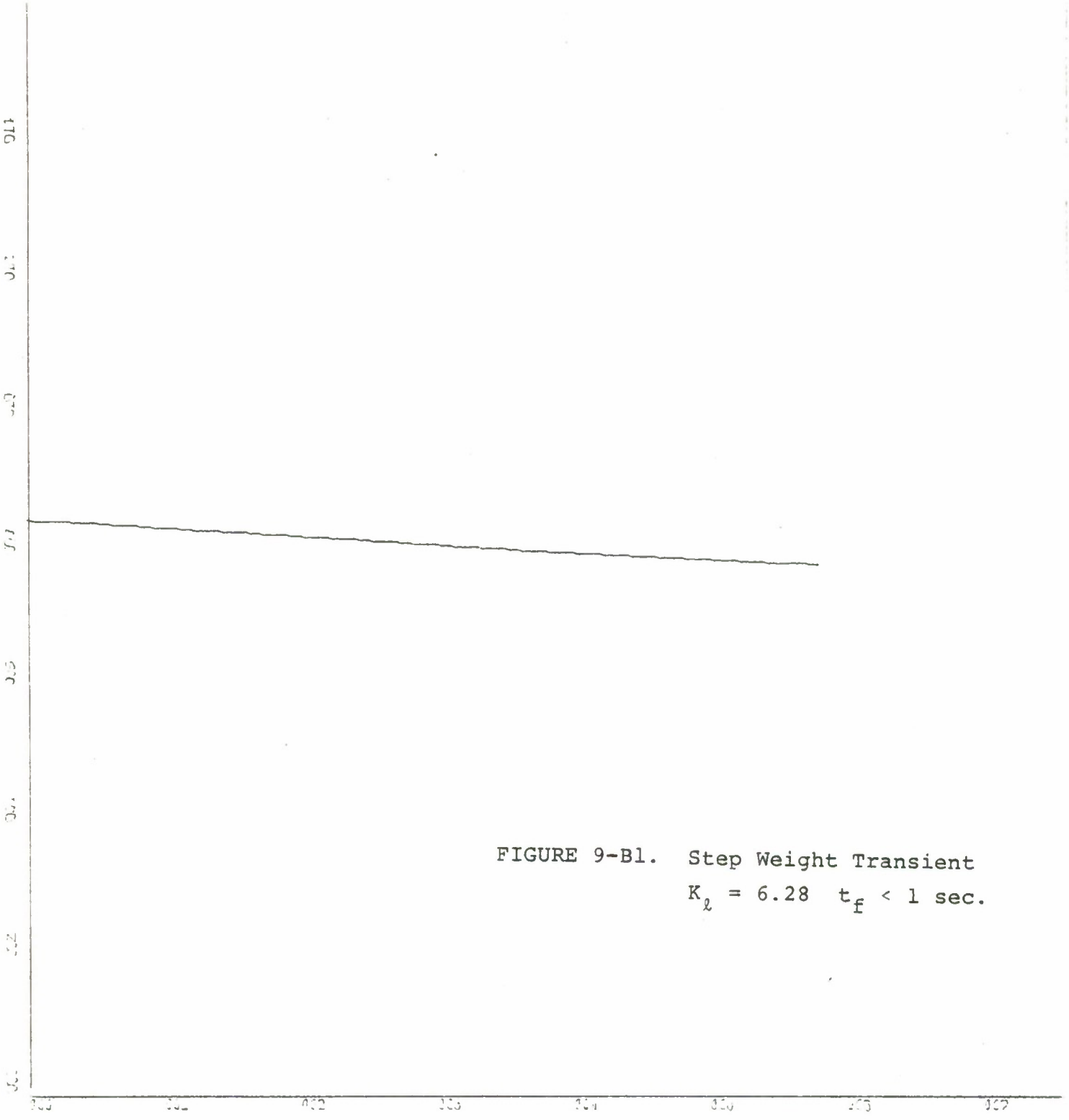

FIGURE 9-B1. Step Weight Transient
$K_{\ell} = 6.28 \quad t_f < 1$ sec.

X-SCALE=1.00E-01 UNITS INCH.
Y-SCALE=2.00E+00 UNITS INCH.
BOX 70 30 KNOT RUN WR1
PLOT IS Z DISPLACEMENT VERSUS TIME

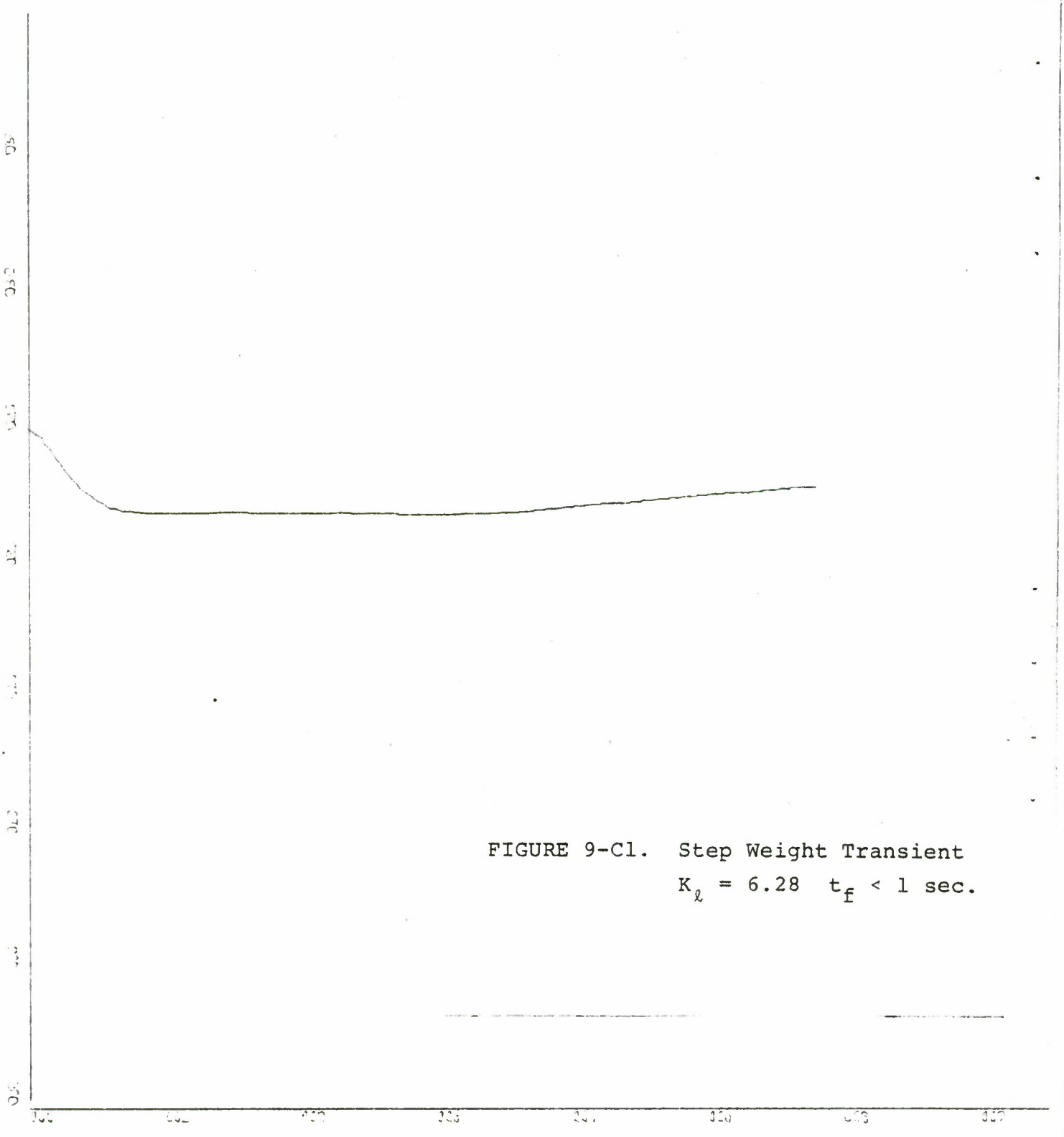

FIGURE 9-C1. Step Weight Transient
$K_\ell = 6.28$ $t_f < 1$ sec.

X-SCALE=1.00E-01 UNITS INCH.
Y-SCALE=5.00E+00 UNITS INCH.
BOX 70 30 KNOT RUN WRT
PLOT IS PLENUM PRESSURE VERSUS TIME

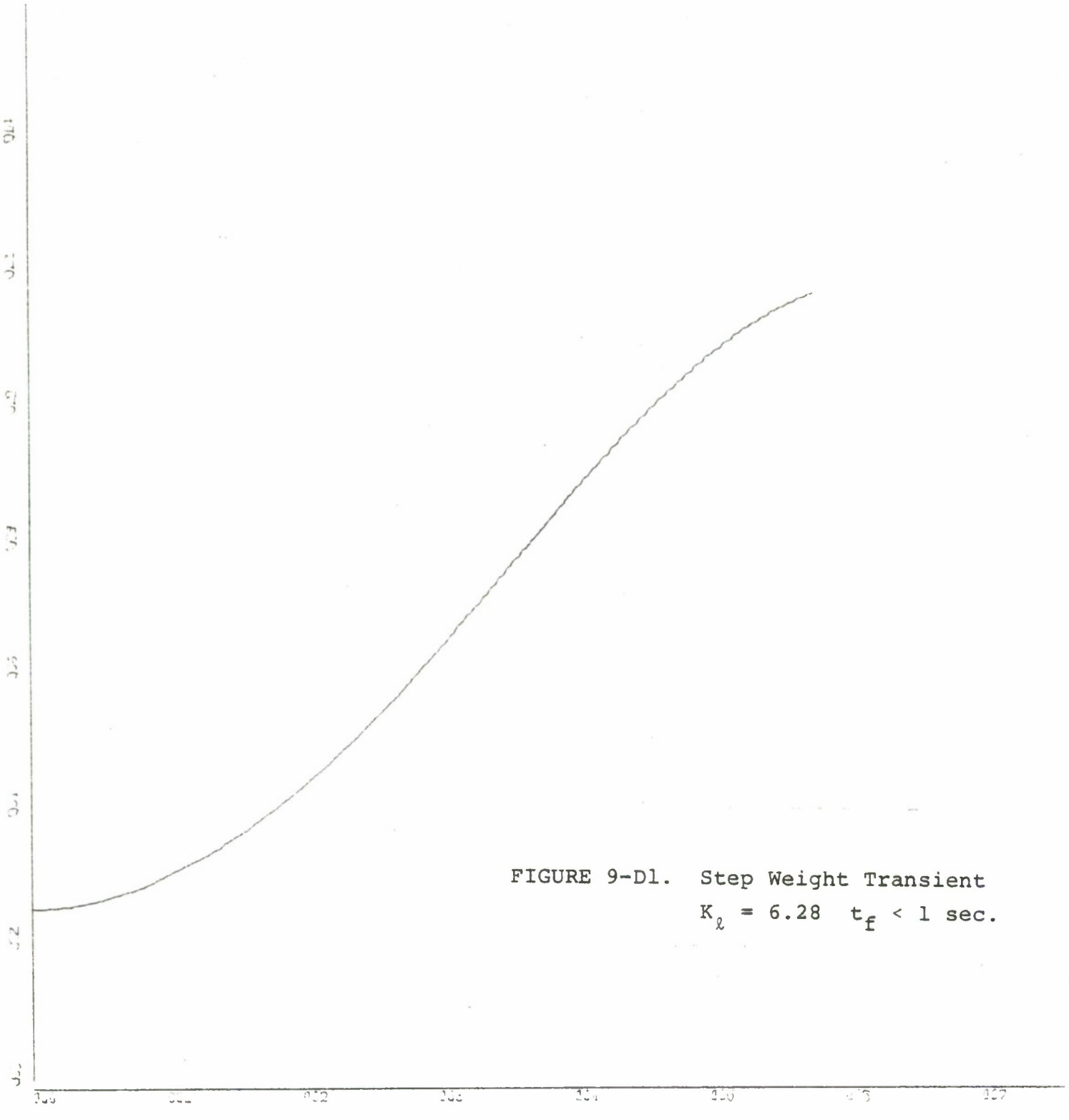

FIGURE 9-D1. Step Weight Transient
$K_\ell = 6.28$ $t_f < 1$ sec.

X-SCALE=1.00E-01 UNITS INCH.
Y-SCALE=2.00E-01 UNITS INCH.
BOX 70 30 KNOT RUN WRL
PLOT IS PITCH ANGLE VERSUS TIME

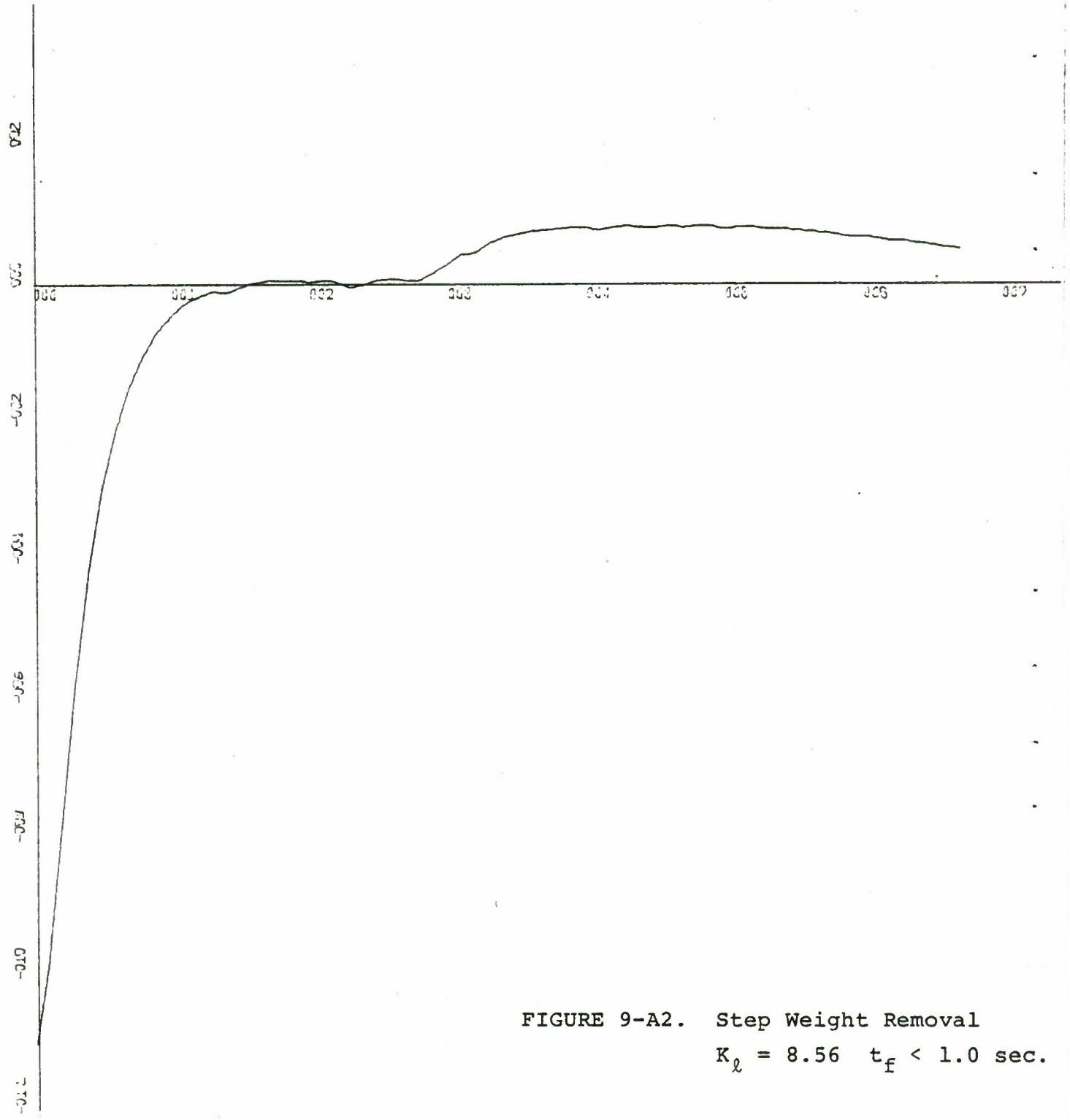

FIGURE 9-A2. Step Weight Removal
$K_\ell = 8.56 \quad t_f < 1.0$ sec.

X-SCALE=1.00E-01 UNITS INCH.
Y-SCALE=2.00E-02 UNITS INCH.
BOX 70 30 KNOT RUN WR2
PLOT IS C.G. ACCELERATION VERSUS TIME

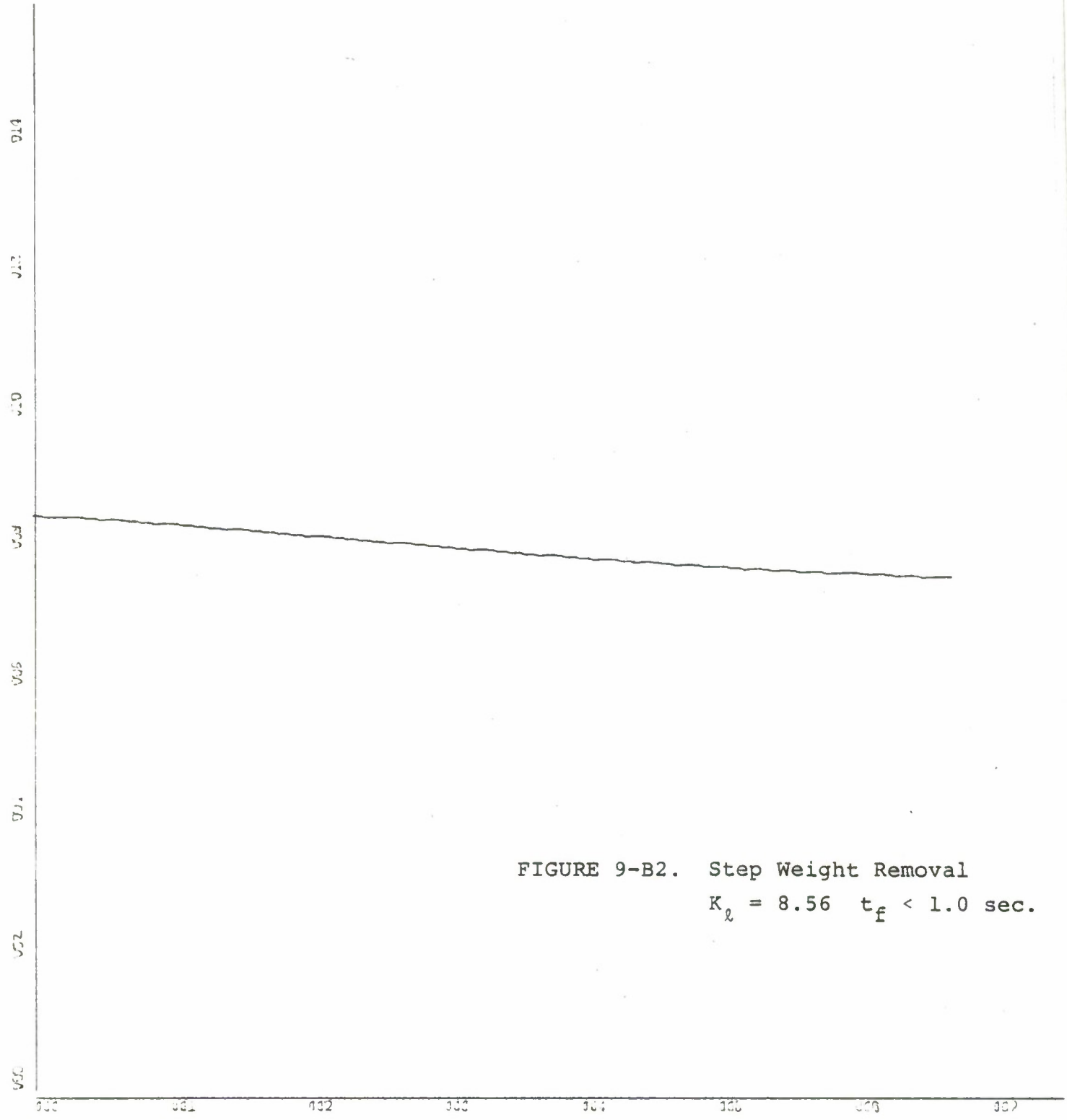

FIGURE 9-B2. Step Weight Removal
$K_\ell = 8.56 \quad t_f < 1.0$ sec.

X-SCALE=1.00E-01 UNITS INCH.
Y-SCALE=2.00E+00 UNITS INCH.
BOX 70 30 KNOT RUN WR2
PLOT IS Z DISPLACEMENT VERSUS TIME

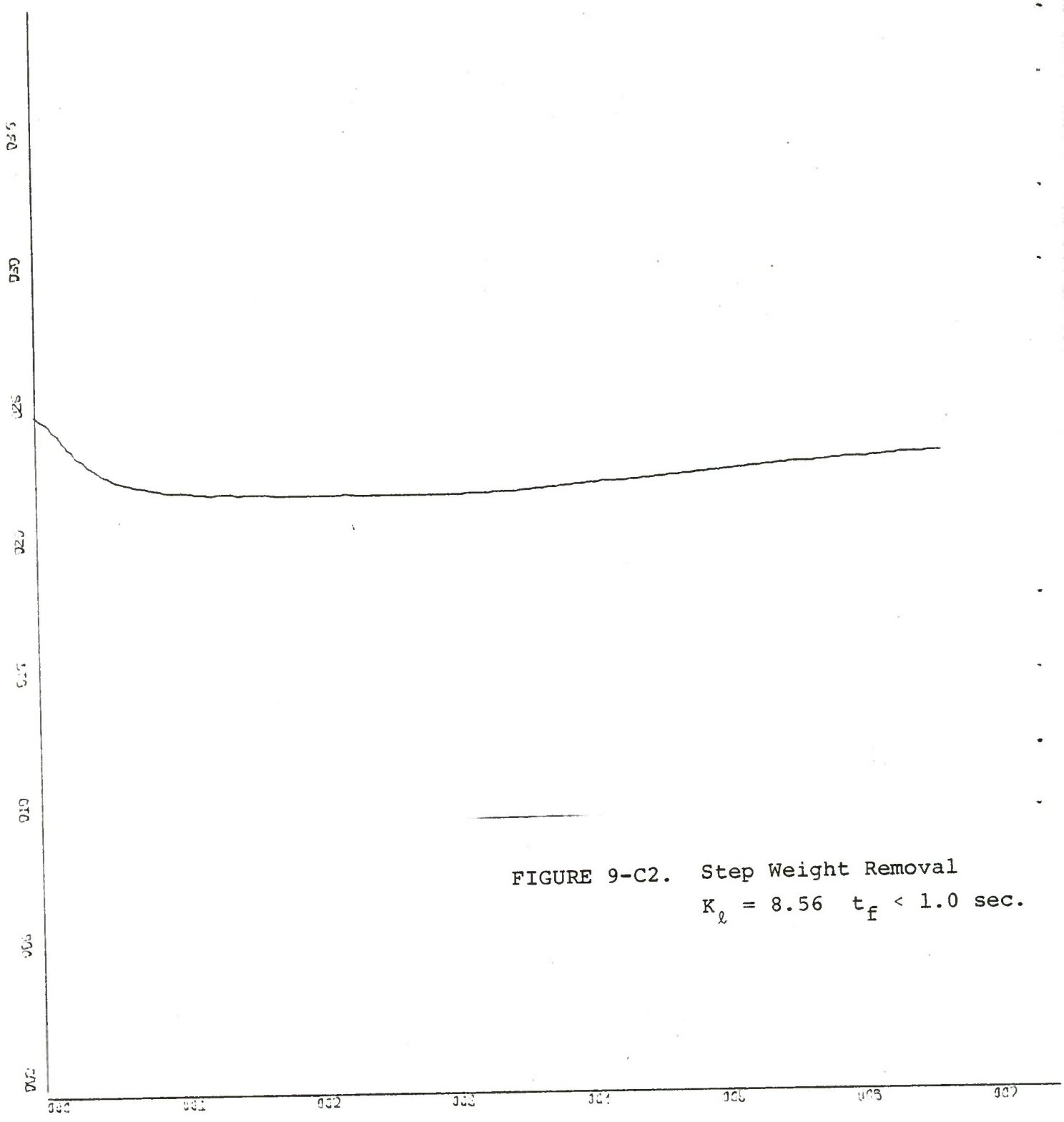

FIGURE 9-C2. Step Weight Removal
$K_\ell = 8.56 \quad t_f < 1.0$ sec.

X-SCALE=1.00E-01 UNITS INCH.
Y-SCALE=5.00E+00 UNITS INCH.
BOX 70 30 KNOT RUN WR2
PLOT IS PLENUM PRESSURE VERSUS TIME

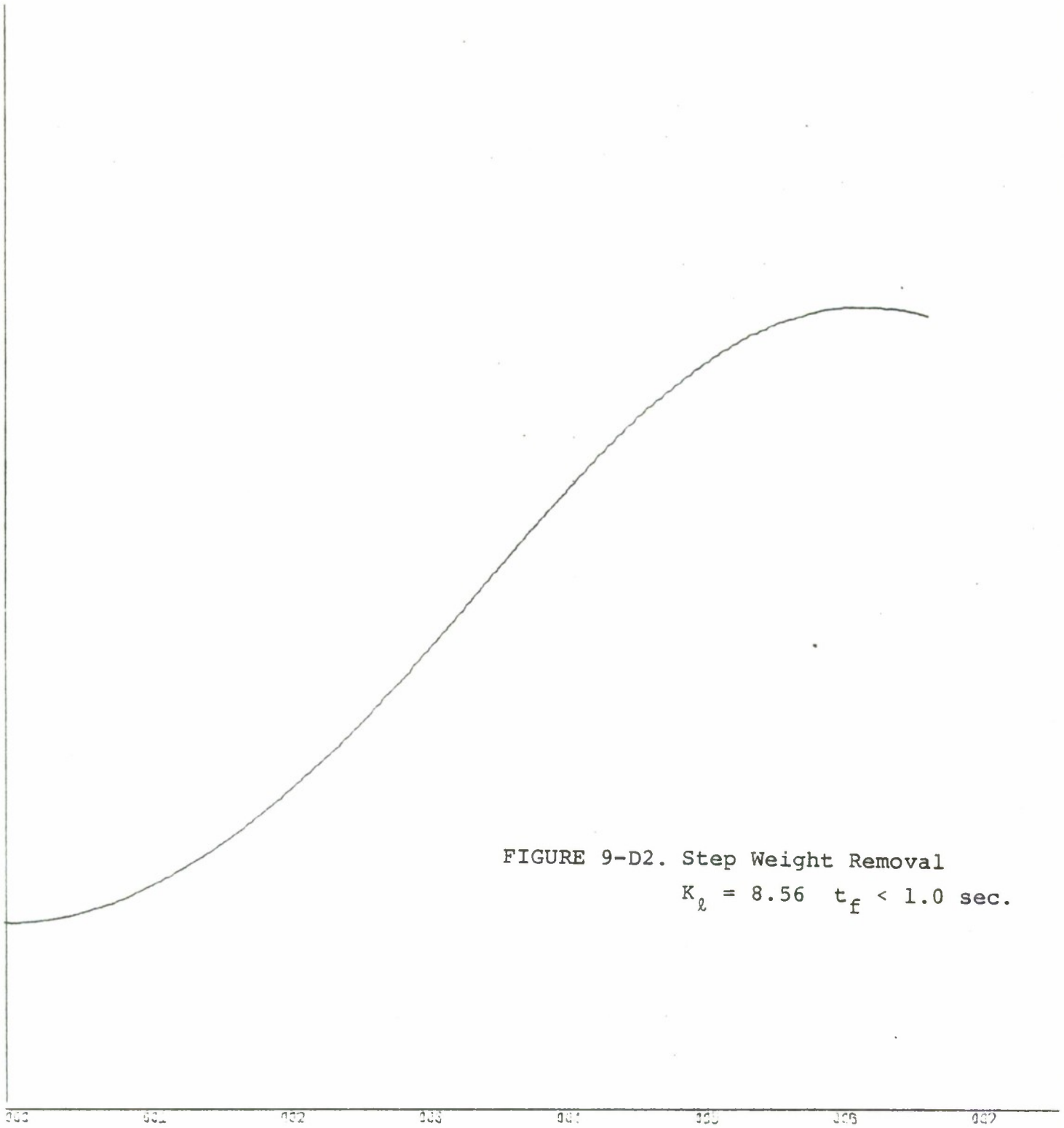

FIGURE 9-D2. Step Weight Removal
$K_\ell = 8.56 \quad t_f < 1.0$ sec.

X-SCALE=1.00E-01 UNITS INCH.
Y-SCALE=2.00E-01 UNITS INCH.
BOX 70 30 KNOT RUN WR2
PLOT IS PITCH ANGLE VERSUS TIME

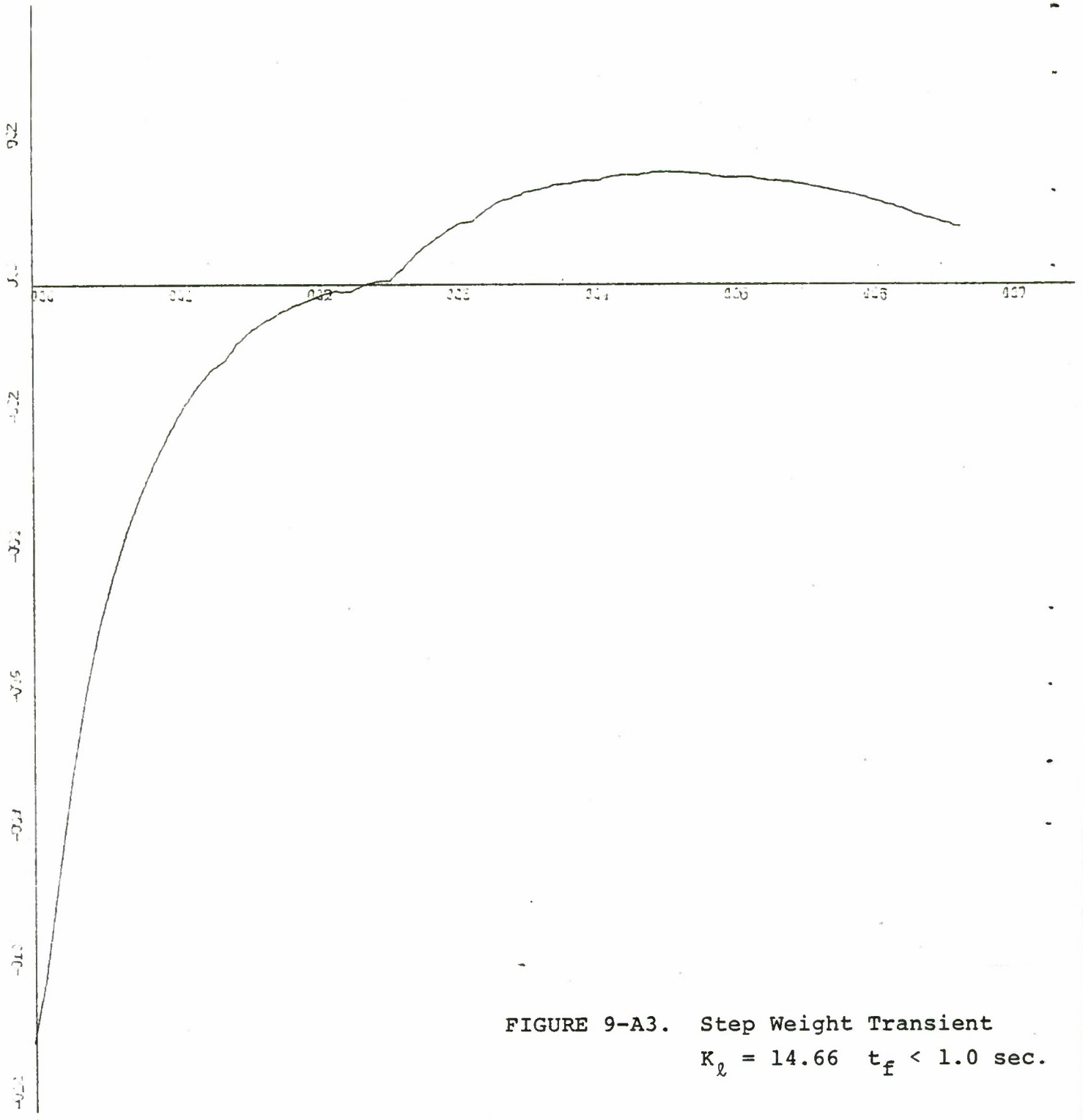

FIGURE 9-A3. Step Weight Transient
$K_\ell = 14.66 \quad t_f < 1.0$ sec.

K-SCALE=1.00E-01 UNITS INCH.
Y-SCALE=2.00E-02 UNITS INCH.
BOX 70 30 KNOT RUN WR4
PLOT IS C.G. ACCELERATION VERSUS TIME

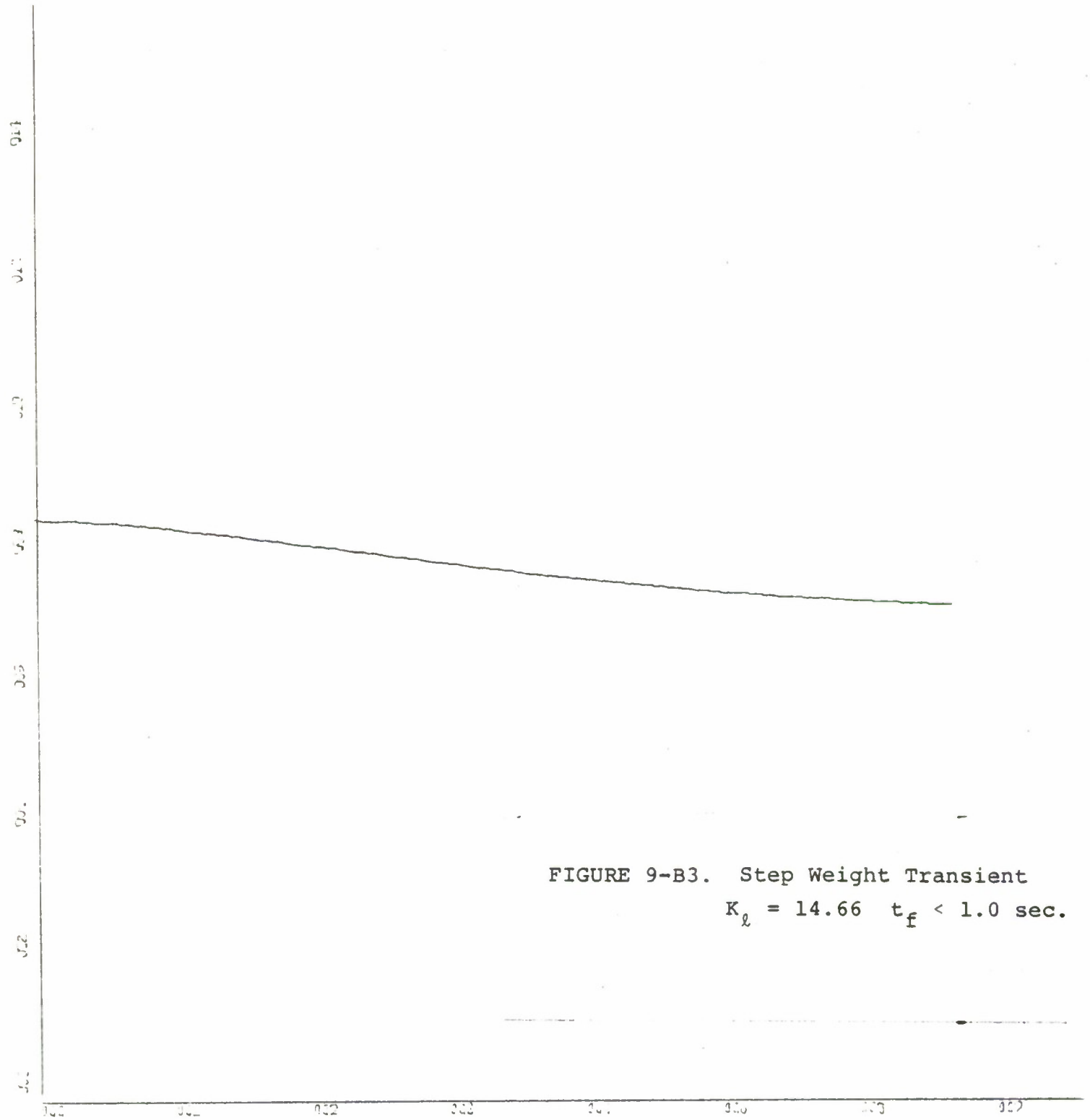

FIGURE 9-B3. Step Weight Transient
$K_\ell = 14.66$ $t_f < 1.0$ sec.

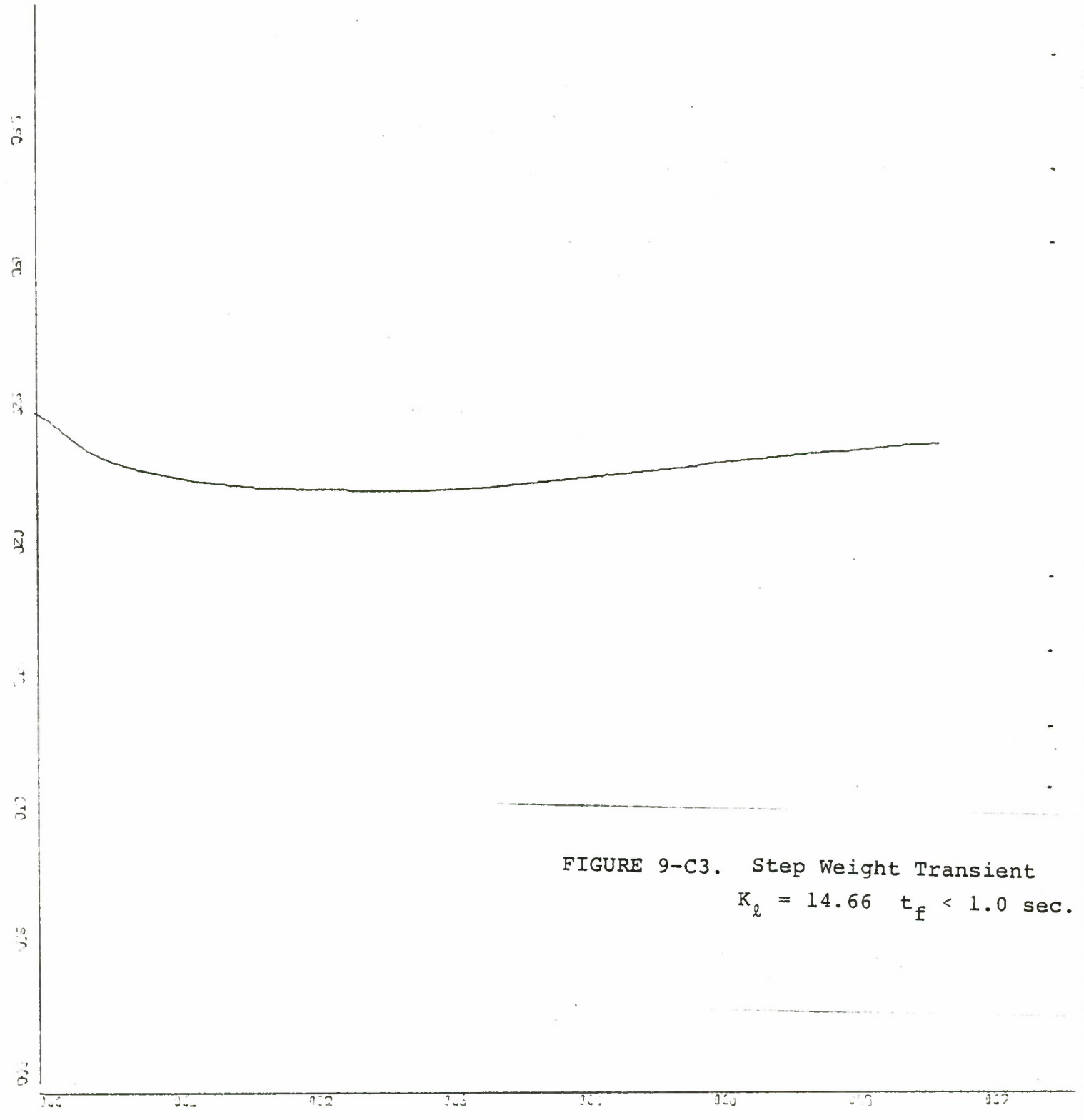

FIGURE 9-C3. Step Weight Transient
$K_\ell = 14.66$ $t_f < 1.0$ sec.

X-SCALE=1.000E-01 UNITS INCH
Y-SCALE=5.000E+00 UNITS INCH
BOX 70 30 KNOT RUN WR4
PLOT IS PLENUM PRESSURE VERSUS TIME

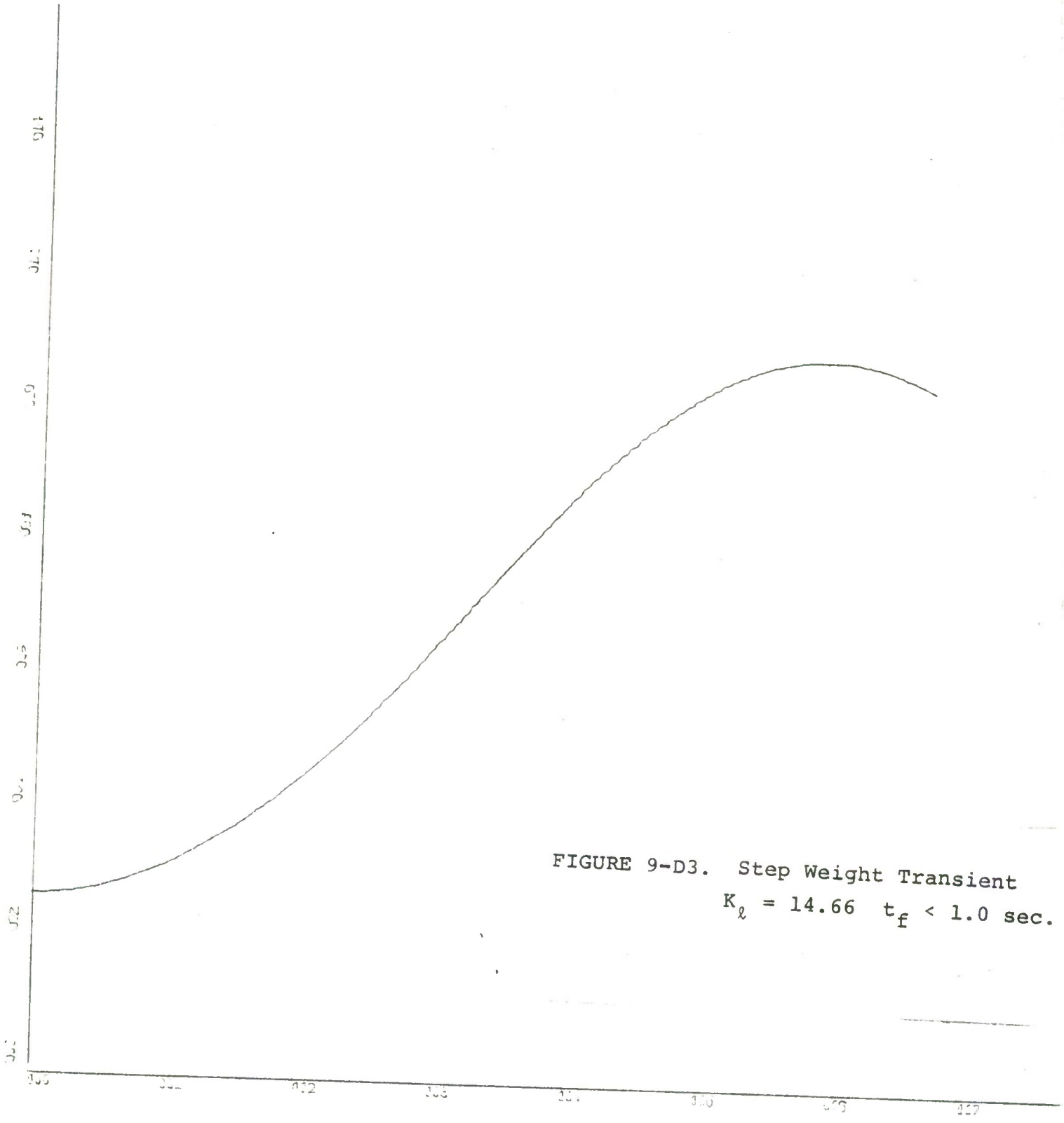

FIGURE 9-D3. Step Weight Transient
$K_\ell = 14.66$ $t_f < 1.0$ sec.

X-SCALE=1.00E-01 UNITS INCH
Y-SCALE=2.00E-01 UNITS INCH
BOX 70 30 KNOT RUN WR4
PLOT IS PITCH ANGLE VERSUS TIME

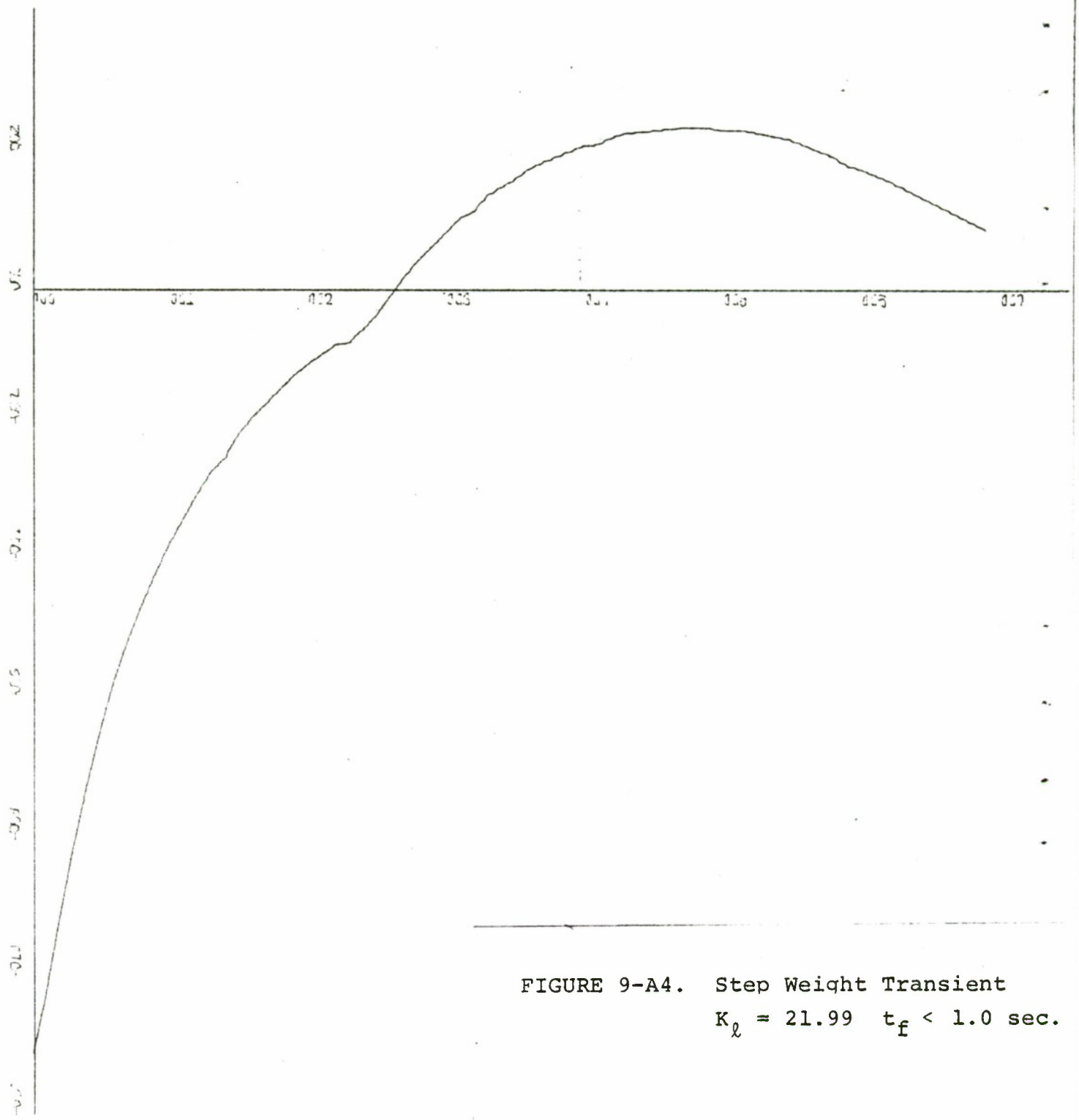

FIGURE 9-A4. Step Weight Transient
K_ℓ = 21.99 t_f < 1.0 sec.

X-SCALE=1.00E-01 UNITS INCH
Y-SCALE=2.00E-02 UNITS INCH
BOX 70 30 KNOT RUN WR6
PLOT IS C.G. ACCELERATION VERSUS TIME

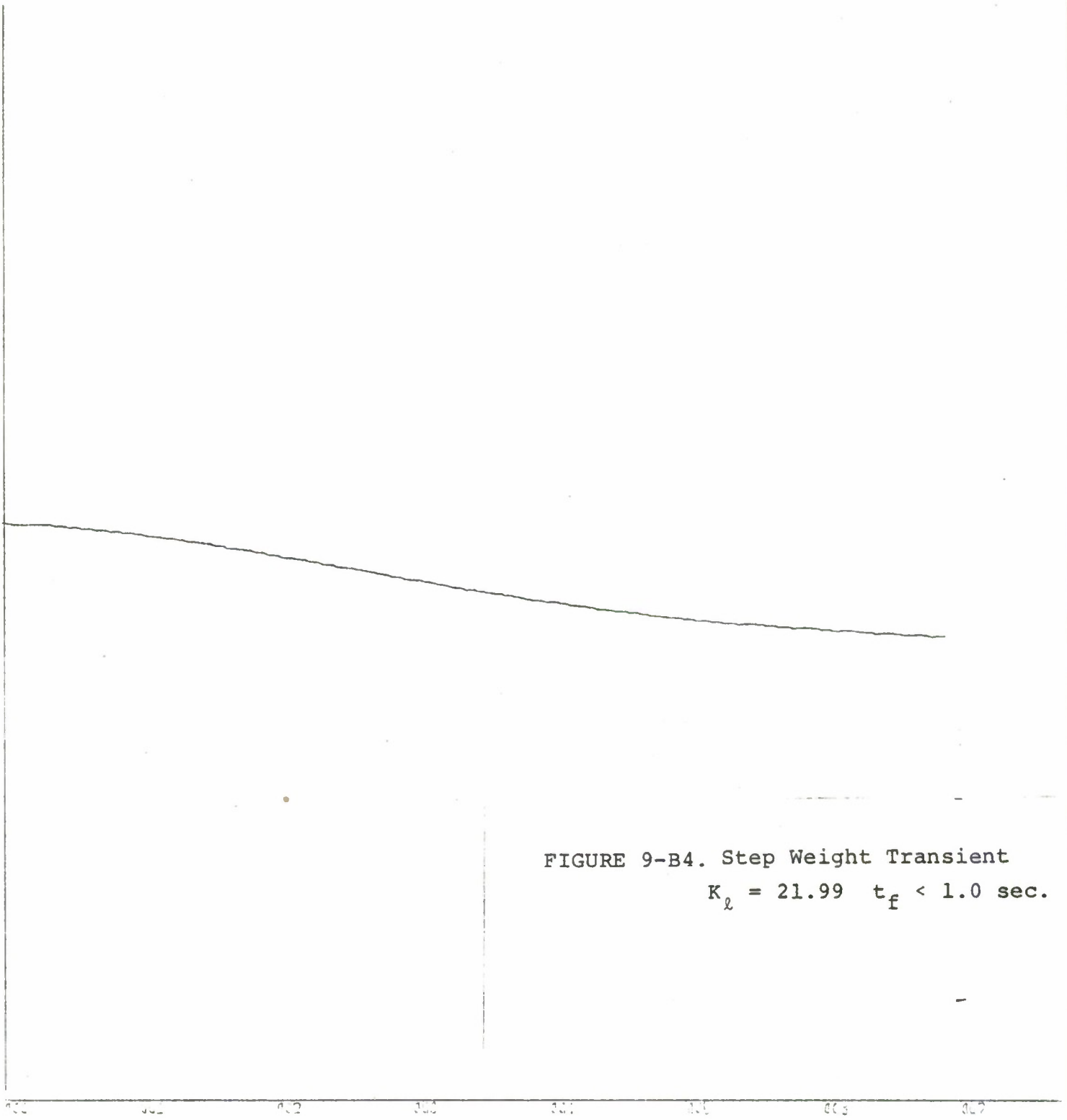

FIGURE 9-B4. Step Weight Transient
$K_\ell = 21.99 \quad t_f < 1.0$ sec.

X-SCALE=1.00E-01 UNITS INCH
Y-SCALE=2.00E+00 UNITS INCH
BOX 70 30 KNOT RUN WR6
PLOT IS Z DISPLACEMENT VERSUS TIME

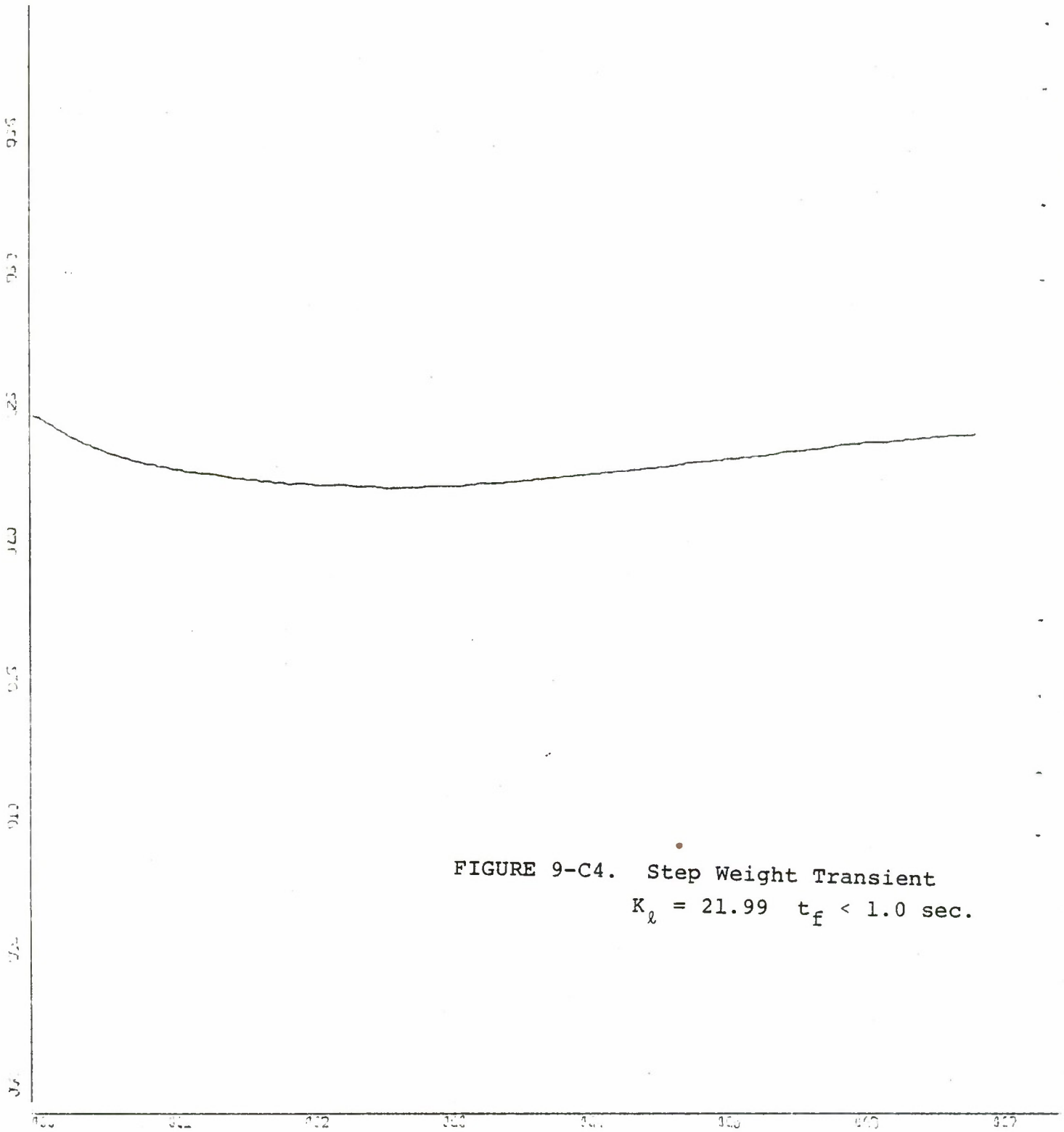

FIGURE 9-C4. Step Weight Transient
$K_\ell = 21.99 \quad t_f < 1.0$ sec.

X-SCALE=1.00E-01 UNITS INCH
Y-SCALE=5.00E+00 UNITS INCH
BOX 70 30 KNOT RUN WR6
PLOT IS PLENUM PRESSURE VERSUS TIME

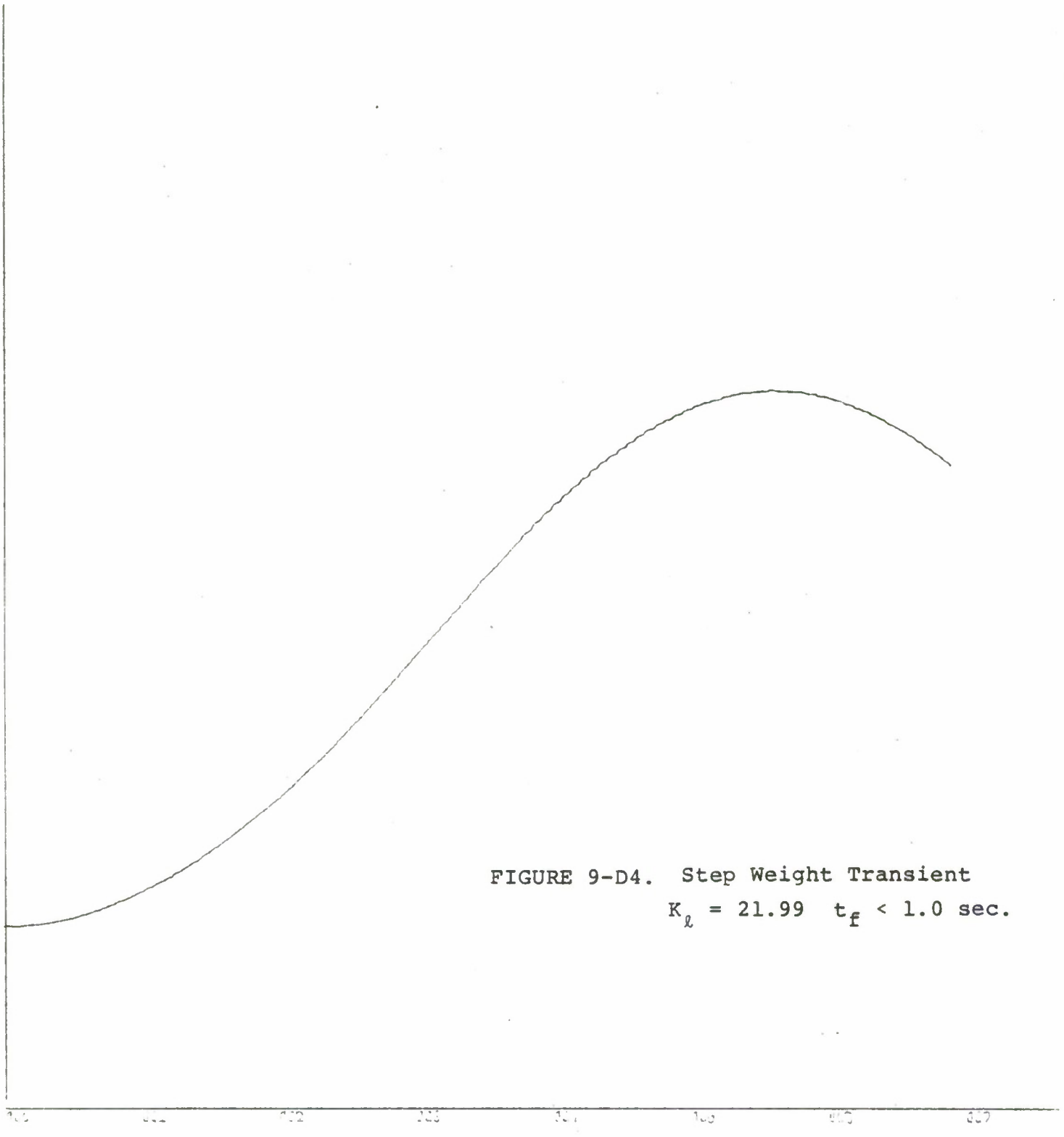

FIGURE 9-D4. Step Weight Transient
K_ℓ = 21.99 t_f < 1.0 sec.

X-SCALE=1.00E-01 UNITS INCH
Y-SCALE=2.00E-01 UNITS INCH
BOX 70 30 KNOT RUN WR6
PLOT IS PITCH ANGLE VERSUS TIME

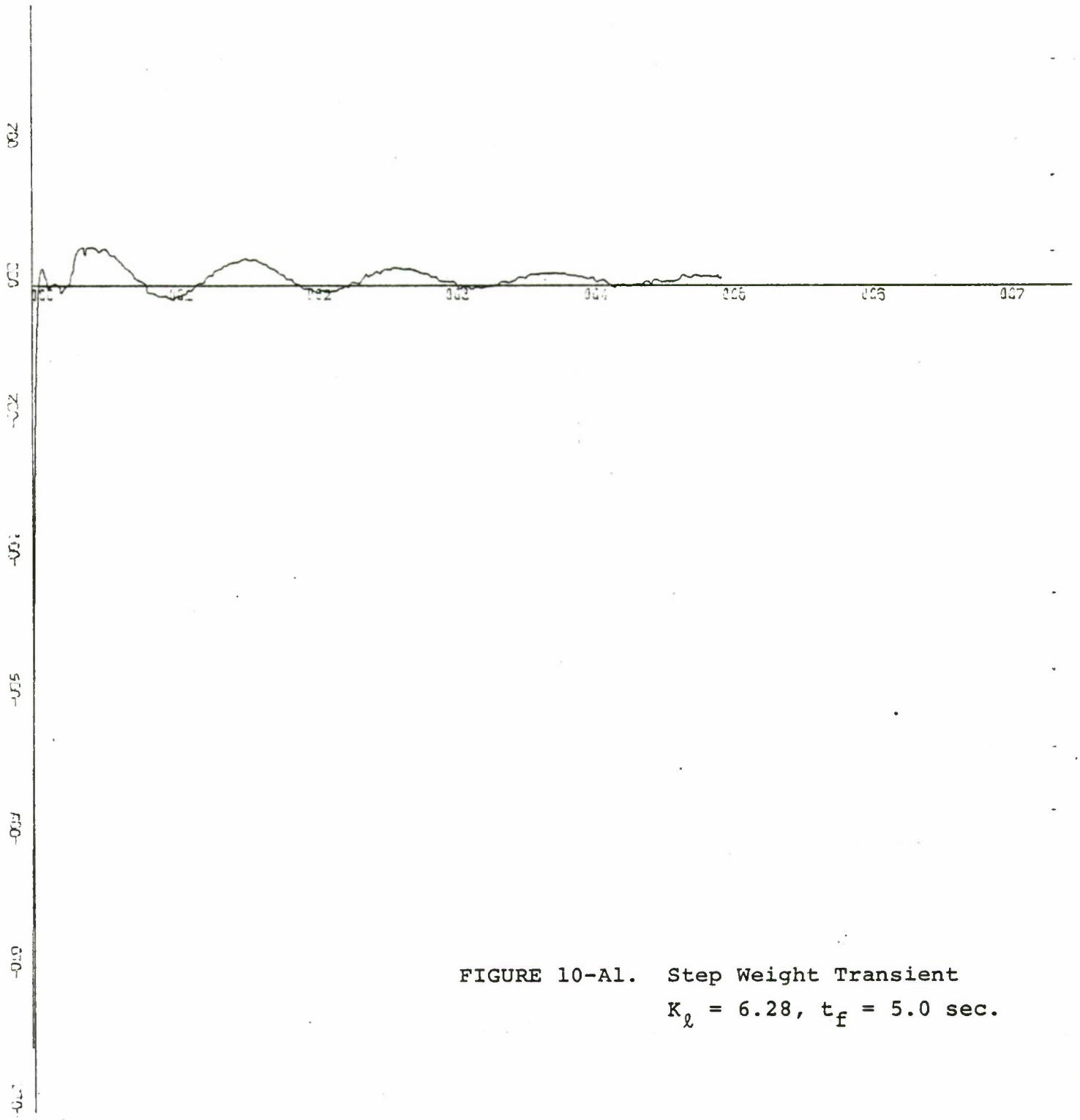

FIGURE 10-A1. Step Weight Transient
$K_\ell = 6.28$, $t_f = 5.0$ sec.

X-SCALE=1.00E+00 UNITS INCH.
Y-SCALE=2.00E-02 UNITS INCH.
BOX 70 30 KNOT RUN WS1
PLOT IS C.G. ACCELERATION VERSUS TIME

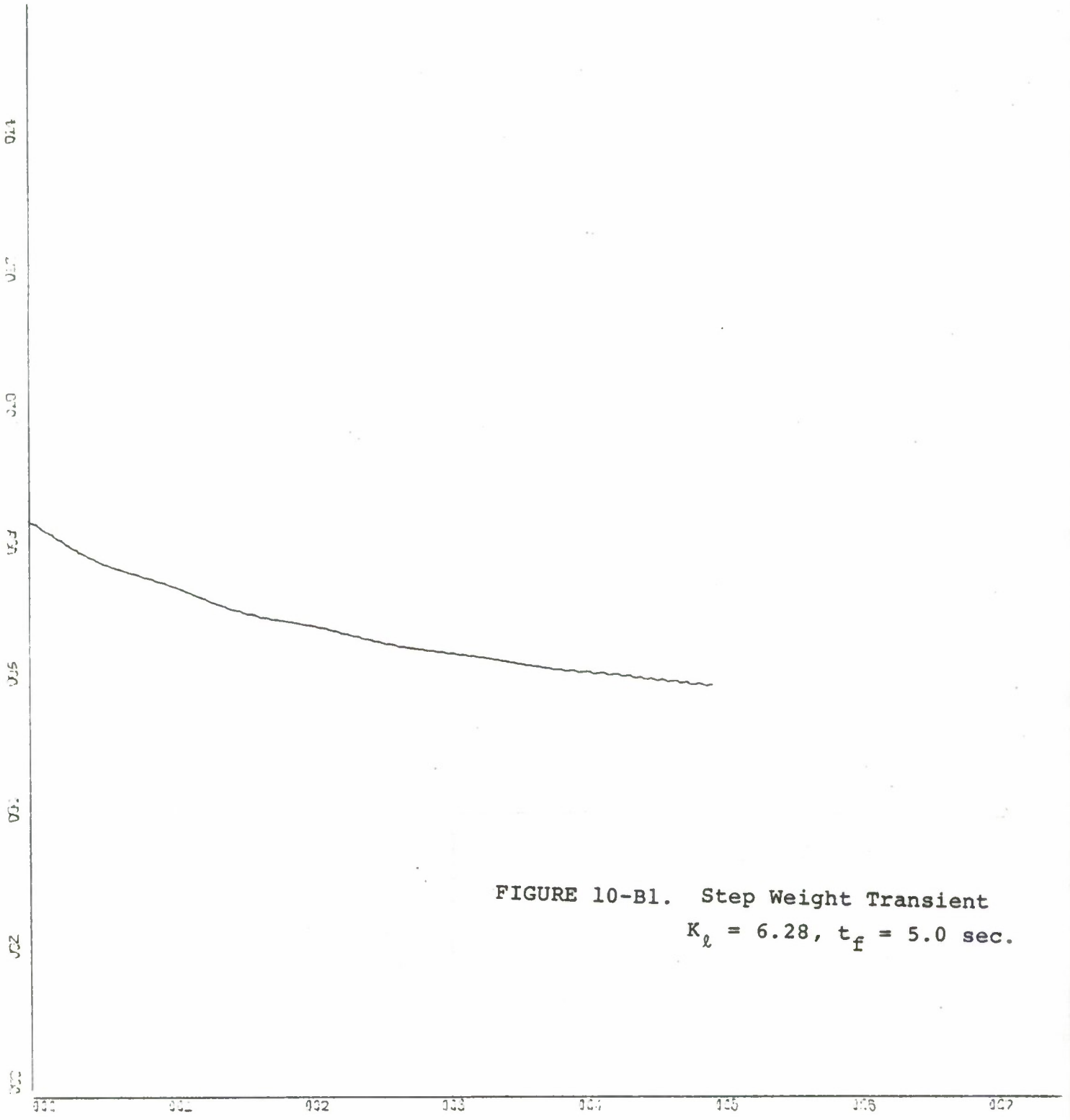

FIGURE 10-B1. Step Weight Transient
$K_\ell = 6.28$, $t_f = 5.0$ sec.

X-SCALE=1.00E+00 UNITS INCH.
Y-SCALE=2.00E+00 UNITS INCH.
BOX 70 30 KNOT RUN WS1
PLOT IS Z DISPLACEMENT VERSUS TIME

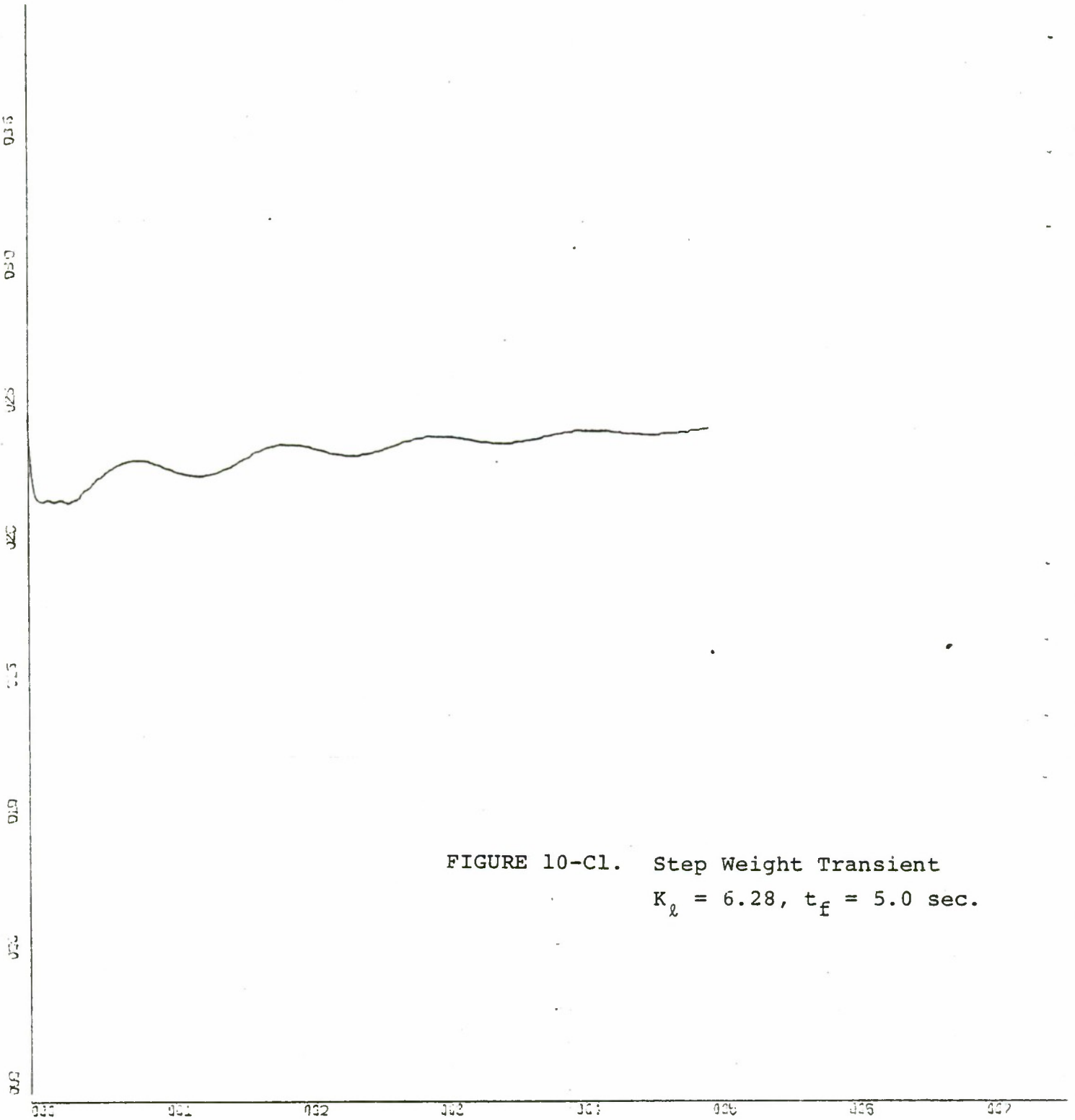

FIGURE 10-C1. Step Weight Transient
$K_\ell = 6.28$, $t_f = 5.0$ sec.

X-SCALE=1.00E+00 UNITS INCH.
Y-SCALE=5.00E+00 UNITS INCH.
BOX 70 30 KNOT RUN WS1
PLOT IS PLENUM PRESSURE VERSUS TIME

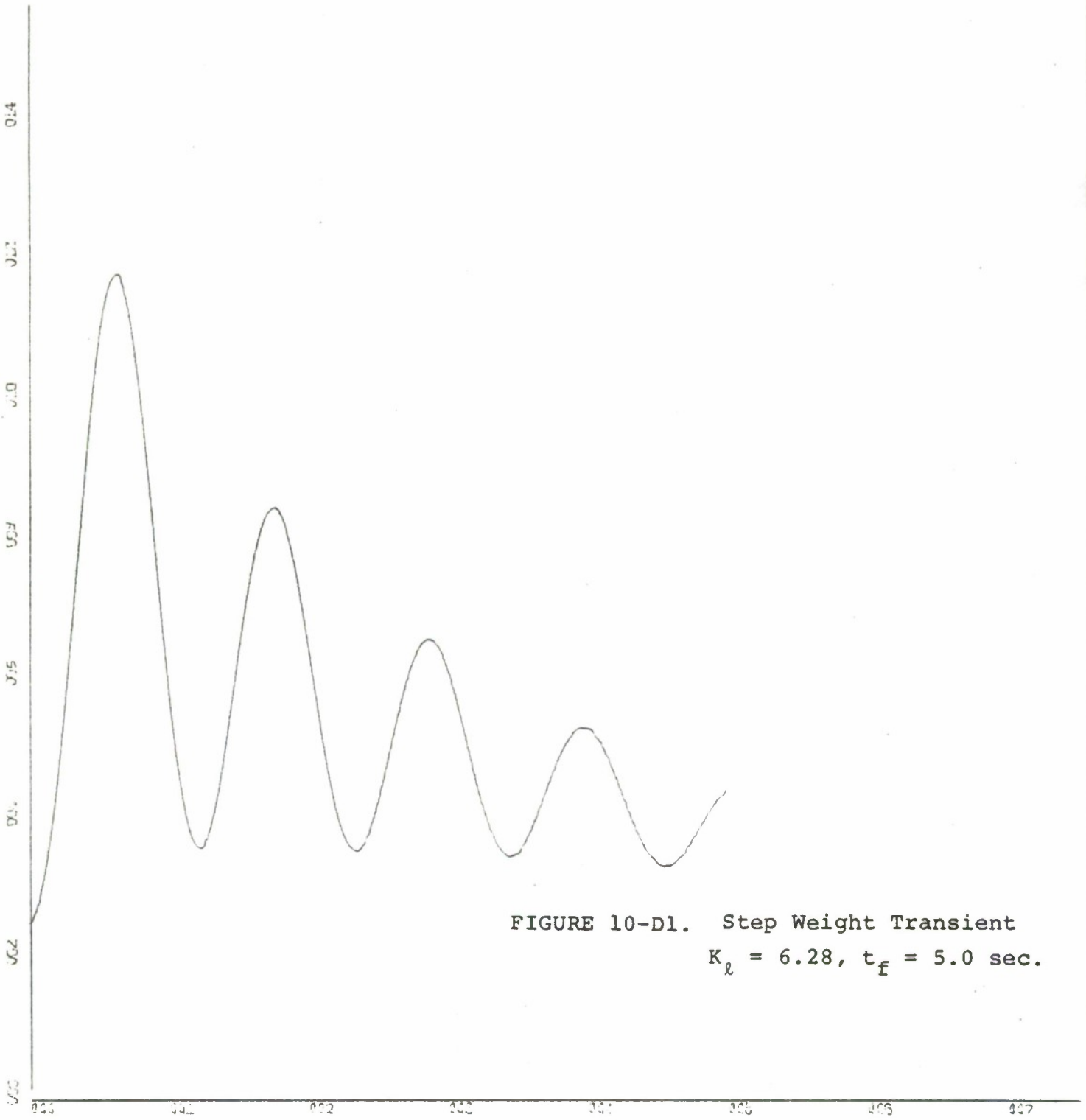

FIGURE 10-D1. Step Weight Transient
$K_\ell = 6.28$, $t_f = 5.0$ sec.

X-SCALE=1.00E+00 UNITS INCH.
Y-SCALE=2.00E-01 UNITS INCH.
BOX 70 30 KNOT RUN WS1
PLOT IS PITCH ANGLE VERSUS TIME

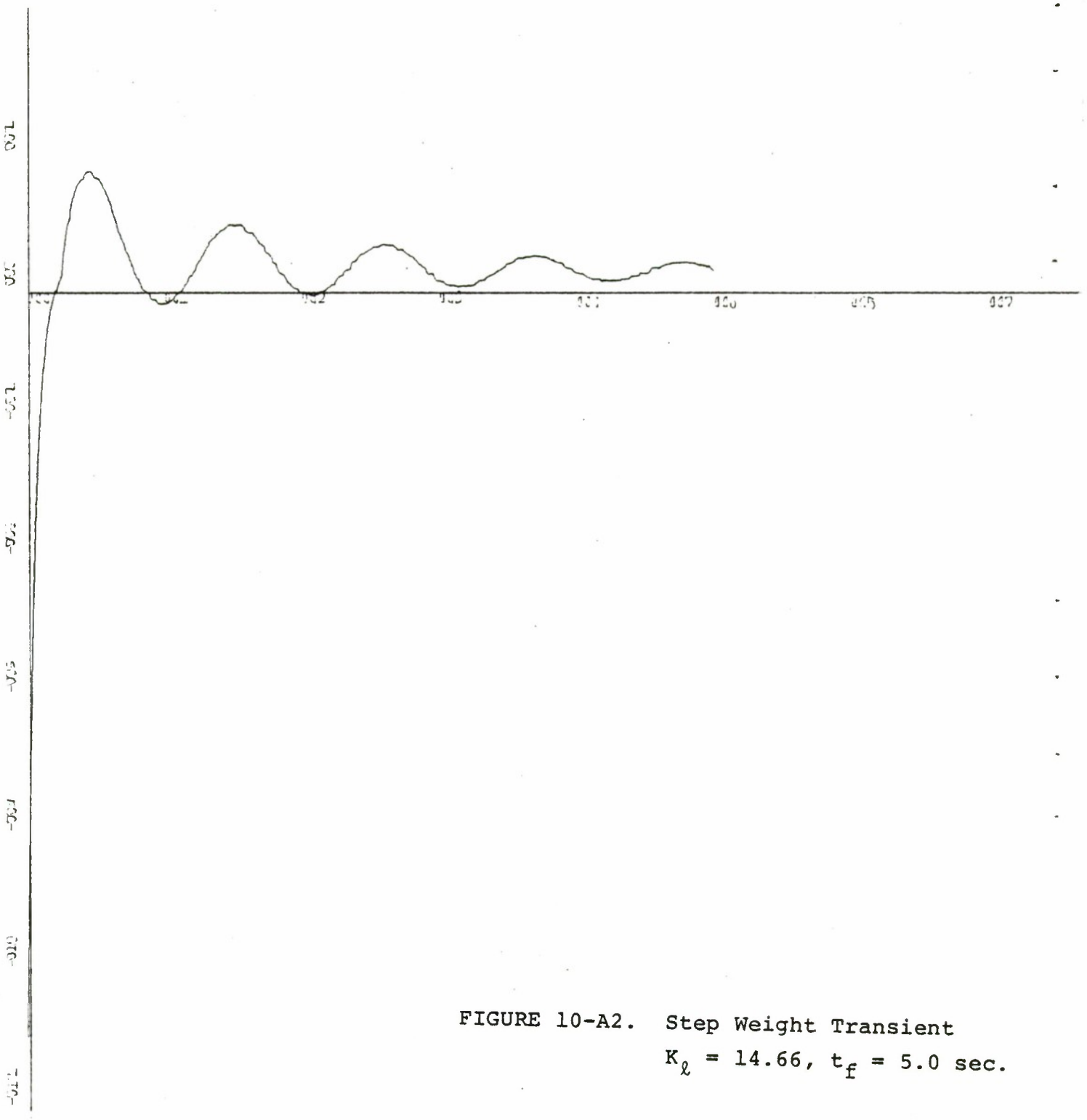

FIGURE 10-A2. Step Weight Transient
K_ℓ = 14.66, t_f = 5.0 sec.

X-SCALE=1.00E+00 UNITS INCH.
Y-SCALE=2.00E-02 UNITS INCH.
BOX 70 30 KNOT RUN WS4
PLOT IS C.G. ACCELERATION VERSUS TIME

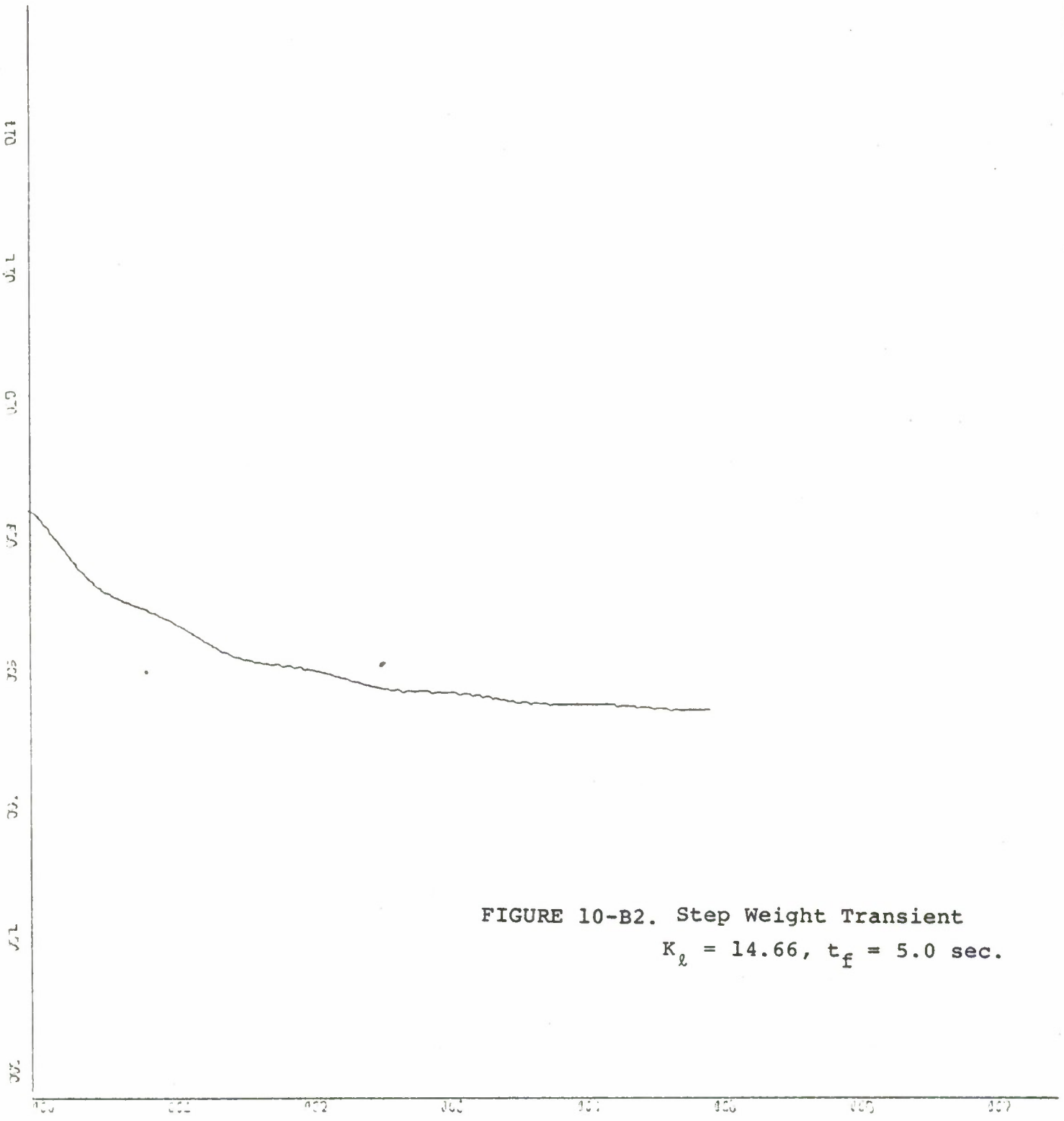

FIGURE 10-B2. Step Weight Transient
K_ℓ = 14.66, t_f = 5.0 sec.

X-SCALE=1.00E+00 UNITS INCH.
Y-SCALE=2.00E+00 UNITS INCH.
BOX 70 30 KNOT RUN 454
PLOT IS Z DISPLACEMENT VERSUS TIME

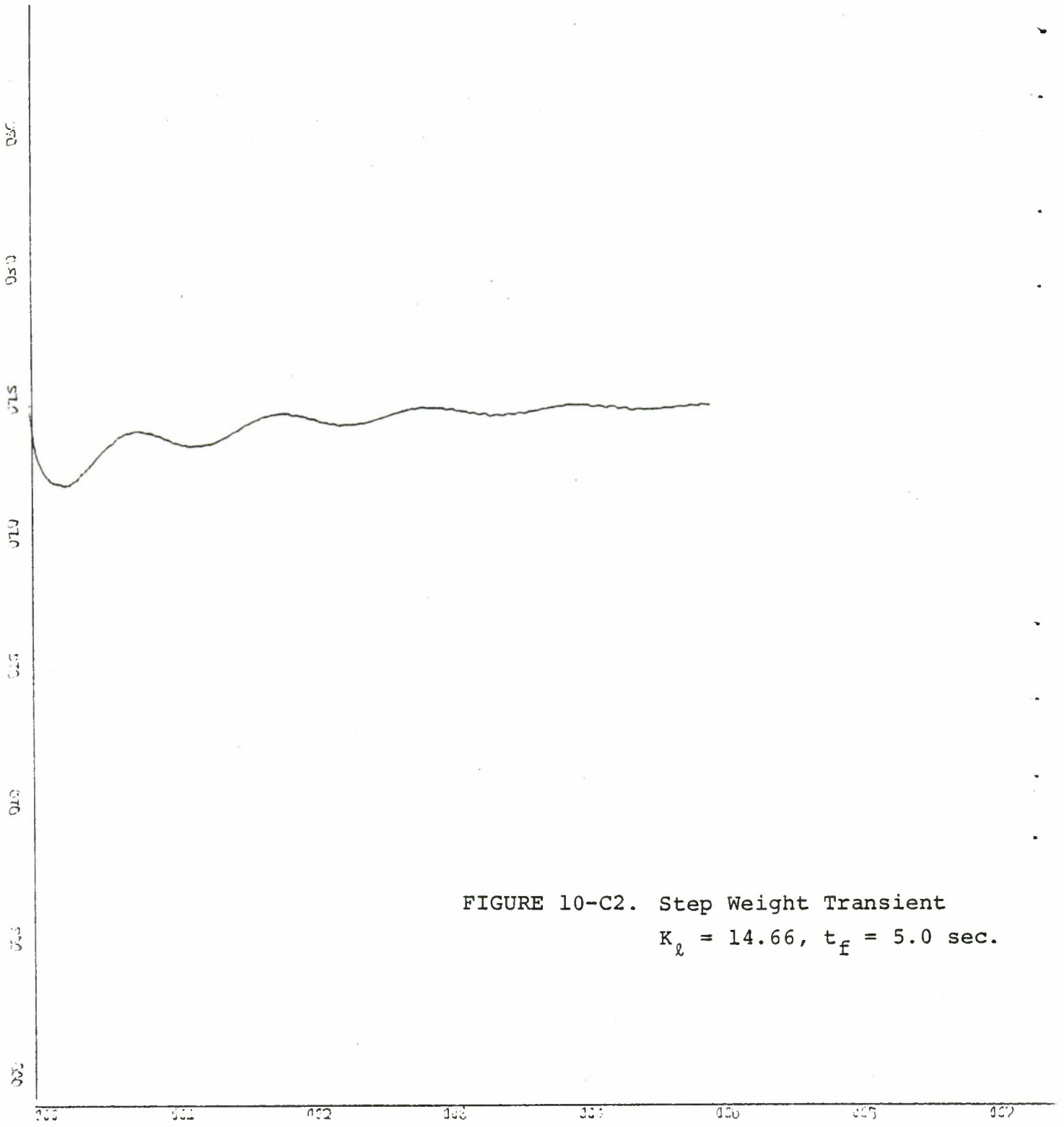

FIGURE 10-C2. Step Weight Transient
K_ℓ = 14.66, t_f = 5.0 sec.

X-SCALE=1.00E+00 UNITS INCH.
Y-SCALE=5.00E+00 UNITS INCH.
BOX 70 30 KNOT RUN WS4
PLOT IS PLENUM PRESSURE VERSUS TIME

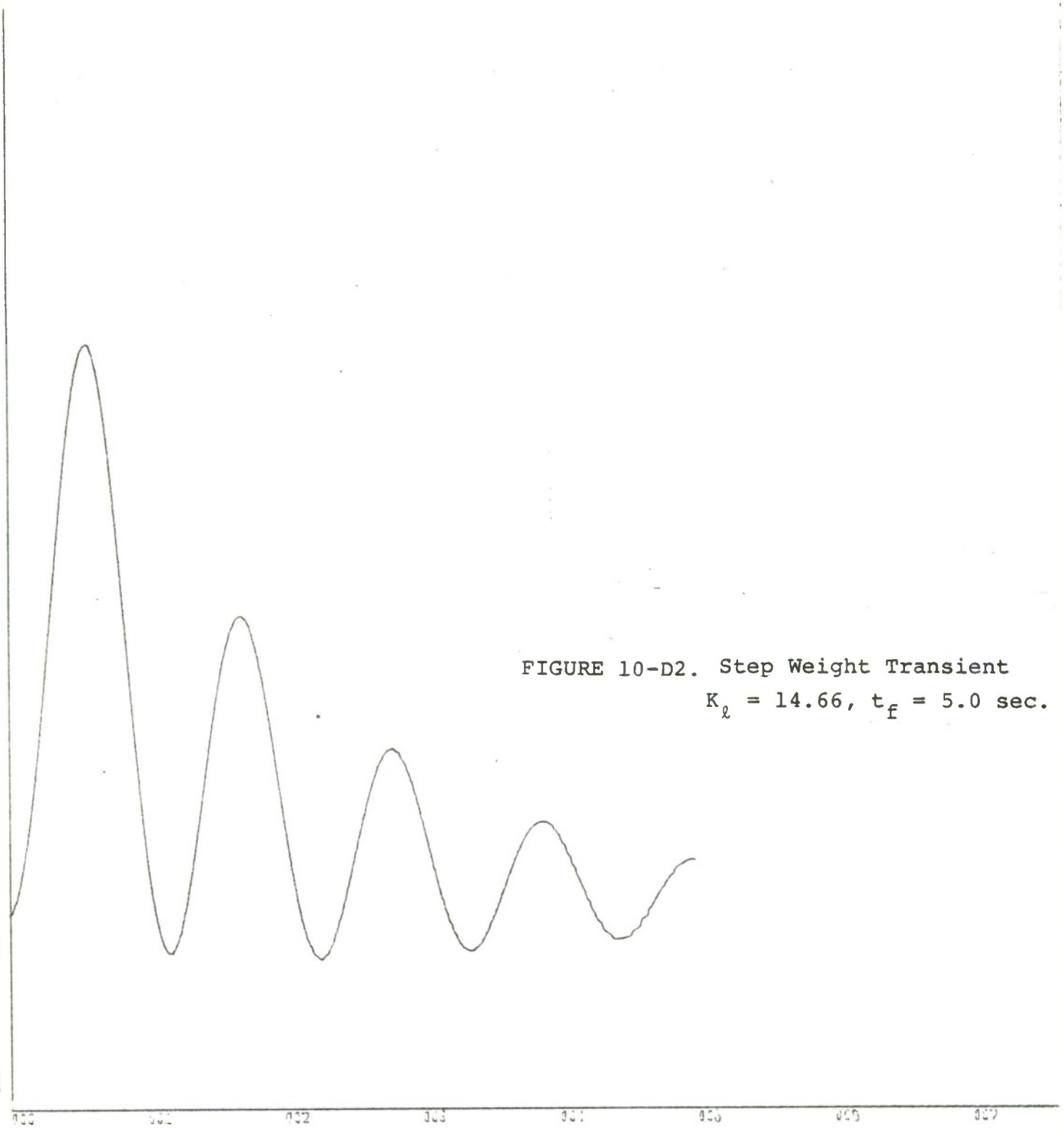

FIGURE 10-D2. Step Weight Transient
K_ℓ = 14.66, t_f = 5.0 sec.

K-SCALE=1.00E+00 UNITS INCH.
[illegible]-SCALE=2.00E-01 UNITS INCH.
BOX 70 30 KNOT RUN 454
PLOT IS PITCH ANGLE VERSUS TIME

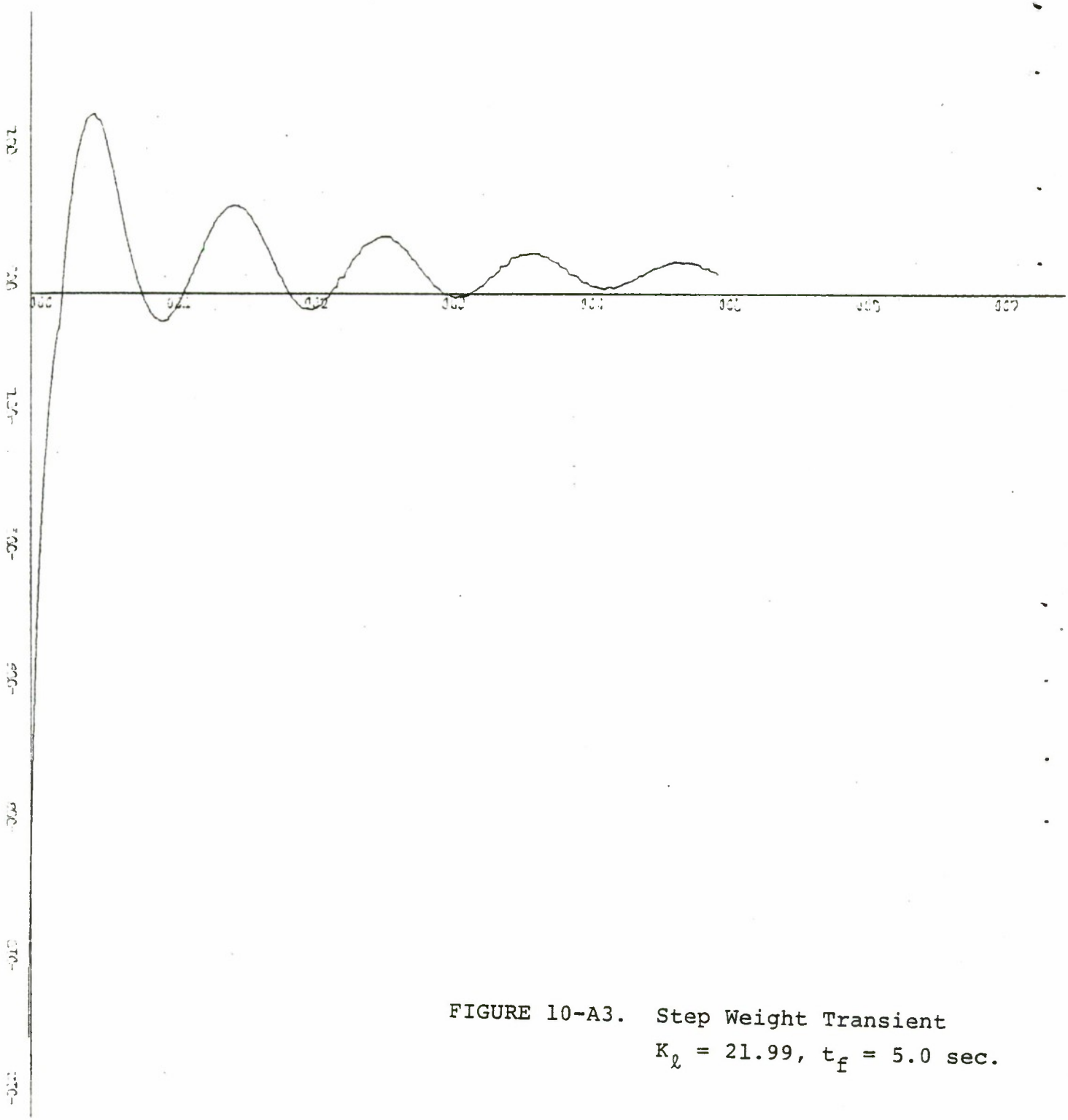

FIGURE 10-A3. Step Weight Transient
K_ℓ = 21.99, t_f = 5.0 sec.

X-SCALE=1.00E+00 UNITS INCH.
Y-SCALE=2.00E-02 UNITS INCH.
BOX 20 30 KNOT RUN HS6
PLOT IS C.G. ACCELERATION VERSUS TIME

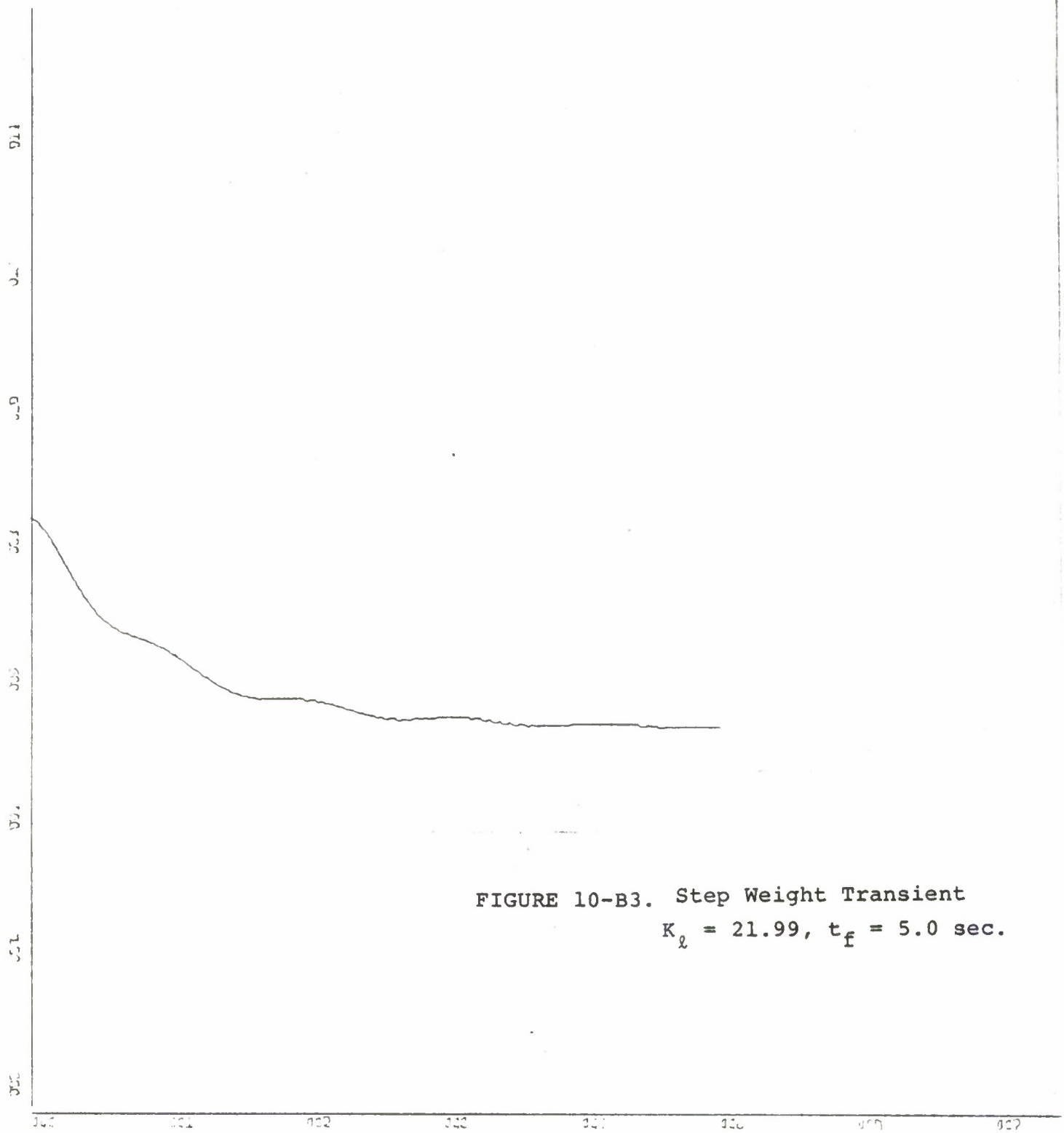

FIGURE 10-B3. Step Weight Transient
K_ℓ = 21.99, t_f = 5.0 sec.

K-SCALE=1.00E+00 UNITS INCH.
Y-SCALE=2.00E+00 UNITS INCH.
BOX 70 30 KNOT RUN 4S6
PLOT IS Z DISPLACEMENT VERSUS TIME

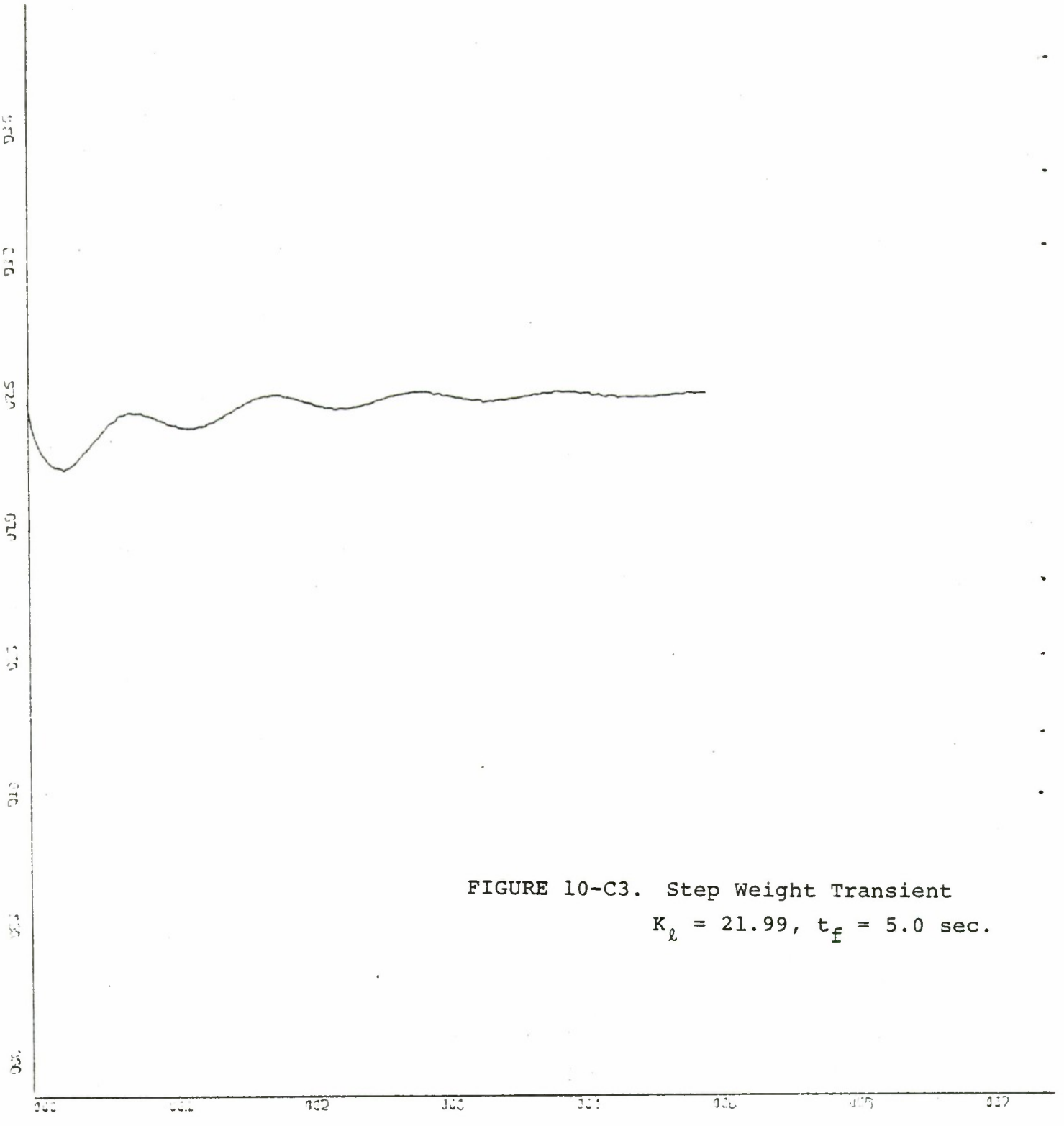

FIGURE 10-C3. Step Weight Transient
K_ℓ = 21.99, t_f = 5.0 sec.

X-SCALE=1.00E+00 UNITS INCH.
Y-SCALE=5.00E+00 UNITS INCH.
BOX 70 30 KNOT RUN WS6
PLOT IS PLENUM PRESSURE VERSUS TIME

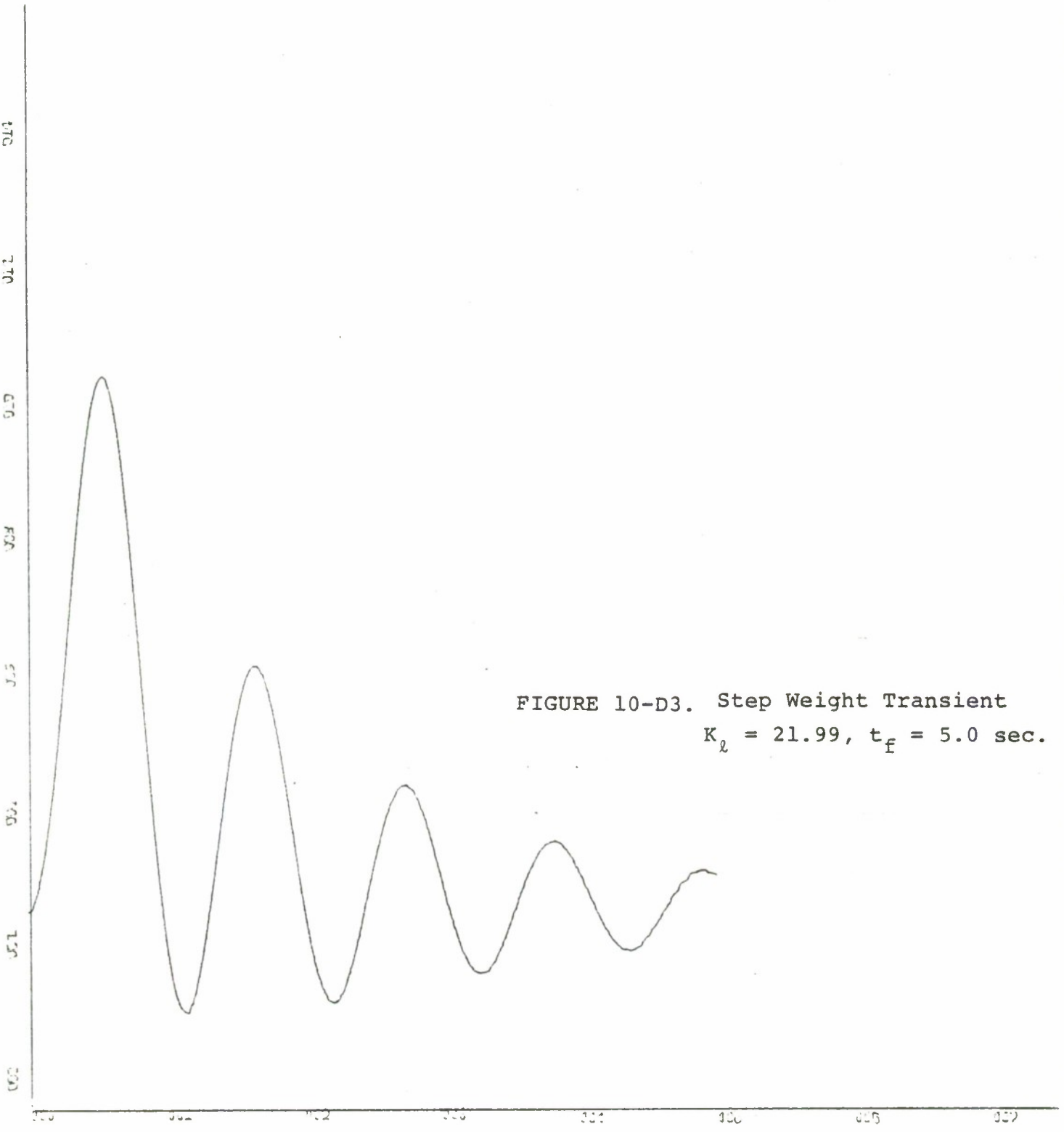

FIGURE 10-D3. Step Weight Transient
K_ℓ = 21.99, t_f = 5.0 sec.

V. CONCLUSIONS

A few specific conclusions may be drawn from the results of this study:

1. The major effect of increasing air flow rates is to attenuate high frequency components in the response of the craft. This is clearly shown by the high frequency response of both the linear and 6 D.O.F. models. It is also shown by the step weight removal transients. Therefore, to reduce the vibrations due to vertical accelerations at high encounter frequencies, the air flow rate should be maintained as high as practical.

2. The pitch mode couples strongly into the vertical motions over the encounter frequency range of 1 to 10 rad/sec. as shown by the 6 D.O.F. model. Therefore, pitch motion should be added to the linear model to account for the changes in air flow leakage rate due to the variations in the pitch angle.

3. The linear model (Heave motion only) is sufficiently accurate for many studies and should be used where applicable to aid in the analysis and design of CAB craft characteristic.

4. The linear model reduces both the CPU execution time and the operating class in the job queue resulting in a reduce interaction (turnaround) time.

5. The complex sea method of developing the frequency response of the 6 DOF model using the Fast Fourier Transform provides approximate results that can be quite inaccurate unless special care is exercised in its application.

VI. RECOMMENDATIONS

One of the long range goals of the analytical studies of the CAB craft at NPS is to develop a simplified model that will provide a reasonable computer execution time for control system design and evaluation in the complex sea operating environment. We feel that we have a reasonable start in this direction and have the following recommendation for future studies:

1. The pitch mode should be modelled and incorporated in the Linear Heave-Only Model. Mr. McIntyre in Reference 7 has made the first effort in this direction and a current study by Mr. Barnes (Reference 8) has improved on the model and shows promise of providing the additional information missing from the Heave-Only Model.

2. Upon the completion of the Linear Pitch-Heave Model and its regular sea frequency response validation with the 6 D.O.F. model, the complex sea frequency response should be computed and compared for both accuracy and speed of computation.

3. Continue experimentation with both software and hardware techniques for the analysis of the complex sea results both for the 6 D.O.F. model and the actual XR-3 craft to provide improved results of the complex sea frequency response analysis.

4. Develop deterministic input tests for the XR-3 craft for validation of the SESCOMP model. The weight removal transient is one such test that shows promise for validation of the Pitch-Heave mode equations.

5. Investigate effect of the addition of a membrane in the plenum chamber to reduce the variations in the vertical motions of the XR-3 craft. The actual XR-3 craft as well as the 6 D.O.F. program and the linear pitch-heave model would be used in this study.

LIST OF REFERENCES

1. Gerba, Jr., A. and Thaler, G. J., Pressure Ratio Effect on the Heave Motion Characteristics and Pressure Dynamics of the XR-3 Loads and Motion Program for Step Weight Transients, NPS Progress Report to SESPO, January 1977.

2. Gerba, Jr., A. and Thaler, G. J., A Method for Scaling the Heave Motion Equations of the C.A.B. 6-D.O.F. Loads and Motion Program from Model to Full-Size Craft., NPS Progress Report to SESPO, December 1977. Report Number NPS62-77-002.

3. Comstock, J. P. (Editor), Principles of Naval Architecture, Society of Naval Architects and Marine Engineers, N.Y., 1967.

4. Booth III, B. F., The Frequency Response and Operating Characteristics of the XR-3 Loads and Motion Program, NPS Master Thesis, June 1976.

5. Menzel, R. F., Study of the Roll and Pitch Transients in Calm Water Using the Simulated Performance of the XR-3 Surface Effect Ship Loads and Motions Computer Program, NPS Master Thesis, December 1975.

6. Gerba, Jr., A. and Thaler, G. J., Frequency Response Studies of Ambient Pressure Effects on the XR-3 Computer Program (6-D.O.F.), NPS Progress Report to SESPO, September 1977.

7. McIntyre, L. F., Investigation of a Linear, Two-Degree-of-Freedom Simulation of the XR-3 Captured Air Bubble (CAB) Craft in the Frequency Domain, NPS Master Thesis, June 1977.

8. Barnes, L. W., Pitch Control Study Using a 2-D.O.F. Model in Heave and Pitch, (Tentative), NPS Master Thesis, March 1979.

APPENDIX A. DESCRIPTION OF THE SIMPLIFIED XR-3 MODEL

A. Nonlinear System

In this model of the XR-3, pitch variations are reduced to zero by assuming 1) the center of pressure (C.P.) directly under the center of gravity (C.G.), 2) the sidewall symmetrical about the C.G. with uniform rectangular cross-section from bow to stern and 3) the pitch moments of the seals and aerodynamics cancel each other. The lift force of plenum pressure and sidewall buoyancy oppose the craft weight. All other lift and drag forces are neglected since constant speed conditions are assumed.

In addition it will be assumed that the rear seal maintains a constant leakage area, that is, the seal follows the water level at a fixed separation.

Figure A1 shows a top and sideview of the simulated CAB craft. All dimensions are chosen to approximate those of the XR-3 craft in order to compare the results of this analysis to the L & M program solution under similar operating conditions.

The equations of motion for this system are given below.

$$\text{Orifice Leakage Rate, } q_{out} = C_n A_\ell \sqrt{\frac{2\bar{P}_b}{\rho_a}} \quad \frac{\text{cu.ft.}}{\text{sec.}} \tag{1}$$

$$\text{Fan Map Input Rate, } q_{in} = n \left[Q_i(o) - k_q \bar{P}_b \right] \quad \frac{\text{cu.ft.}}{\text{sec.}} \tag{2}$$

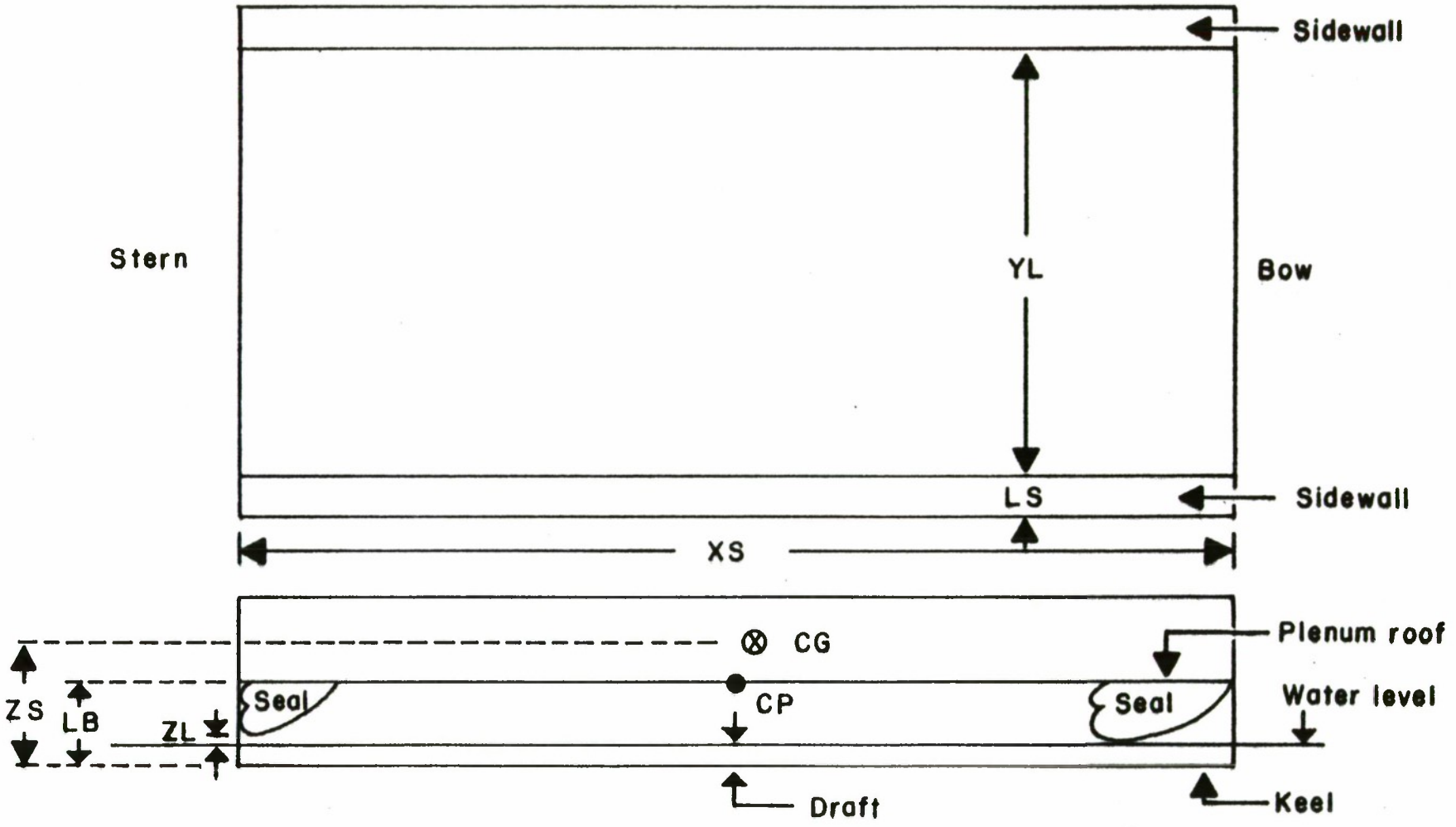

FIGURE A1. – Top and Side View of Simplified XR-3

Absolute Plenum Pressure, (Adiabatic Process) $P_b = P_a \left(\frac{M_b}{V_b \rho_a}\right)^{\gamma}$ Psf (3)

Plenum Volume, $V_b = (V_n - A_b \ell_d)$ cu.ft. (4)

Plenum Air Flow Rate, $\dot{M}_b = \rho_a (q_{in} - q_{out})$ $\frac{\text{lbs.}}{\text{sec.}}$ (5)

Heave Acceleration, $\ddot{Z} = \left(\frac{W}{M} - \frac{F_p}{M} - \frac{F_\ell}{M}\right)$ $\frac{\text{ft.}}{\text{sec.}^2}$ (6)

Heave Velocity, $\dot{Z} = \left[\int \ddot{Z}\, dt\right]$ $\frac{\text{ft.}}{\text{sec.}}$ (7)

Heave, $Z = \left[\int_o^\tau \dot{Z}\, dt + Z(o)\right]$ ft. (8)

Plenum Pressure Lift Force, $F_p = A_b \bar{P}_b$ lbs. (9)

Buoyancy Lift Force, $F_\ell = \left[2(A_\delta \ell_d)\rho g\right]$ lbs. (10)

Plenum Gage Pressure, $\bar{P}_b = (P_b - P_a)$ Psf. (11)

Draft, $\ell_d = Z + Zs$ feet (12)

The system parameters and constants are listed below.

Adiabatic process coefficient, $\gamma = 1.4$

Leakage area, $A_\ell = Y_L\, Z_L = 0.438$

Leakage orifice coefficient, $C_n = 0.90$

Air density, $\rho_a = .002378$

Atmospheric pressure, $P_a = 2116.$

Plenum area,	$A_b = 200.$
Empty plenum volume,	$V_n \doteq 383.$
Craft weight,	$W = 6007$
Keel line area of sidewall,	$A = 75/4$
Draft, initial condition,	$\ell_d(o) = 0.5$
Density of water,	$\rho = 2.$
Gravity acceleration,	$g = 32.$
Center gravity location,	$Zs = 2.5$
Number of fans,	$n = 5.$
Steady state fan output,	$Q_i(o) = 35.$
Fan map slope,	$kq = 1.0$

The schematic diagram of signal flow is shown in Figure A2.

The coordinate system and initial conditions for heave and draft are shown in Figure A3.

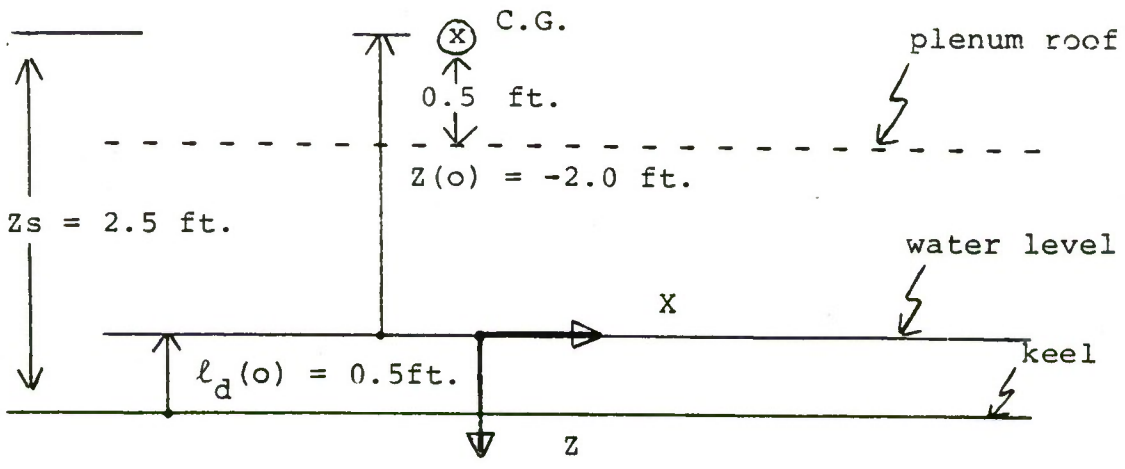

Figure A3 - Coordinate System and Initial Condition of Heave and Draft.

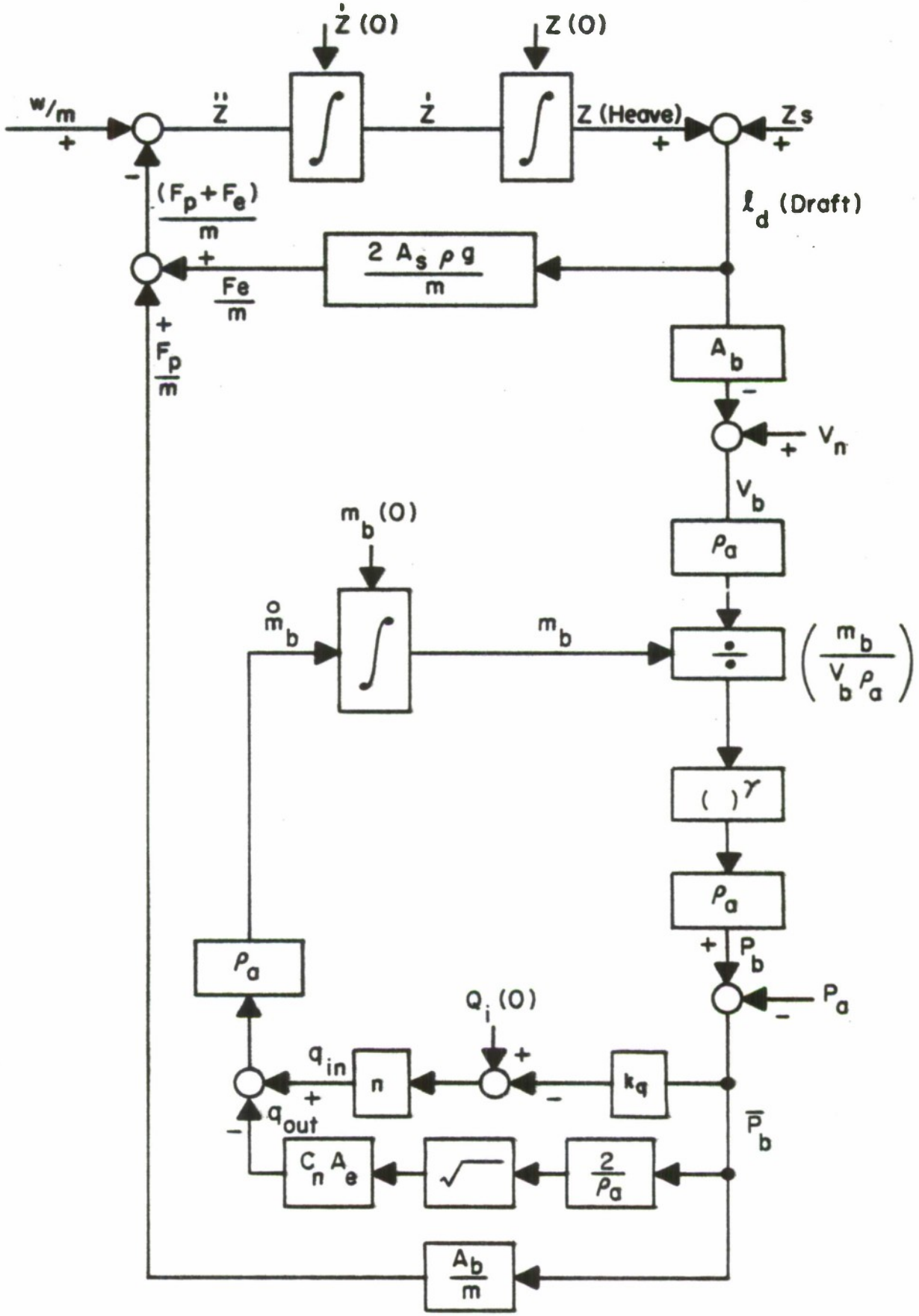

FIGURE A2.—Schematic Diagram of Signal Flow.

It should be noted that the range of heave motion is $-2.5 < Z < -0.5$ since -2.5 feet would put the water level at the keel line and -0.5 feet would put the water level at the plenum roof. Draft is measured from the keel and would have the range $0 < \ell_d < 2.0$. Also note that if the craft "drops" into the water, ℓ_d increases and Z becomes less negative, that is, Z increases in the positive (downward) direction.

At steady-state condition, the plenum pressure assumed is $\bar{P}_b(o) \doteq 24.$ PSF producing a $F_p(o) = 4800$ lbs. For the draft of $\ell_d(o) = 0.5$ feet, the buoyancy force $F_\ell(o) = 1200$ lbs.

The air mass in the plenum for the above steady-state where $q_{in}(o) = q_{out}(o) = 55$ cu. ft./sec. is $M_b(o) = 0.71878$ pounds.

B. Linear System

The linear system equations are arrived at by application of the Taylor Series expansion[a] about the steady-state operating point. The development is shown below for the two differential equations.

---

a) Steady State and incremental variations are noted as follows using heave as an example.

$$z = z(o) + \delta z$$

Equation (1), let $W/M = W_m$; $F_p/M = F_{pm}$

and $F_\ell/M = F_{\ell m}$

then,

$$\ddot{z}(o) + \dot{\delta z} = W/M - (F_{pm}(o) + \delta F_{pm}) - (F_{\ell m}(o) + \delta F_{\ell m})$$

or,

$$\dot{\delta z} = -\delta F_{pm} - \delta F_{\ell m} \qquad (1a)$$

Equation (2), let $m/\rho_a = V_m$

then,

$$\dot{V}_m(o) + \dot{\delta V}_m = nQ_i - nk_q\,(\bar{P}_b(0) + \delta\bar{P}_b) - C_n A_\ell \left(\frac{2\bar{P}_b(o)}{\rho_a}\right)^{\frac{1}{2}} - C_n A_\ell \tfrac{1}{2} \left(\frac{2\bar{P}_b(o)}{\rho_a}\right)^{-\frac{1}{2}} \left(\frac{2}{\rho_a}\right) \delta\bar{P}_b$$

or,

$$\dot{\delta V}_m = -(nk_q)\,\delta\bar{P}_b - \frac{C_n A_\ell}{\rho_a} \left(\frac{\rho_a}{2\bar{P}_b(o)}\right)^{\frac{1}{2}} \delta\bar{P}_b \qquad (2a)$$

Next, the auxiliary algebraic equations are linearized.

$$F_p(o) + \delta F_p = A_b\,(\bar{P}_b(o) + \delta\bar{P}_b)$$

$$\delta F_p = A_b\,\delta\bar{P}_b \qquad (3a)$$

$$F_\ell\ (o) + \delta F_\ell = 2A_s\ \rho_w g\ (\ell_d(o) + \delta \ell_d)$$

$$\boxed{\delta F_\ell = (2A_s\ \rho_w g)\ \delta \ell_d} \qquad (4a)$$

Eq. (5a) and (6a) have already been developed they are:

$$\boxed{\delta q_{in} = -(nk_q)\ \delta \bar{P}_b} \qquad (5a)$$

and

$$\boxed{\delta q_{out} = -\frac{C_n A_\ell}{\rho_a}\ \left(\frac{\rho_a}{2\bar{P}_b(o)}\right)^{\frac{1}{2}}\ \delta \bar{P}_b} \qquad (6a)$$

For equation 7a

$$\frac{(P_b(o) + \delta P_b)}{P_a} = \left(\frac{V_m(o)}{V_b(o)}\right)^\gamma + \gamma \left(\frac{V_m(o)}{V_b(o)}\right)^{\gamma-1} \left\{\left[\frac{1}{V_b(o)}\right]\ \delta V_m - \frac{(V_m(o))}{[V_b(o)]^2}\ \delta V_b\right\}$$

$$\delta P_b = P_a \gamma\ (\quad)^{\gamma-1} \left\{\left[\frac{V_m(o)}{V_b(o)}\ \frac{\delta V_m}{V_m(o)} - \frac{V_m(o)}{V_b(o)}\ \frac{\delta V_b}{V_b(o)}\right]\right\}$$

$$\boxed{\delta P_b = \gamma P_b(o)\ \left[\frac{1}{V_m(o)}\ \delta V_m - \frac{1}{V_b(o)}\ \delta V_b\right]} \qquad (7a)$$

and equation 8, 9, and 10 follow.

$$V_b(o) + \delta V_b = V_n - A_b\ (\ell_d(o) + \delta\ell_d)$$

$$\boxed{\delta V_b = -\ (A_b)\,\delta\ell_d} \qquad (8a)$$

$$\bar{P}_b(o) + \delta\bar{P}_b = P_b(o) + \delta P_b - P_a$$

$$\boxed{\delta\bar{P}_b = \delta P_b} \qquad (9a)$$

$$\ell_d(o) + \delta\ell_d = z(o) + \delta z + Z_\delta$$

$$\boxed{\delta\ell_d = \delta z} \qquad (10a)$$

Combining (1a), (3a), (4a), (7a) and (8a) as follows:

$$\ddot{\delta z} = -\left(\frac{A_b}{M}\right)\ \delta\bar{P}_b - \left(\frac{2A_\delta \rho_w g}{M}\right)\ \delta z$$

recall that $\delta\ell_d = \delta z$

$$\ddot{\delta z} = -\frac{A_b}{M}\ \left\{\gamma\ P_b(o)\left[\frac{1}{V_m(o)}\ \delta V_m - \frac{1}{V_b(o)}\ (-A_b)\ \delta z\right]\right\}$$

$$-\left(2\ \frac{A_\delta \rho_w g}{M}\right)\ \delta z$$

$$\ddot{\delta z} = -\left\{\left[\left(\frac{2A_{\Delta}\rho_w g}{M}\right) + \left(\frac{\gamma P_b(o) A_b^2}{MV_b(o)}\right)\right] \delta z + \left[\frac{\gamma P_b(o) A_b}{MV_m(o)}\right] \delta V_m\right\}$$

Also for equation (2a)

$$\dot{\delta V}_m = -\left[nk_q + \frac{C_n A_\ell}{\rho_a}\left(\frac{\rho_a}{2\bar{P}_b(o)}\right)^{\frac{1}{2}}\right] \gamma P_b(o) \left[\frac{\delta V_m}{V_m(o)} - \frac{\delta V_b}{V_b(o)}\right]$$

$$\dot{\delta V}_m = -\left[nk_q + \frac{C_n A_\ell}{\rho_a}\left(\frac{\rho_a}{2\bar{P}_b(o)}\right)^{\frac{1}{2}}\right] \gamma P_b(o) \left[\left(\frac{1}{V_m(o)}\right) \delta V_m + \left(\frac{A_b}{V_b(o)}\right) \delta z\right]$$

and for equation (7a)

$$\delta P_b = \gamma P_b(o) \left[\frac{1}{V_m(o)} \delta V_m + \frac{A_b}{V_b(o)} \delta z\right]$$

Now define the state vector

$$\underline{x} \triangleq [\delta z \quad \dot{\delta z} \quad \delta V_m]^T$$

and output variable, $y = \delta P_b$ with

$$y \triangleq c_{11} x_1 + c_{13} x_3$$

Then the state equations are

$$\dot{x}_1 = x_2$$
$$\dot{x}_2 = a_{21} x_1 + a_{23} x_3$$
$$\dot{x}_3 = a_{31} x_1 + a_{33} x_3$$

where $c_{11} = \frac{\gamma P_b(o) A_b}{V_b(o)}$ and $c_{13} = \frac{\gamma P_b(o)}{V_m(o)}$

$$a_{21} = -\left(\frac{2A_\delta \rho_w g}{M} + \frac{\gamma P_b(o) A_b^2}{MV_b(o)}\right)$$

$$a_{23} = -\left(\frac{\gamma P_b(o) A_b}{MV_m(o)}\right)$$

$$a_{31} = -\gamma P_b(o) \left[nk_q + \frac{C_n A_\ell}{\rho_a} \sqrt{\frac{\rho_a}{2\bar{P}_b(o)}}\right] \frac{A_b}{V_b(o)}$$

$$a_{33} = -\gamma P_b(o) \left[nk_q + \frac{C_n A_\ell}{\rho_a} \sqrt{\frac{\rho_a}{2\bar{P}_b(0)}}\right] \frac{1}{V_m(o)}$$

The characteristic equation for this system is given by $(\delta I - A)$ where

$$A = \begin{vmatrix} o & 1 & o \\ a_{21} & o & a_{23} \\ a_{31} & o & a_{33} \end{vmatrix}$$

Then $$(\delta I - A) = \begin{bmatrix} \delta & -1 & o \\ -a_{21} & \delta & -a_{23} \\ -a_{31} & o & \delta - a_{33} \end{bmatrix}$$

and the characteristic equation is

$$\delta^3 - a_{33}\delta^2 - a_{21}\delta + (a_{21}a_{33} - a_{23}a_{31}) = o$$

Using the given numerical values the characteristic equation is

$$\delta^3 + 62.\delta^2 + 2183\delta + 789 = o$$

This cubic equation will factor into one real root near the origin and a complex pair far removed from the jw axis. (See Sec. IVA) Thus a step weight response will have a complex pair of poles which can be approximated by the quadratic form,

$$\delta^2 - a_{33}\,\delta - a_{21} = 0$$

For the given numerical values it can be shown that a rough approximation for the coefficients are:

$$-a_{33} \doteq n k_{eq}\,\gamma\, P_b(o)/V_m(o)$$

$$-a_{21} \doteq \frac{A_b^2}{M}\,\gamma\, P_b(o)/V_b(o)$$

Using the above approximation yields a natural frequency of:

$$w_n = \sqrt{-a_{21}} = \left[\frac{A_b^2}{M}\;\gamma\;P_b(o)/V_b(o)\right]^{1/2}$$

$$w_n = K_n \sqrt{P_b(o)/V_b(o)} \qquad (13)$$

where $K_n = A_b \sqrt{\gamma/M}$

and a damping factor

$$\zeta = \frac{-a_{33}}{2w_n} = \left[\frac{n^2 k_q^2\,\gamma^2\,P_b^2(o)\;/\;V^2_m(o)}{4\;\frac{A_b^2}{M}\,\gamma\,P_b(o)\;/\;V_b(o)}\right]^{1/2}$$

$$\zeta = K_f \sqrt{\frac{P_b(o)\;V_b(o)}{V^2_m(o)}} \qquad (14)$$

where $K_f = \frac{n k_q}{2A_b}\sqrt{\gamma m}$

APPENDIX B. COMPUTATION OF THE WAVE INPUT TRANSFER FUNCTION

The block diagram of Figure 1 given in Section IIIA can be drawn as a signal flow graph as shown in Figure B-1. To obtain the system transfer functions, the Mason Gain Rule (MGR) can be applied as follows:

$$\Delta = 1 - (L_1 + L_2 + L_3) + L_2L_3 + L_2L_4$$

where

$$L_1 = -k_2\ k_3\ k_4\ k_8\ \delta^{-2}$$

$$L_2 = -k_3\ k_6\ k_7\ \delta^{-1}$$

$$L_3 = -k_5\ \delta^{-2}$$

$$L_4 = -k_9\ \delta^{-1}$$

For the incremental heave (draft), δz, the MGR yields for the wave input, δW

$$\delta z = \frac{1}{\Delta}\ (P_1\ \Delta_1 + P_2\Delta_2)\ \delta W$$

where

$$P_1 = -k_0\delta^{-2} \qquad \Delta_1 = 1 - L_2$$

$$P_2 = -k_1\ k_2\ k_3\ k_4\ \delta^{-2} \qquad \Delta_2 = 1$$

thus,

$$\delta z = \frac{1}{\Delta}\left[(-k_0\delta^{-2})\ (1 + k_3k_6k_7\delta^{-1}) + (-k_1k_2k_3k_4\delta^{-2})\ (1)\right]\ \delta W$$

where the gain coefficients for any particular operating conditions are:

$$k_0 = \left(\frac{2W_sV_w}{\omega_i}\right) \sin\left(\frac{\omega_i L_p}{2V_w}\right)\left(\frac{2\rho_w g}{M}\right)$$

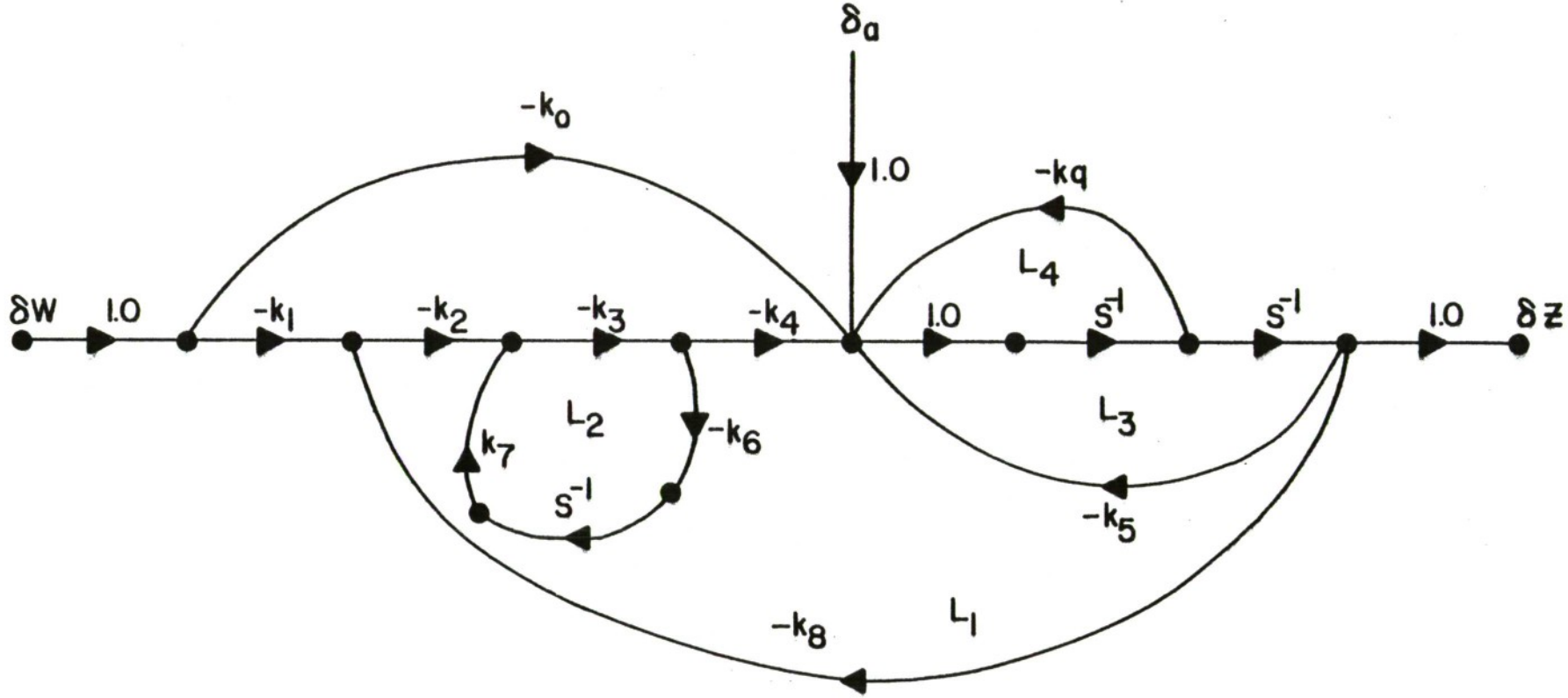

FIG B-1 SIGNAL FLOW GRAPH OF HEAVE EQUATIONS FOR WAVE INPUT

$$k_1 = \left(\frac{2W_p V_w}{\omega_i}\right) \sin \left(\frac{\omega_i L_p}{2V_w}\right)$$

$$k_2 = 1/V_b\ (o)$$

$$k_3 = \gamma P_b\ (o)$$

$$k_4 = A_b/M$$

$$k_5 = 2A_\delta \rho_w g/M$$

$$k_6 = \left(nk_q + \frac{C_n A_\ell}{\rho a}\sqrt{\frac{\rho a}{2\bar{P}_b\ (o)}}\right)$$

$$k_7 = 1/V_m\ (o)$$

$$k_8 = A_b$$

$$k_9 = \left(\frac{UC_v \rho_w B^2}{8M}\right)$$

By applying substitution and reduction, the transfer function becomes,

$$\frac{\delta z}{\delta w} = \frac{-(a\delta + b)}{\delta^3 + c\delta^2 + d\delta + e}$$

with

$$a = (k_0 + k_1 k_2 k_3 k_4)$$

$$b = k_0 k_3 k_6 k_7$$

$$c = (k_3 k_6 k_7 + k_9)$$

$$d = (k_5 + k_2 k_3 k_4 k_8 + k_3 k_6 k_7 k_9)$$

$$e = k_3 k_5 k_6 k_7$$

It should be noted that the transfer function of draft to wave height has a numerator whose coefficients "a" and "b" are functions of the incident wave, ω_i, and therefore will change in value for each frequency of the sinusoidal sea input.

In addition, it should be noted that the incremental heave (draft) is 180 degrees out of phase with the wave input as would be expected since a positive value of wave height produces (1) increased buoyancy and (2) reduction in plenum volume which increases the plenum pressure and thus the lift force.

Further, it is observed that the denominator polynomial is of third order as would be expected since the characteristic roots of this system are obtained by solution of the equation

$$s^3 + cs^2 + ds + e = 0$$

as given in Section IV-A. The transfer function of c.g. acceleration, $\ddot{\delta z}$, to wave height, δw, is obtained from the signal flow graph as follows,

$$\frac{\ddot{\delta z}}{\delta W} = \frac{-k_1k_2k_3k_4(1) - k_0(1 + k_3k_6k_7s^{-1})}{\Delta}$$

$$\frac{\ddot{\delta z}}{\delta W} = \frac{-s^2(as + b)}{s^3 + cs^2 + ds + e}$$

where the coefficient a, b, c, d and e are the same as those in the draft-wave height transfer function.

The minus sign appearing in this transfer function represents the 180 phase shift which is also shown in the draft-wave height transfer function as would be expected.

In like manner, the transfer function of plenum pressure, δP_b, to wave height, δW is

$$\frac{\delta P_b}{\delta W} = \frac{k_1 k_2 k_3 (1 + k_5 \delta^{-2} + k_9 \delta^{-1}) - k_0 k_2 k_3 k_8 \delta^{-2}}{\Delta}$$

$$\frac{\delta P_b}{\delta W} = \frac{\delta (a^1 \delta^2 + b^1 \delta + c^1)}{\Delta} = \frac{\delta^2 (a^1 \delta + b^1)}{\Delta}$$

where

$$a^1 = k_1 \; k_2 \; k_3$$

$$b^1 = k_1 \; k_2 \; k_3 \; k_9$$

$$c^1 = k_2 \; k_3 \; (k_1 k_5 - k_0 k_8) = \text{zero}$$

APPENDIX C. RELATIONSHIP OF ENCOUNTER FREQUENCY TO INCIDENT WAVE FREQUENCY FOR THE XR-3 CRAFT

Booth (in Appendix A of Reference 4) gives a brief development of the equation for encounter frequency and for the case of ahead seas, the incident frequency, ω_i is shown to be

$$\omega_i = \frac{g}{2V}\left[\sqrt{1 + \left(\frac{4V}{g}\right)\omega_e} - 1\right]$$

This relationship was plotted by Booth and is repeated below in Figure C-1. For the XR-3 craft operating at a steady-state speed of 30 knots, V = 50.67 ft/sec., the incident wave frequency becomes

$$\omega_i = 0.318\left[\sqrt{1 + (6.3)\omega_e} - 1\right]$$

An approximation to this functional relationship that is useful over the range

$$1 < \omega_e < 20 \text{ rps}$$

is $\omega_i^2 = \omega_e/2$ for the 30 knot speed fo the XR-3 craft.

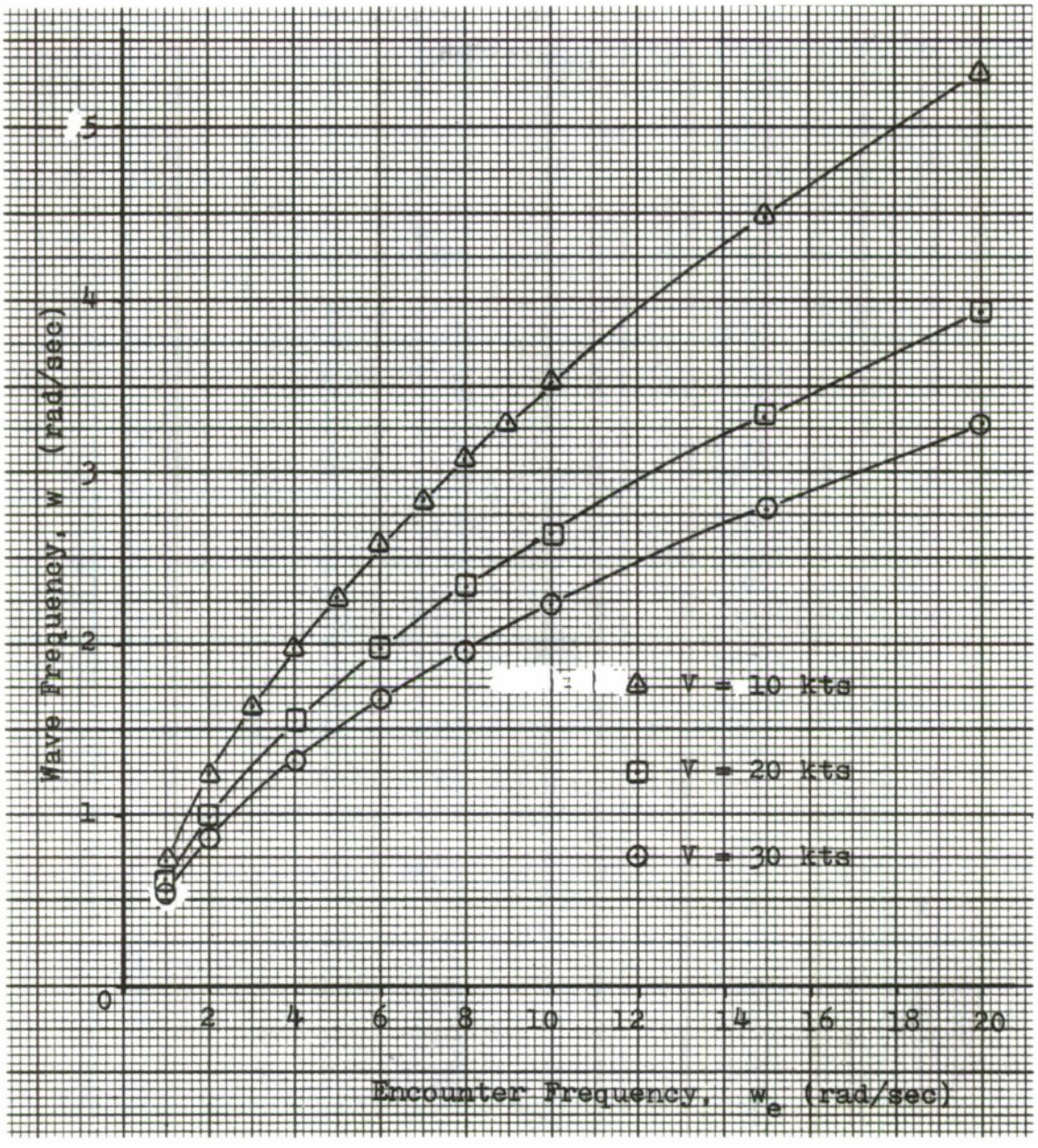

Figure C-1. Wave Frequency vs. Encounter Frequency

DISTRIBUTION LIST

	No. of Copies
Library Code 0142 Naval Postgraduate School Monterey, CA 93940	2
Research Administration Code 012A Naval Postgraduate School Monterey, CA 93940	1
Naval Sea Systems Command Washington, D. C. 20362	6
Professor A. Gerba Department of Electrical Engineering Naval Postgraduate School Monterey, CA 93940	5
Professor G. Thaler Department of Electrical Engineering Naval Postgraduate School Monterey, CA 93940	5